4-30-1993

One-Dimensional Computer Modeling of Thermal and Water Quality Characteristics of Coldwater Lake, WA

David Kevin Whitaker
Portland State University

AN ABSTRACT OF THE THESIS OF David Kevin Whitaker for the Master of Science in Civil Engineering presented April 30, 1993.

Title: One-Dimensional Computer Modeling of Thermal and Water Quality Characteristics of Coldwater Lake, WA.

APPROVED BY THE MEMBERS OF THE THESIS COMMITTEE:

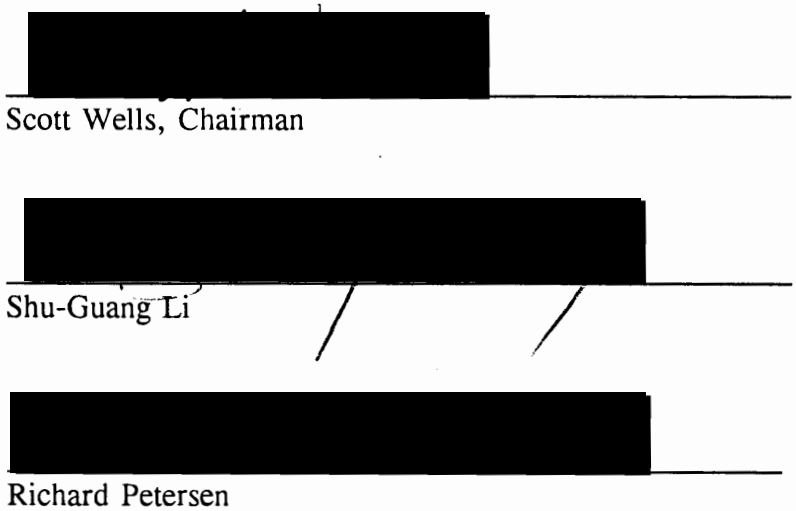

Scott Wells, Chairman

Shu-Guang Li

Richard Petersen

Coldwater Lake is a new lake formed when a massive mudflow down the Toutle River Valley, caused by the eruption of Mount St. Helens on May 18, 1980, blocked the natural outlet of Coldwater Creek. This research utilizes physical, biological and chemical data collected at Coldwater Lake during the summers of 1989 and 1990 to calibrate and verify the one-dimensional computer models CE-THERM-R1 and CE-QUAL-R1 for Coldwater Lake.

CE-THERM-R1 was used to simulate thermal characteristics in Coldwater Lake during the summer stratification periods of 1989 and 1990. The model was calibrated to 1989 data and was verified with 1990 data. The model performed well with respect to typical stratification features such as depth and temperature of the epilimnion, gradient of the thermocline and temperature of the hypolimnion. The 1990 verification simulation indicated a lack of heat in the epilimnion and metalimnion towards the end of the summer. This is thought to be a product of inaccurate cloud cover data.

Model simulations predicted vertical eddy diffusion coefficients (Ez) throughout the water column. These were compared to Ez values in the hypolimnion calculated from temperature data collected by Kelly (1991). Model simulated Ez values in the hypolimnion were near molecular diffusion while field calculated values were one to two orders of magnitude greater than molecular diffusion. The model simulation assumed no lake inflow or outflow so the hypolimnion was more stable than the natural system.

The amount of photosynthetically available radiation (PAR) to Coldwater Lake was determined from output derived from the model simulation. This will be useful in determining primary productivity within the lake.

CE-QUAL-R1 was used to simulate water quality in Coldwater Lake. The model was calibrated using dissolved oxygen (D.O.) data collected in 1989. The model adequately predicted the D.O. profile in the hypolimnion but tended to over

predict D.O. concentration in the epilimnion by 1.0 - 3.0 mg/l. This may be caused by an under estimation of the vertical diffusion coefficient in the model simulation.

Mean phytoplankton concentrations were similar to field data in the surface layer assuming a 1 mg/l phytoplankton to 10 ug/l chlorophyll a ratio. However, concentrations at 10 m and 20 m were under predicted. The phytoplankton - chlorophyll a comparison may not be valid for these lower regions because a significant portion of algal cells within this region are non-viable and are found as particulate detritus in various stages of decomposition.

Model simulated nutrient concentrations were in good agreement with the field data. NO_3 concentration in the hypolimnion increased slightly throughout the model simulation due to decay of the assumed initial condition of 2 mg/l refractory dissolved organic matter which was contributed to the lake during the eruption of Mt. Saint Helens on May 18, 1980. The model simulation predicted that the phytoplankton were nitrogen limited.

An analysis of potential changes in water clarity and water temperature due to the addition of fish in the summer of 1989 was made. The 1990 model simulation predicted that the addition of 200 kg/hectare of Rainbow Trout had little change on water temperature and water clarity.

Collection of further site specific data such as; cloud cover estimates, primary productivity rates and quantity of dissolved organic matter contributed by the May 18, 1980 eruption of Mt. Saint Helens would be useful in building a reliable water quality model at Coldwater Lake.

ONE-DIMENSIONAL COMPUTER MODELING OF THERMAL AND WATER QUALITY CHARACTERISTICS OF COLDWATER LAKE, WA.

by

DAVID KEVIN WHITAKER

A thesis submitted in partial fulfillment of the
requirements for the degree of

MASTER OF SCIENCE
in
CIVIL ENGINEERING

Portland State University
1993

TO THE OFFICE OF GRADUATE STUDIES:

The members of the Committee approve the thesis of David Kevin Whitaker presented April 30, 1993.

Scott Wells, Chair

Shu-Guang Li

Richard Petersen

APPROVED:

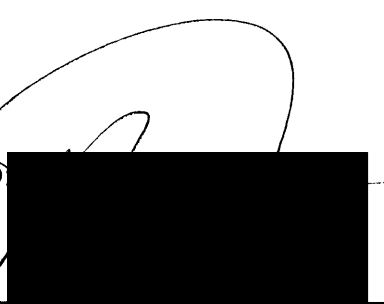

Franz N. Rad, Chair, Department of Civil Engineering

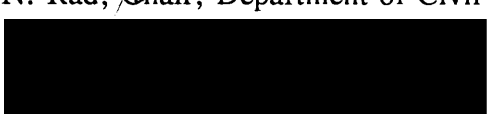

Roy W. Koch, Vice Provost for Graduate Studies and Research

ACKNOWLEDGEMENTS

Thank you Dr. Richard Peterson for the limnology class and the field experience which stirred my interest in lake ecology. Also, thanks to Valerie Kelly for allowing an engineer to tag along on those wonderful journeys to Coldwater and Castle Lakes.

Many thanks go out to Dr. Scott Wells for the encouragement and the technical assistance in water quality modeling. His input proved to be quite useful and certainly was appreciated.

Much, much gratitude goes out to my friends which put up with my moods and my inability to return phone calls promptly. I would like to especially thank my friend Kristin for the many graphs, the cutting and pasting, and all the love.

YEE HA!

TABLE OF CONTENTS

APPENDICES

LIST OF TABLES

LIST OF FIGURES

INTRODUCTION

The study and understanding of freshwater ecosystems is of major importance in our society. There is a finite amount of freshwater available to an exponentially growing population. This has become evident over the past decade in Oregon and Washington where much of the available freshwater has been appropriated for human needs and little is left to maintain the health of the freshwater ecosystems. This promotes conflict between various users of the freshwater such as irrigators, municipalities and power generators, and those who wish to protect these ecosystems through passionate appeal to leave them as they are. All of this transpires with limited understanding of the interactions which occur within freshwater ecosystems.

The eruption of Mt. St. Helens on May 18, 1980 and the subsequent impoundment of Coldwater Creek provided a unique opportunity to examine the freshwater ecology of newly formed Coldwater Lake. Water quality field data taken by Kelly (1991) have provided an opportunity to research an ecosystem from its very inception.

The objective of this study was to research the structure and function of various water quality interactions within Coldwater Lake. These objectives included:
(1) Development of a thermal model predicting the onset, extent and duration of thermal stratification using recently collected limnological data (1989-1990)
(2) Analysis of the lake mixing processes which drive the lakes thermal structure

phenomena (3) Analysis of the amount of photosynthetically available radiation (PAR) available for use by phytoplankton (4) Development of a water quality model which could be used as a tool for further understanding of water quality dynamics in Coldwater Lake and an (5) Investigation of the potential changes in water quality due to the addition of fish to the lake in 1989.

METHODS

SITE DESCRIPTION

Physical Setting

Coldwater Lake (46° 18' N, 122° 15' W) is approximately 12 km NW of Mt. St. Helens in Southwestern Washington on the western side of the Cascade mountain range. The surface of the lake is at approximately 760 m elevation, and the lake resides in a deeply incised canyon with ridges ranging from elevation 1200 m to 1400 m surrounding all sides of the lake except the outlet location which faces the southwest (see Figure 1). The outlet drains to Coldwater Creek and then into the North Fork Toutle River. A 13 km^2 area that directly borders the lake is drained by intermittent flows from minor streams. Two perennial streams also feed into Coldwater Lake. Coldwater Creek flows into the farthest eastern section of the lake and drains approximately 15 km^2 of mountainous terrain. South Coldwater Creek flows into the lake near the outlet in the southwestern region of the lake. It also drains approximately 15 km^2 of mountainous terrain plus the 45 km^2 watershed of Spirit Lake to the east. The total area which drains to Coldwater Lake is 93 km^2, of which 48 km^2 is within the Coldwater Lake drainage boundaries and 45 km^2 is from a trans-basin diversion from Spirit Lake.

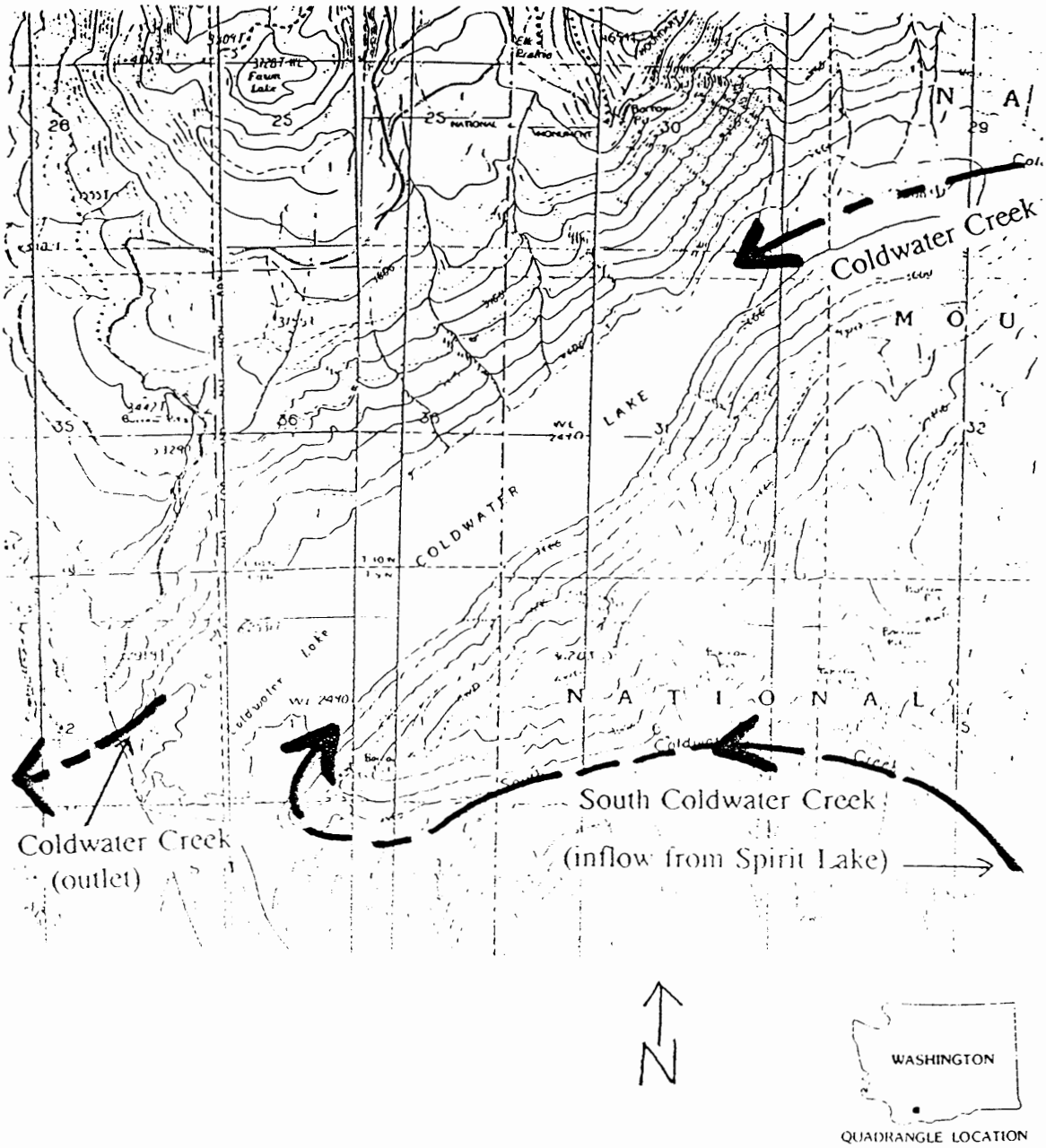

Figure 1. Topographic map, Coldwater Lake, 1983.

A diversion tunnel was constructed by the Corps of Engineers (COE) in 1984-85 to spill water from Spirit Lake through South Coldwater Creek into Coldwater Lake (Figure 2). This diversion structure serves as the main outlet control system for Spirit Lake.

The surface area of Coldwater Lake is approximately 3.4 km^2 with a maximum breadth of 1 km. It has a maximum depth of 62 m and a corresponding volume of $6.94*10^7$ m^3. The steepness of the upper reaches of the lake compared with the relatively mild slopes and flat bottom of the lake at the middle and lower sections indicate that sediment and debris from the May 18, 1980 eruption and previous eruptions of Mt. St. Helens have entered the canyon near the confluence of Coldwater and South Coldwater Creeks (Kelly 1991).

Precipitation in the Coldwater Lake area is principally marine in origin due to the dominant winds out of the west and its close proximity to the Pacific Ocean (90 miles to the west). The predominant rainy season occurs between October and April and is due to a southwesterly to westerly stream of moist cool air from the common Aluetian low which is centered in the Gulf of Alaska (Uhrich 1990). Approximately 75% of the annual precipitation falls between October and March. The historical average annual precipitation as measured at Spirit Lake from 1961-85 is 103.8 inches (Uhrich 1990). The maximum rainfall intensity for a 24 hour period from 1981 to 1986 as measured at the Coldwater Lake outlet is 2.87", which occurred on February 23, 1986. This compares to a rainfall amount of 3.53" on the same day at Castle Lake which is at elevation 796 m and is approximately 5 km to the southwest (Uhrich

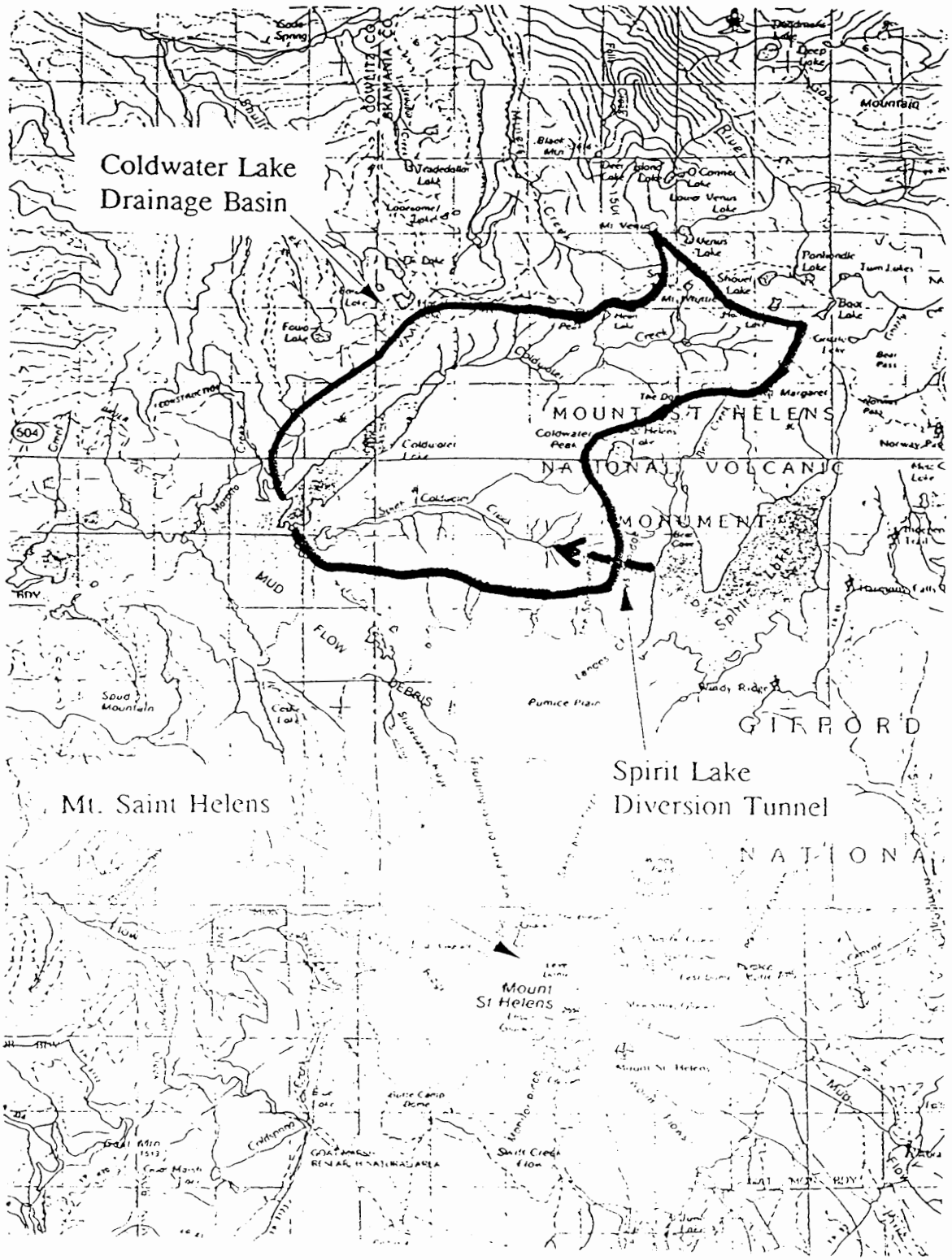

Figure 2. Coldwater Lake and surrounding area.

1990). Rainfall amounts vary significantly in this mountainous terrain as a function of altitude and location.

Coldwater Lake is usually covered by ice and snow during the winter months. The length of time the lake is ice covered is highly variable and dependent upon regional temperature patterns. The average annual maximum, minimum and mean air temperatures for Spirit Lake are 10.0°C, 1.0°C and 5.6°C, respectively (Uhrich 1990). Spirit Lake is at elevation 987 m and typically has cooler temperatures than Coldwater Lake. The average annual snow depth at Spirit lake from 1932-56 was 282.6 inches (Uhrich 1990).

History of the Lake

The landscape around what is now Coldwater Lake was significantly altered on May 18, 1980. At approximately 8:37 a.m. an earthquake of magnitude 5.1 destabilized the bulging north face of Mt. St. Helens causing a series of landslides to cascade down the northern reaches of the mountain. The largest of these landslides evolved into a tremendous lahar. Approximately 2.8 km^3 of volcanic debris flowed north from the mountain into Spirit Lake partially flowing up and over Coldwater Ridge (Kelly 1991). However, the main part of the flow was deflected by the ridge and continued by flowing down the North Fork Toutle River, the path of least resistance (Figure 2). The lahar finally stopped after flowing 22 km from the mountain down the Toutle River valley. The deposits which were left behind ranged from 25 m to 150 m thick (Fairchild 1985). The deposits effectively dammed both

Coldwater and Castle Creeks, the Spirit Lake outlet, as well as other smaller, less significant streams. Coldwater Creek was dammed at the confluence of Coldwater and South Coldwater Creeks.

The lahar which flowed down the North Fork Toutle did not begin movement down the valley until 4.5 hours after the eruption began and lasted approximately 8 hours (Fairchild 1985). The lahar consisted of various materials which were primarily gravel in a highly erodible matrix of silt and clay. These flows supported cobbles, boulders, and ice chunks from the glaciers and downed trees picked up along the way. The flow velocities ranged from 1.5 m/s near the end of the flow to up to 40 m/s near the base of the mountain (Janda 1981). Soon after the eruption, Coldwater Lake began filling behind the debris dam which blocked the outlet to Coldwater Creek. Typically lakes formed by landslides are transitory in nature because the unconsolidated nature of the debris blockage leaves it susceptible to erosion from the out flowing waters (Wetzel 1983). However, the landslide which blocked the Coldwater Creek outlet was so massive that it took many months to fill the lake. There was concern that structural failure of the debris blockage due to erosion from flow over the blockage would lead to catastrophic flooding in the Toutle River basin. To prevent flooding, the U.S Army Corp of Engineers (COE) constructed a spillway during summer 1981 in the southwestern portion of the lake to serve as the lake outlet.

Coldwater Lake receives inflows from Spirit Lake via a trans-basin diversion tunnel through Harry's Ridge and into South Coldwater Creek (Figure 2). The tunnel

became operational in May 1985 and discharged 20% of the lake volume in 6 months (Janda 1985). This increase in stream flows caused significant erosion in South Coldwater Canyon, removing approximately 900,000 m^3 of material from the canyon within 6 months (Janda 1985). Much of the material was deposited in Coldwater Lake, which greatly increased the size of the South Coldwater Creek delta near the lake outlet. Evidence from water quality observations during the summer of 1986 suggested that the inflow from South Coldwater Creek did not fully mix with Coldwater Lake prior to discharge (Larson, 1987). The incomplete mixing may be attributed to the closeness of the stream inlet to the lake outlet.

Studies of the lakes within the Mt. St. Helens blast zone were undertaken soon after the May 18, 1980 eruption. Lakes within the zone were studied and compared to lakes outside the blast zone to determine how they were affected. An excellent review of studies which investigated major ions, dissolved organic carbon, temperature, dissolved oxygen, alkalinity, light extinction, biological processes, and nutrient cycling in Coldwater Lake and other lakes from June 1980 through 1982 is Kelly (1991), a thesis entitled "Limnology of Two New Lakes, Mount St. Helens, WA." Kelly (1991) provides a comprehensive review of limnological data collected at Coldwater Lake during the summers of 1989 and 1990. These data were used to calibrate the numerical model used in this thesis.

The Forest Service has stocked 30,000 Rainbow Trout fingerlings in Coldwater Lake since 1989 (Charlie Chrisifuli, 1993). Visual observations have shown that during the summer of 1990 some large trout were present. Fishing will be

open to the public beginning 7/15/93 with a one fish per day limit.

Coldwater Lake has been in the Forest Service designated red zone of Mt. St. Helens since the eruption. This zone was established to restrict access to the lake. Therefore, Coldwater Lake has had practically no human pressure on it since its birth, 13 years ago. This will soon change with the opening of the Spirit Lake Memorial Highway which leads to Coldwater Lake. In the summer of 1993 thousands of visitors will travel to Coldwater Lake to recreate along its shores and hike the surrounding ridges to find some viewing spot to look down the throat of a live volcano. The introduction of humans into the Coldwater Lake environment may alter the ecological development of the lake system.

Hydrology of the Watershed

The hydrologic characteristics of the watersheds surrounding Mt. St. Helens were changed significantly after the May 18, 1980 eruption. The post eruption 6 hour unit hydrograph for the lower Toutle River during the 1980-1981 winter had a peak discharge 1.75 times higher than the peak discharge before the eruption. Additionally, the time to peak was reduced from 15 hours to 9 hours. Stream gaging in the lower Toutle River indicated that peak discharges typically related to 25 year recurrence interval storms occurred 3 times during the three years after the eruption (Janda 1985).

The increase in storm runoff in this basin since the eruption were attributed to 3 characteristics; decreased infiltration, reduction in the hydraulic roughness in

affected channels, and bulking of flows because of increased suspended sediment concentration (Janda 1985).

Prior to the eruption, streams surrounding Mt. St. Helens flowed through forests of Douglas Fir and Hemlock. Many parts of the forest had not been logged and were in a pristine state. The iniltration capacity of the soils, pre-eruption were typically 50 mm hr^{-1}, with values exceeding 100 mm hr^{-1} common (Janda 1985). This high infiltration rate reduced the runoff excess and decreased the time to peak of maximum discharge. The presence of large cobbles, boulders and downed woody debris in the stream channels increased the channel roughness which increased the time at which the peak discharge occured.

The ridges surrounding Coldwater Lake were effectively denuded of all vegetation during the eruption blast. Infiltration capacities were reduced to 1 - 4 mm hr^{-1} after the silty crust of the airfull tephra was deposited. This reduced the infiltration capacities of the soils in the watershed tremendously (Janda 1985). Infiltration capacities soon increased however, due to sheet erosion of the ash tephra and rill and gully erosion down to pre-eruption soils. Erosional processes increased sediment load into Coldwater Lake. Much of this sediment was deposited in the deltas at the inlets of both North and South Coldwater Creeks. The outflow from the lake is much clearer than the inflow indicating that sediment accumulates in the lake.

Fine materials such as sand (0.0625 to 2 mm grain size) and silt and clay (<0.675 grain size) eroded during the first year after the blast. Coldwater Lake received 2.11×10^6 tons of sediment within this period (Kelly 1991).

Sediment traps were placed 2.3 meters above the deepest part of the lake on June 24, 1982. They were recovered in August 4, 1983, replaced, and recovered again on August 8, 1984 (Anderson 1985). Daily sediment yields from minor streams with intermittent flows into Coldwater Lake during 1982 (excluding North and South Coldwater Creek drainages), ranged from $2g/m^2$ during the dry season to as much as 115 g/m^2 during the "first-flush" or turbite phase of the season. The annual yield at this time was appoximately 8600 metric tons/km^2 (Anderson 1985). The area drained by these minor streams is approximately 13 km^2. This translates to a contribution to Coldwater Lake of approximately 100,000 metric tons of sediment per year from this drainage area. The North and South Coldwater Creek sediment inputs were not included in the sediment calculations because most of the sediment from these creeks is deposited in their respective deltas. Both streams do contribute sediment to the lake. Only South Coldwater Creek has been investigated for sediment transport and it has been estimated that its drainage basis contributes 25,000 metric tons/km^2. This translates to a denudation rate of 1.16 cm/yr (Janda 1985). The sedimentation rate has decreased since 1983 because of the introduction of more vegetation to the hill slopes and stream channels. Also, much of the highly erodible tephra material has been eroded exposing more cohesive soils.

DATA COLLECTION

Meteorological Data

Meteorological data used in the model include daily mean values for dry-bulb temperature, dewpoint temperature, wind speed, cloud cover and barometric pressure. Cloud cover data were taken as the daily mean value from sunrise to sunset. The wind speed and dry-bulb temperatures were obtained from the COE meteorological station SLZW for the 1989 model period and from the COE meteorological station CSLW for the 4/25/90 - 7/31/90 model period (Figure 3). Wind speed and dry-bulb air temperature data for these COE meteorological stations was incomplete after 7/31/90. Linear regressions of air temperature and wind speed were used to calculate values from 8/1/90 - 11/24/90 by utilizing paired values of data from station CSLW and data from the NOAA weather service station at the Portland International Airport (PIA) approximately 50 km to the south at elevation 0.6 m (Figures 4 and 5).

Dew point temperatures were obtained by relating dry-bulb temperatures to relative humidities using a psychrometric chart (Van Nostrand 1983). Relative humidities were taken from the NOAA weather station at PIA for both 1989 and 1990. Since no data for relative humidity were available near Coldwater Lake, PIA values were used to represent relative humidity at the Lake.

Cloud cover data were taken from the NOAA weather station at PIA. The PIA station was located on the western end of the Columbia River Gorge on the south bank of the Columbia River. Airflow patterns were typically northwesterly during

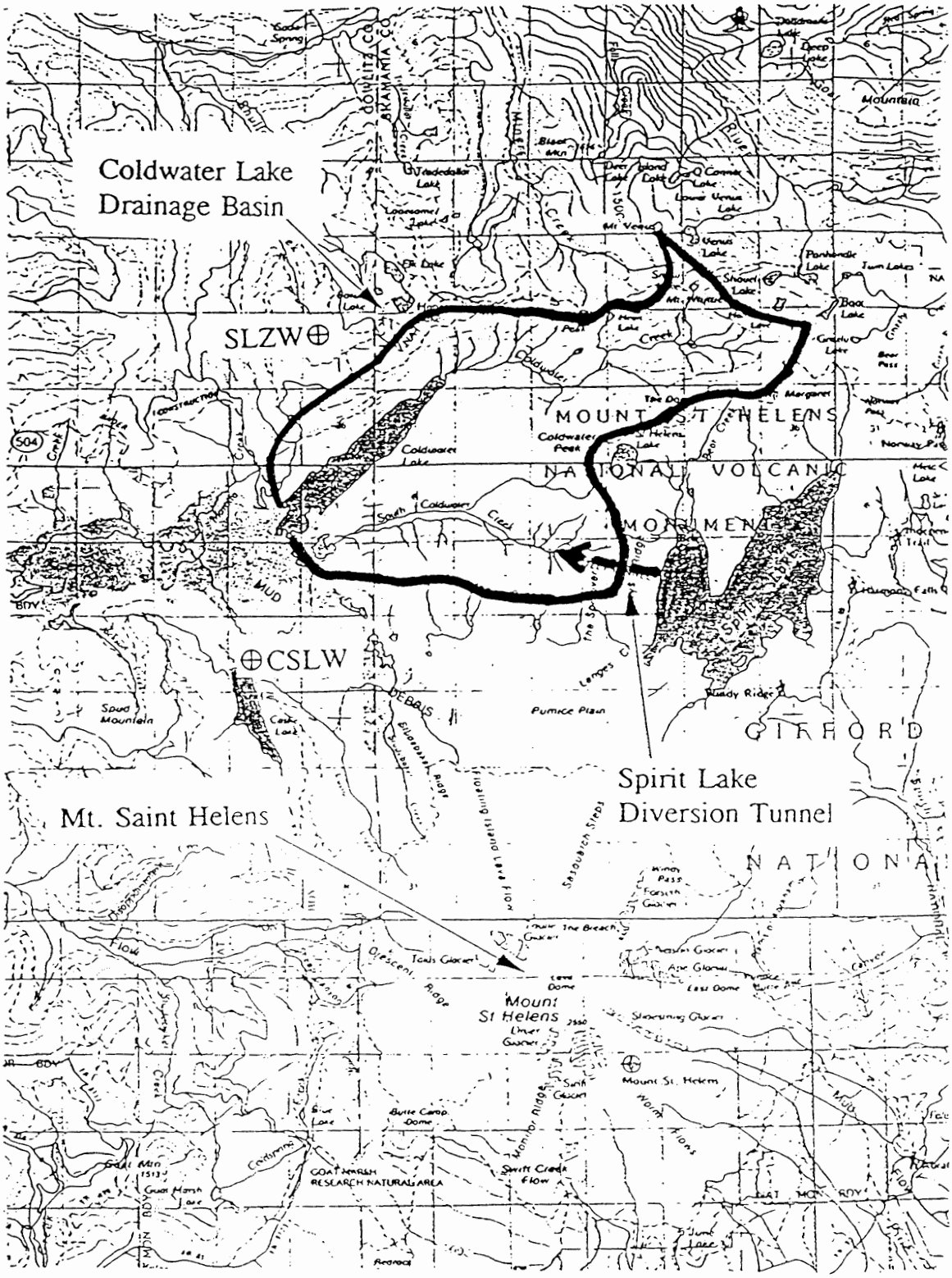

Figure 3. Meteorological Stations.

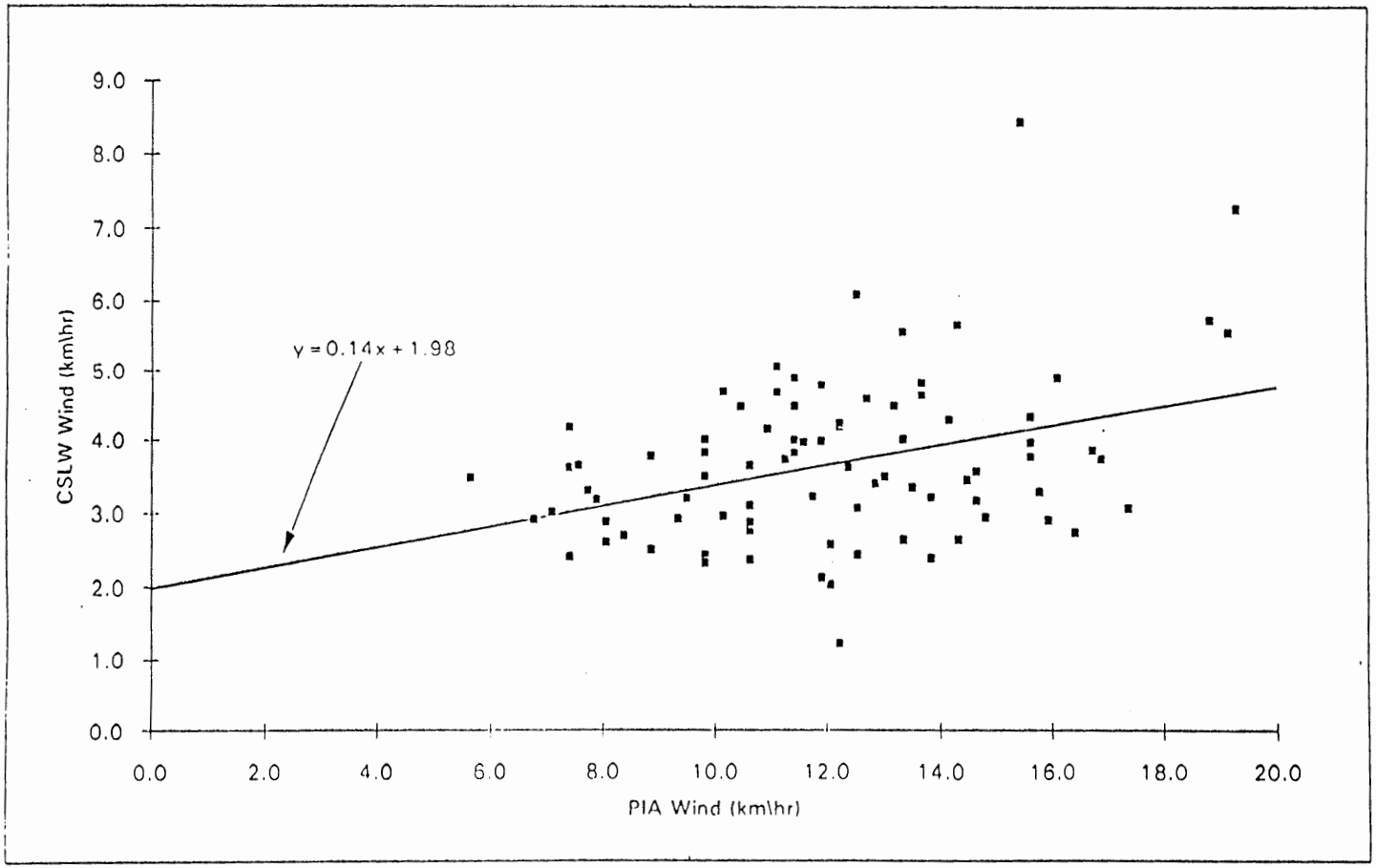

Figure 4. 1990 Wind speed linear regression (PIA/CSLW Pairs).

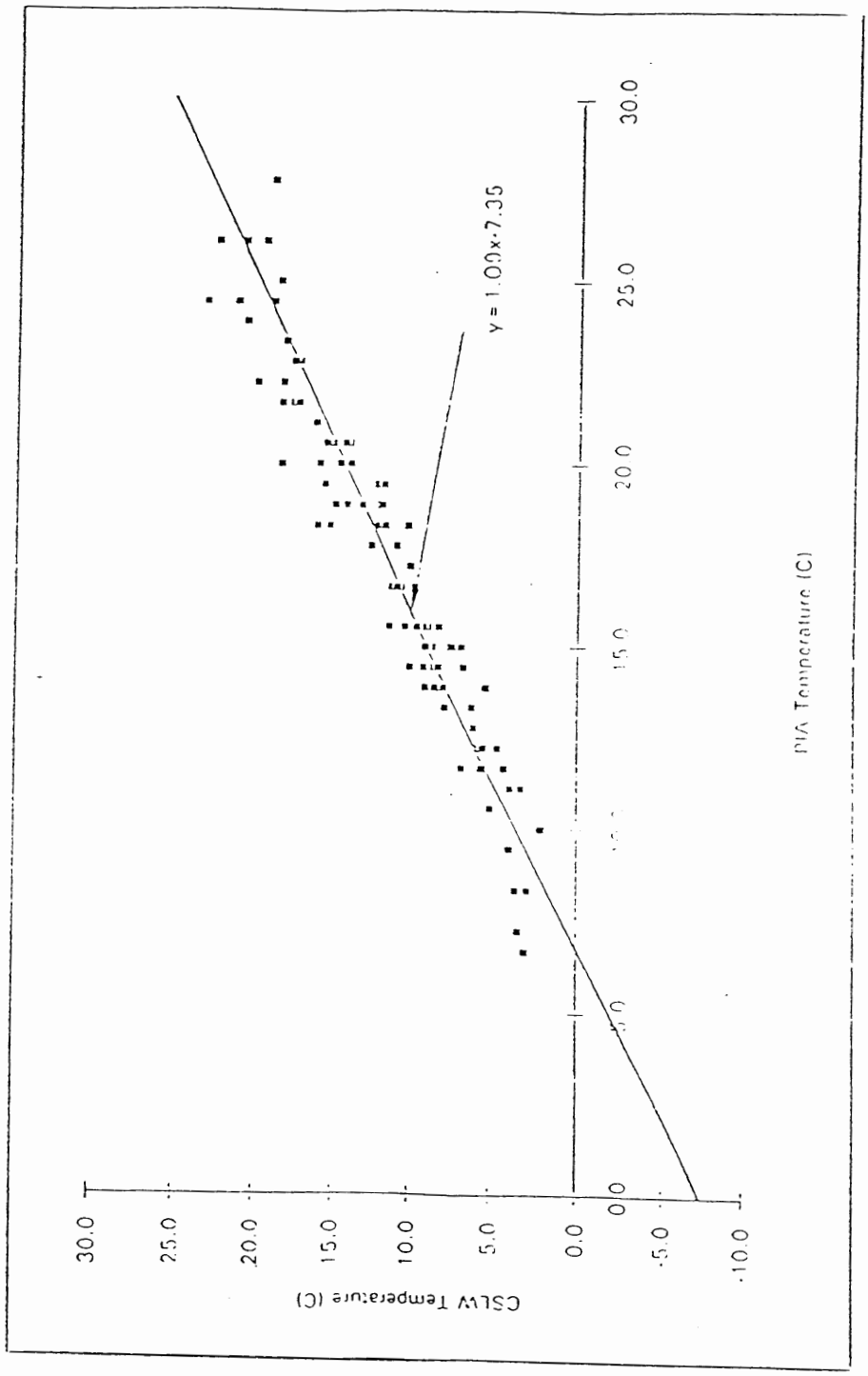

Figure 5. 1990 Temperature linear regression (PIA/CSLW Pairs).

the late spring and summer months (NOAA 1990). Coldwater Lake was at elevation 760 m on the western side of the Cascade mountain range and had airflow patterns predominately north-northwesterly during the late spring and summer months of 1989 and 1990. The Cascade Mountain Range disrupts the predominate air-flow pattern by promoting convection and forcing air to rise along its westward slope. This promotes a greater amount of precipitation and cloud cover on these slopes than would occur in the lower elevations. Therefore, the mean daily cloud cover data collected at PIA under represented the cloud cover at Coldwater Lake. Table I summarizes the sources used for meteorological data.

Physical Data

Data used in the modeling effort were collected during field sampling visits to Coldwater Lake by Kelly (1991) in the summers of 1989 and 1990. The lake was visited nine times in 1989 and eight times in 1990. The first sampling visit occurred when the snow had melted sufficiently to allow access to the lake. Sampling was done out of a 10' aluminum boat with a 5 hp outboard engine. Data were routinely collected from a shallow and a deep station in the lake (Figure 6). Data reported by Kelly (1991) from the station located over the deepest part of the lake were used in the model simulation.

Bathymetric data were collected during the summer of 1990 with a Monow depth sounder. The depth sounder generated a continuous tape of the lake bottom elevation while transecting the lake at a continuous velocity. Depths from the tape

TABLE I

SOURCES OF METEOROLOGICAL DATA USED IN MODELING OF COLDWATER LAKE 1989 - 1990

DATA	YEAR	SOURCE
Air Temperatures (Dry Bulb)(° C)	1989	COE meteorological station SLZW (see figure 2)
	04/25/90 - 07/31/90	COE meteorological station CSLW (see figure 2)
	08/01/90 - 11/24/90	DBT=1.09 (T_{PIA}) - 7.47 (where T_{PIA} is the dry-bulb temperature at the NOAA, PIA weather station from 07/31 - 11/24) ; this linear regression was determined from CSLW/PIA pairs from 04/25/90 - 07/31/90; R^2= 0.923
Wind Speed (km/hr)	1989	COE meteorological station SLZW
	04/25/90 - 07/31/90	COE meteorological station SLZW
	08/01/90 - 11/24/90	WS=0.14(WS_{PIA})+1.98 (where WS_{PIA} is the wind speed measured at the NOAA, PIA weather station); this linear regression was determined from CSLW/PIA pairs from 04/25/90 -07/31/90; R^2= 0.142
Relative Humidity %	1989 & 1990	NOAA measurements at the PIA weather station
Cloud Cover (0-10; 10 = 100 percent cloud cover)	1989 & 1990	NOAA measurements at the PIA weather station
Barometric Pressure (mb)	1989 & 1990	All values were estimated at 1000 mb

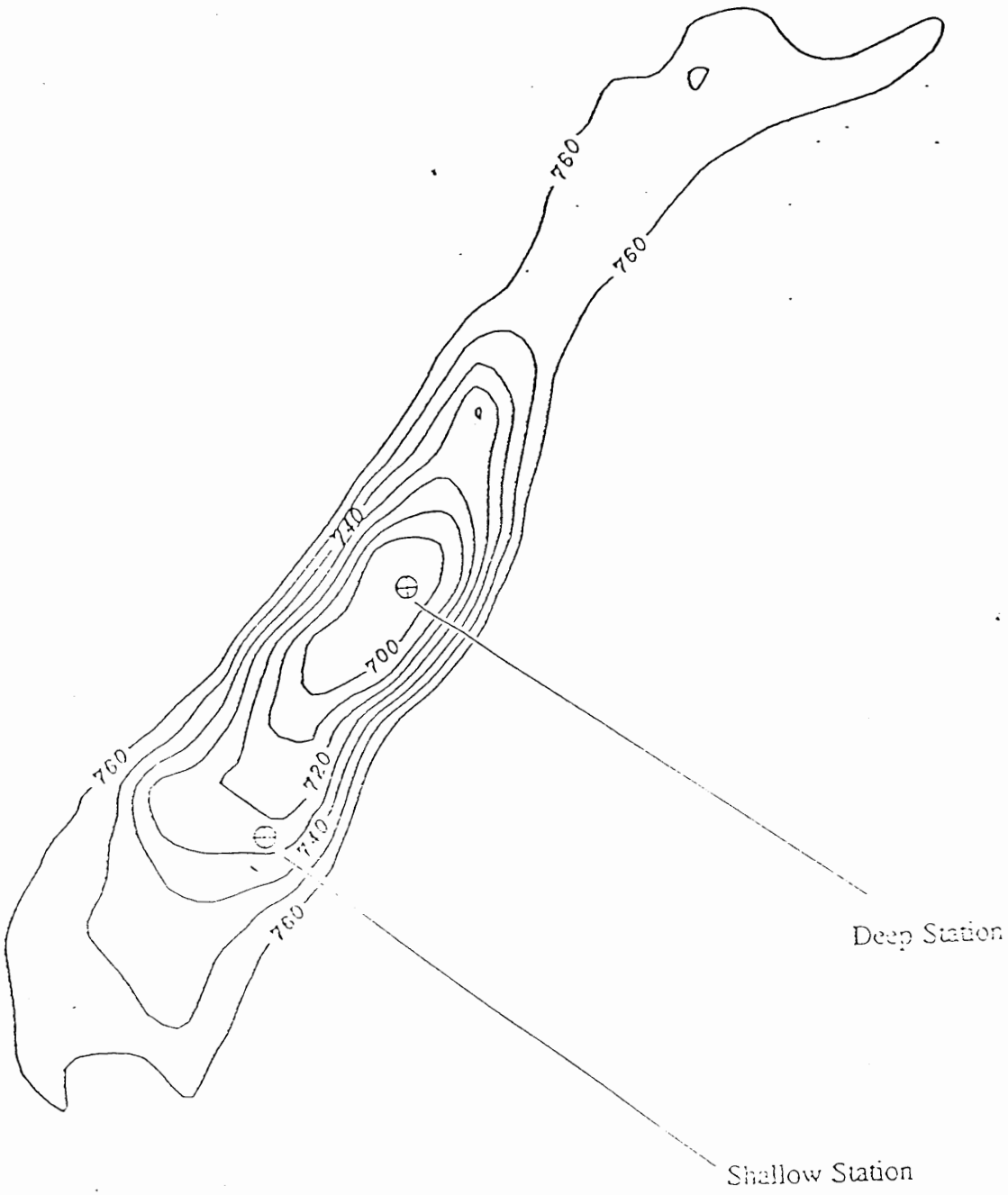

Figure 6. Bathymetric map in meters (MSL), Coldwater Lake, summer 1990.

were digitized with a CAD system and then transferred into an ASCII file that the computer program SURFER could read. The SURFER program was used to generate a bathymetric map of the lake (Figure 6) and to calculate water surface area as a function of lake depth. Water surface area vs. lake depth is shown in Figure 7 with a least squares power curve and 2nd order polynomial curve fit to the data. The reservoir morphometry was represented by the equations from these curves.

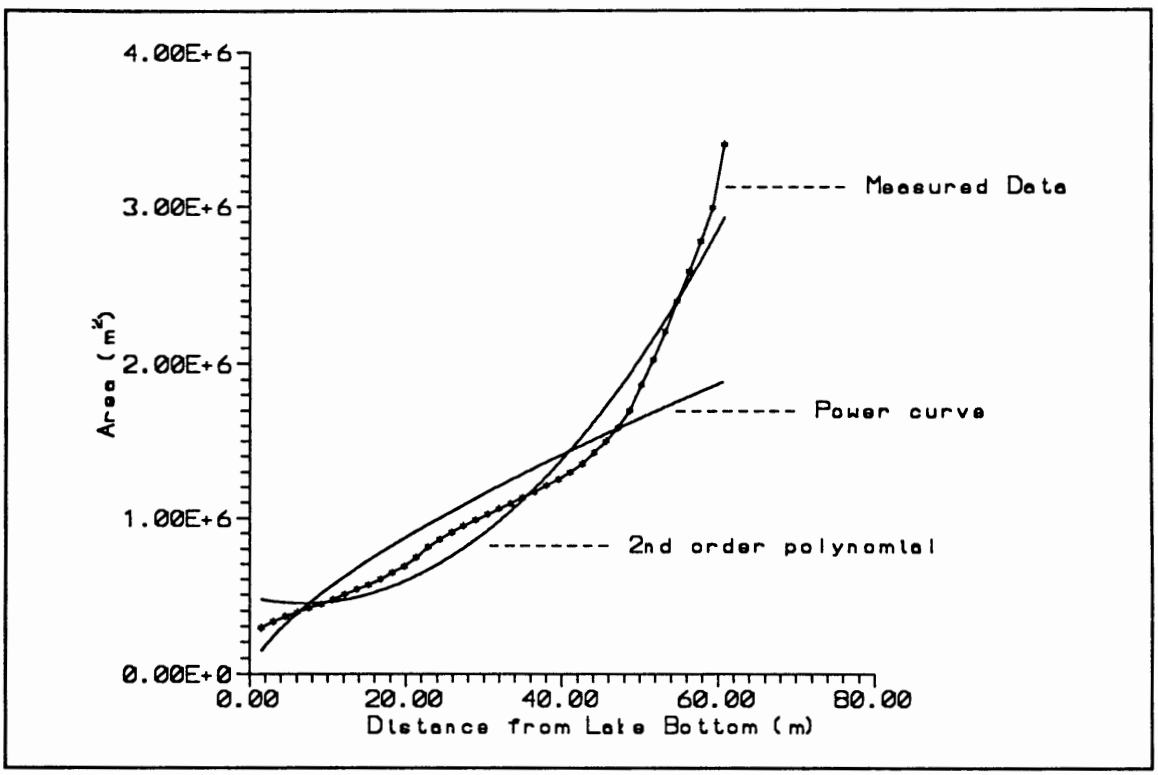

Figure 7. Water surface vs. lake depth plot with a power curve and 2nd order polynomial curve to fit the plot.

The area of individual layers (I) was calculated by the following equation for the 2nd degee polynomial:

$$AREA(I) = ACOEF(1)+ACOEF(2)*Z(I)+ACOEF(3)*[Z(I)]^2 \quad (1)$$

AREA (I)=cross-sectional area for layer I (m^2)

ACOEF(1)=489871

ACOEF(2)=11827.7

ACOEF(3)=850.9

Z(I)=distance from lake bottom (m)

The volume of individual layers (I) in m^3 was calculated by taking the integral of the area equation which is:

$$VOL(I)=ACOEF(1)*Z(I)+ACOEF(2)*[Z(I)]^2/2+ACOEF(3)*[Z(I)]^3/3 \quad (2)$$

The area of individual layers (I) was calculated by the following equation for the power curve:

$$AREA(I)=ACOEF(1)*Z(I)**ACOEF(2) \quad (3)$$

ACOEF(1)=110524

ACOEF(2)=0.69071

The volume at individual layers (I) was calculated by taking the integral of the area equation which is:

$$VOL(I)=ACOEF(1) / (ACOEF(2) + 1)*Z(I)**(ACOEF(2) + 1) \quad (4)$$

Since neither of these curve fits adequately represented the depth - area relationship the model was modified to accept a 3rd degree polynomial as in Figure 8.

The area of individual layers (I) was calculated by the following equation for the 3rd degree polynomial:

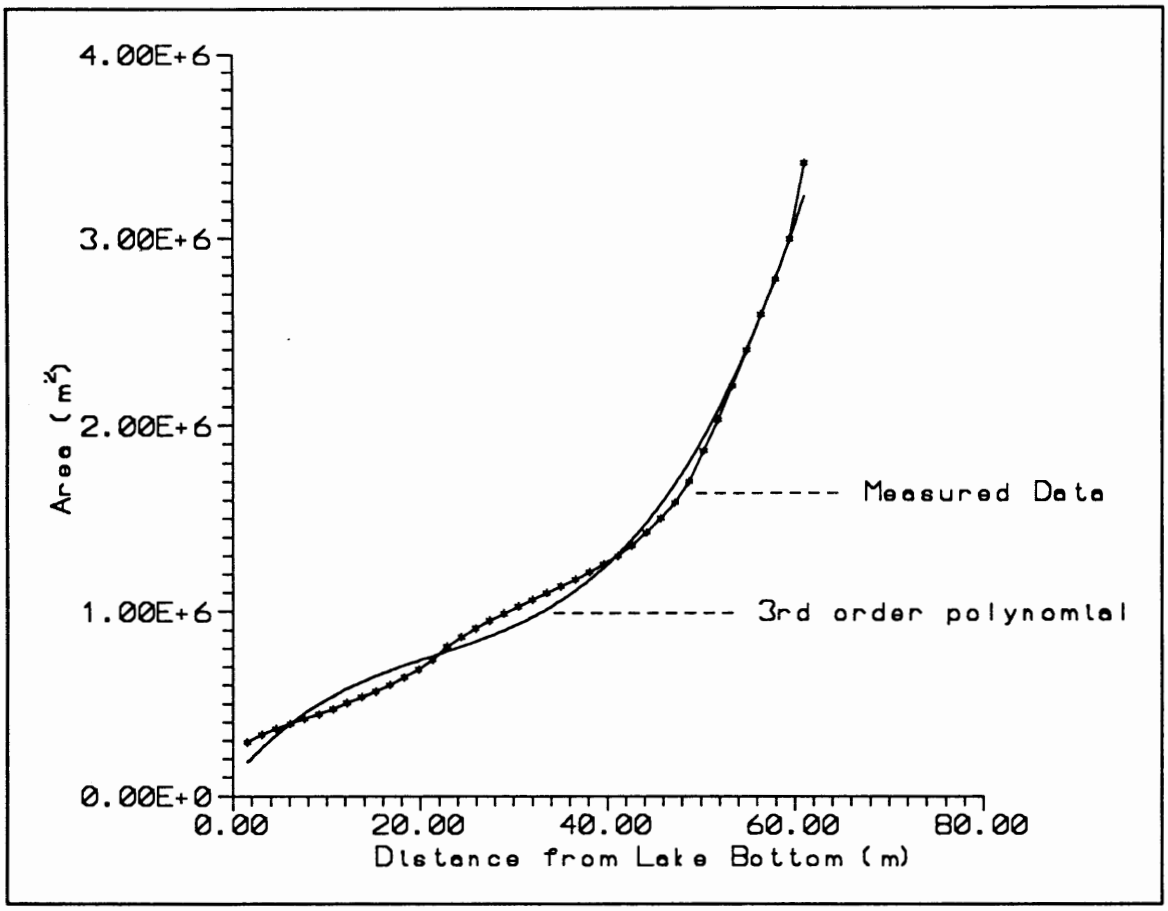

Figure 8. Water surface vs. lake depth plot with a 3rd order polynomial curve fit to the plot.

$$AREA(I) = ACOEF(1)+ACOEF(2)*Z(I)+ACOEF(3)*[Z(I)]^2 + ACOEF(4)*[Z(I)]^3 \quad (5)$$

ACOEF(1)=96420.8

ACOEF(2)=59379.4

ACOEF(3)=-1963.33

ACOEF(4)=30.028

The volume at individual layers (I) was calculated by taking the integral of the area

equation which was:

$$VOL(I) = ACOEF(1)*Z(I) + ACOEF(2)*[Z(I)]^2/2 + ACOEF(3)*[Z(I)]^3/3 \quad (6)$$
$$+ ACOEF(4)*[Z(I)]^4/4$$

During each sampling trip, water temperature was measured at one meter intervals from the lake surface to a depth of 20 meters and at 5 meter intervals from 20 to 60 meters in depth. Transparency was measured using a 30 cm secchi disk. Dissolved oxygen (DO) samples were taken at varying depths, fixed on site, and analyzed within 24 hours (Kelly 1991).

Chemical/Biological Data

Chemical and biological field data collected during the summers of 1989 and 1990 included: nutrient and chlorophyll a samples which were collected in a Van Dorn sampler at five depths per sampling trip; phytoplankton samples which were collected at 5 meter intervals from the lake surface to a depth of 20 meters; zooplankton samples which were collected at various depths using a plankton net; and major ion samples which were collected only in 1989 on three occasions near the lake surface, at mid-lake depth and at the bottom of the lake (Kelly 1991). Laboratory analyses were coordinated by Kelly (1991). Minimum and maximum values for these parameters are summarized in Table II.

MODEL DESCRIPTION AND ASSUMPTIONS

Governing Equation

CE-QUAL-RI is a one-dimensional, integral energy model developed at the U.S. Army Corps of Engineers Waterways Experiment Station in Vicksburg, Mississippi. The model was designed to simulate major physical, chemical and

TABLE II

BIOLOGICAL DATA FOR SUMMERS OF 1989 AND 1990

PARAMETERS	MIN VALUE	DEPTH (meters)	MAX VALUE	DEPTH (meters)
chlorophyll a	0.33 ug/1	20	4.74 ug/1	10
zooplankton	40 (Indivs/m^3)	0 - 5	15906 (Indivs/m^3)	0 - 5
SiO_2	12.78 mg/1	0	18.20 mg/1	55
NO_3	1.44 ug/1	0	15.26 ug/1	35
PO_4	6.32 ug/1	0	144.58 ug/1	60
DO	4.87 mg/1	55	9.97 mg/1	15
temperature	4.11°C	50	18.96 °C	5

biological processes which occurred within a lake or reservoir. A Lagrangian grid system was used to simulate the exchange of thermal energy and constituent concentrations between fully mixed horizontal layers. There was no vertical flow between the layers. Instead, the layer thicknesses were allowed to vary accounting

for the net flow of water into or out of a layer (Ford 1980). The mathematical structure of the model used the conservation of mass equation (Equation 7) as the basis for determining constituent concentrations in layer Z_i, as functions of time and depth:

$$\partial/\partial t(VC) = \Sigma Q_{in}C_{in} - Q_{out}C + \partial/\partial z(DA\ \partial C/\partial z)\Delta Z + \text{Source Rates} - \text{Sink Rates} \quad (7)$$

where
V = layer volume, m^3
C = constituent concentration, g/m^3
Q_{in} = layer inflow, m^3/hr
C_{in} = inflow concentration, g/m^3
Q_{out} = layer outflow, m^3/hr
D = diffusion coefficient, m^2/hr
A = horizontal surface area of the layer, m^2
ΔZ = layer thickness, m
t = time, hr
z = layer elevation, m

All terms are presented in units of mass per unit time. Two boundary conditions are required since Equation 7 is second order in space. In the Coldwater Lake modelling simulation the boundary conditions were at the lake surface and the lake bottom. Equation 7 is of first order in time, so one initial condition was required which occurred at $t = 0$. Equation 7 is used for heat conservation by substituting the concentration of heat $\rho c_p T$, where ρ is fluid density, c_p is specific heat of water, and T is temperature for C.

Assumptions

Computer models are simplified representations of the natural system being modeled. Assumptions must be made to simplify reactions which occur within the natural system. The major assumptions in this version of CE-QUAL-R1 were:

- Conservation of mass and energy
- One-dimensional solution (horizontal layers were homogenous throughout area of the vertical layer)
- Simplified ecological interactions
  - ▸ No competition of species
  - ▸ Does not consider all ecological processes
  - ▸ Does not predict numbers of any species
- Anaerobic processes modeled: reduced forms of magenese, iron and sulfide
- No groundwater inflows into the lake

Other assumptions specific to Coldwater Lake were made also:

- Some values for ecological parameters were assumed from suggested values in the CE-QUAL-RI manual. See Appendix A for a complete listing of parameter values and their sources and Appendix B for a listing of initial values.
- Lake inflow and outflow were assumed to be insignificant based on a mean annual detention time of approximately 340 days (Figure 9).

The Coldwater Lake mean annual detention time was calculated from a 6.6 m^3/s mean annual outflow measured at the Coldwater Lake outlet canal during water year 1986. This outflow represented runoff discharge from the 93 km^2 drainage basin area encompassing both the Coldwater Lake and Spirit Lake drainage basins. It was assumed that inflows from South Coldwater Creek did not completely mix with Coldwater Lake because of the close proximity of the inflow channel to the lake outlet. Therefore, only inflows from Coldwater Creek and from the minor intermittent streams around the lake were assumed detained. The drainage area contributing these flows is 28 km^2 which is approximately 30% of the 93 km^2 drainage area which

contributed the 6.6 m^3/s mean annual outflow in water year 1986. By taking a ratio of

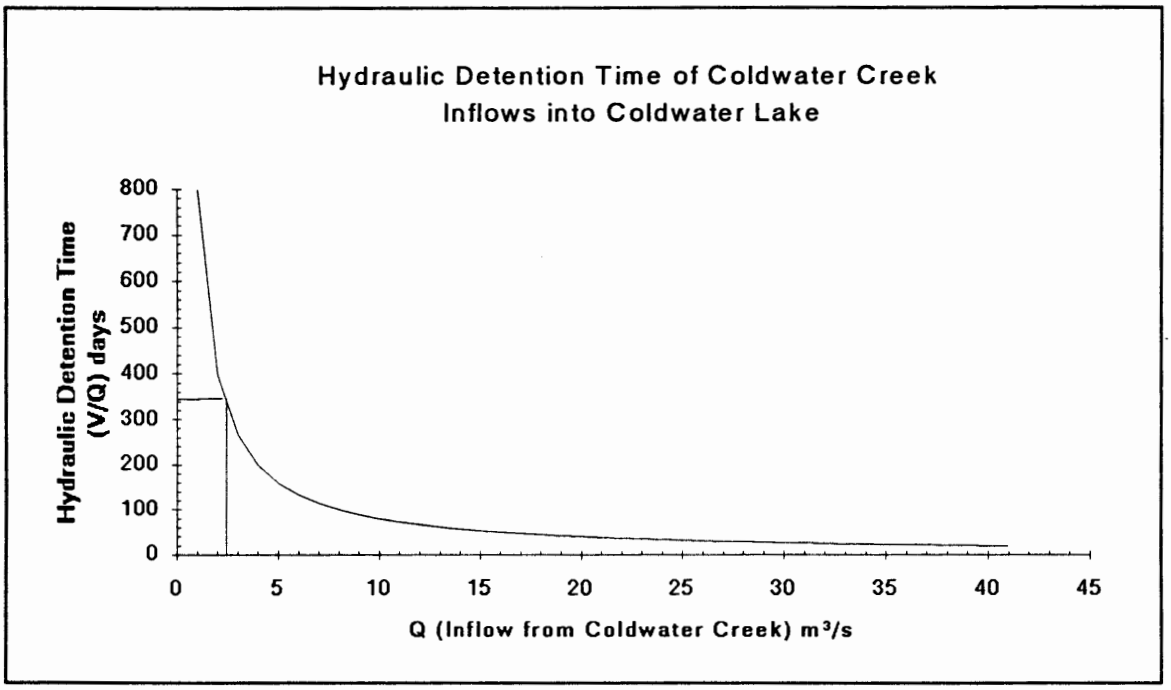

Figure 9. Hydraulic detention time of Coldwater Creek inflows into Coldwater Lake vs. predicted average monthly inflow from Coldwater Creek.

drainage basin area to inflow (assuming total inflow = total outflow), a mean annual inflow of approximately 2 m^3/s will come from Coldwater Creek and the minor intermittent streams around the lake. Figure 9 shows the relationship between hydraulic detention time and inflow.

Thermal Energy

Thermal energy distribution within a lake has a significant influence on the lake's water quality. Temperature changes within the lake, caused by heat fluxes from solar radiation and inflows to the lake control biological and chemical rate processes,

distribution of inflows and the density profile of the lake. Temperature was treated as a thermal energy concentration which is applied to the conservation of mass equation. For any layer i, the general thermal energy equation was:

$$\rho_i c_p \partial/\partial t\,(T_i V_i) = \partial/\partial z(\rho_i c_p D_i A_i \partial T/\partial z)\Delta Z_i + \partial/\partial z(\phi_i A_i)\Delta Z_i + \rho_i c_p (Q_{in} T_{in} + Q_p T_p - T_i Q_{out}) \quad (8)$$

[Rate of change kcal/hr] = [Diffusion kcal/hr] +

[Internal Absorption of Solar Radiation kcal/hr] + [Advection kcal/hr]

where:

ρ_i = density of water, kg/m^3
c_p = specific heat of water, kcal/°C - kg
T_i = temperature, °C
V_i = layer volume, m^3
D_i = diffusivity, m^2/hr
A_i = layer area, m^2
ΔZ_i = layer thickness, m
ϕ_i = flux of solar radiation, kcal-m^2/hr
Q_{in} = layer inflow volume, m^3/hr
T_{in} = inflow temperature, °C
Q_p = pumpback volume, m^3/hr
T_p = pumpback temperature, °C
Q_{out} = layer outflow volume, m^3/hr

Solar Radiation

The solar radiation component of the thermal energy equation is one of many heat fluxes forming the heat budget which was calculated from meteorological data. The components of the heat budget include shortwave radiation, longwave radiation, back radiation, evaporative heat loss and the conductive-convective term. Solar radiation was absorbed exponentially with depth while all other fluxes acted only on

the water surface (Ford 1980).

Solar radiation was assumed to be absorbed exponentially with depth within a water column, except in the top meter or so where a certain fraction β, of the solar radiation, Q_{ns}, was assumed to be absorbed in a 0.6 m thick zone (Ford 1980). The remaining light was absorbed exponentially with depth with a light extinction coefficient, η m^{-1}. The equation used in the model to determine flux of radiation with depth was:

$$\phi(Z) = (1 - \beta)Q_{ns}e^{-\eta Z^*} \quad (9)$$

where

β = percent of solar radiation absorbed within 0.6 m of the surface
Q_{ns} = net solar radiation at the water surface, kcal/m^2/sec
$\phi(Z)$ = flux of solar radiation at depth Z, kcal/m^2/sec
Z^* = water depth starting 0.6 m below the surface (i.e., $Z^* = Z - 0.6$ m)

The extinction coefficient, η, was derived from Secchi disc measurements. The Secchi disc was lowered into the water column until it disappeared from view. This depth corresponds to a light intensity which was approximately 10% of surface light (Wetzel 1983). The extinction coefficient was calculated as follows:

$$\eta = (\ln I_s - \ln I_{.10})/z = 2.3/z \quad (10)$$

where:

η = extinction coefficient, m^{-1}
$I_s = (1-\beta)Q_{ns}$, light intensity at the surface, kcal/m^2/sec
$I_{.10} = \phi(Z) = 0.10\ (1-\beta)Q_{ns}$, 10% of surface light intensity, kcal/m^2/sec
z = Secchi disk depth, m

Diffusion

The diffusion term in the mass balance equation accounted for mixing which occured because of concentration gradients. The eddy diffusion coefficient dominated the diffusion terms since non-molecular reactions occured at a much greater scale than molecular reactions. The diffusion modeling approach was used in conjunction with a mixed layer approach where an energy balance was used to determine mixed layer depth. The eddy diffusion coefficient was expressed in m^2/hr, and is based on the assumption that the flux of a concentration is equal to the eddy diffusion coefficient times a concentration gradient analogous to the molecular diffusion (Ford 1980).

Eddy diffusivities in this model simulation were functions of wind speed, stability of thermal stratification, and the size of space and time scales. Wind is a major source of mixing for large lakes with theoretical hydraulic residence times of several months (Ford 1980). When wind blows over a lake, it creates a shear stress along the water surface which creates turbulent kinetic energy (TKE). TKE available to the system from this wind shear was estimated by:

$$TKE_w = \int_{A_s}(CW_*Z\Delta)tdA \qquad (11)$$

where

TKE_w = wind shear turbulent kinetic energy, $kg\text{-}m^2/s^2$
A_s = water surface area, m^2
C = empirical sheltering coefficient
W_* = shear velocity of water, m/s
Z = shear stress at the air-water interface $kg/m^2\ s^2$
Δt = time step, sec

TKE was also produced from the convective cooling which occured as the mean air temperature dropped. The TKE available from convective cooling was:

$$TKE_c = -C_c Q_n A_s Z_{mix} g \alpha \Delta t / C_p \quad (12)$$

where

TKE_c = convective turbulent kinetic energy, kg-m^2/s^2
C_c = empirical convective cooling calibration coefficient
Q_n = heat flux along the air-water interface, kcal/m^2-s
Z_{mix} = depth of mixed region, m
g = acceleration due to gravity, m/s^2
α = coefficient of thermal expansion of water, per °C
c_p = specific heat of water, kcal/kg - °C

When there was a positive heat flux (Q_n) across the air-water interface $TKE_c = 0$.

Total TKE available for entrainment was:

$$TKE = TKE_w + TKE_c \quad (13)$$

This total TKE value was modified by a Richardson number function to account for mixing inefficiencies at the base of the mixed layer.

The depth of the mixed layer where entrainment occured (epilimnion) was dependent upon the total TKE from wind shear and convective mixing and the work (W_L) required to lift a volume of metalimnetic water from the bottom of the mixed region to the center of mass of the mixed region. If TKE was greater than W_L, the depth and volume at the epilimnion were increased. This occurred during the time of the fall turnover when water in the lake became well-mixed throughout the water column. Entrainment continued until TKE was no longer greater than W_L.

Numerical Accuracy

An additional source of mixing occured in the model which was not in the conservation of mass equation. This was numerical diffusion which had to do with

the numerical accuracy of the model scheme. Numerical accuracy could be estimated through an analysis of the truncation error which occured through the transition from an analytical to a numerical solution. The truncation error is in the finite difference equation and could create instability in the equation. The instability could cause a significant error in the solution of the equation. The way to circumvent these stability problems is by using an implicit calculation method which approximates the differential equation at $t + \theta\Delta t$, rather than at time t where $\frac{1}{2} \leq \theta \leq 1$. CE-QUAL-R1 utilizes an implicit method similar to the Crank-Nicholson method.

An example of the transition from differential to finite difference form is shown in the diffusion term of equation 14:

$$\partial/\partial z \, (DA \, \partial C/\partial z) \, \triangle Z \tag{14}$$

In finite difference form this equation is replaced by

$$(AD/\triangle Z)_{i+1} C_{i+1} - [\, (AD/\triangle Z)_{i+1} + (AD/\triangle Z)_i] C_i + (AD/\triangle Z)_i \, C_{i-1} \tag{15}$$

The numerical model utilized an implicit algorithm where the concentrations for the next point in time were expressed directly from present concentrations and their rates of change and implicitly in terms of the concentration and rates of change at the next time level. This implicit formulation incorporated a Thomas algorithm to solve a system of algebraic equations at each time step. The simultaneous equations were set up in a tridiagonal matrix form incorporating equations from each layer and from the boundary conditions (Vreugdenhil 1989). This implicit method was unconditionally stable numerically.

Oxygen

Oxygen is an important element of any aquatic natural system and is a very important indicator of the health of an aquatic ecosystem.

CE-QUAL-R1 includes compartments for calculations of both aerobic and anaerobic processes. If anaerobic processes dominate, the model will continue the simulation through these processes until aerobic processes dominate again. The oxygen calculations provide the user with insights into algal blooms, oxygen depletion rates and zones of oxygen depletion. The model defines zones of depletion in both the hypolimnion and metalimnion. Oxygen is probably the single most important parameter to be field measured because it provides the maximum information about the state of the ecosystem (Ford 1980).

The change in oxygen concentrations over space and time was dependent upon many variables: diffusion, tributary inflow, outflow, algal production, algal respiration, nitrification, detritus decomposition, sediment decomposition, zooplankton respiration, fish respiration, decay of labile DOM, decay of refractory DOM, oxidation of Mn^{+2}, oxidation of Fe^{+2}, oxidation of S^{-2}, macrophyte respiration, macrophyte production and the exchange of oxygen at the air-water interface.

Other Model Components

The structure of the model consists of over 50 subroutines which calculate numerous biological and chemical constituents and parameters. All of the model constituents and their interactions are shown in Figure 10. The CE QUAL-R1

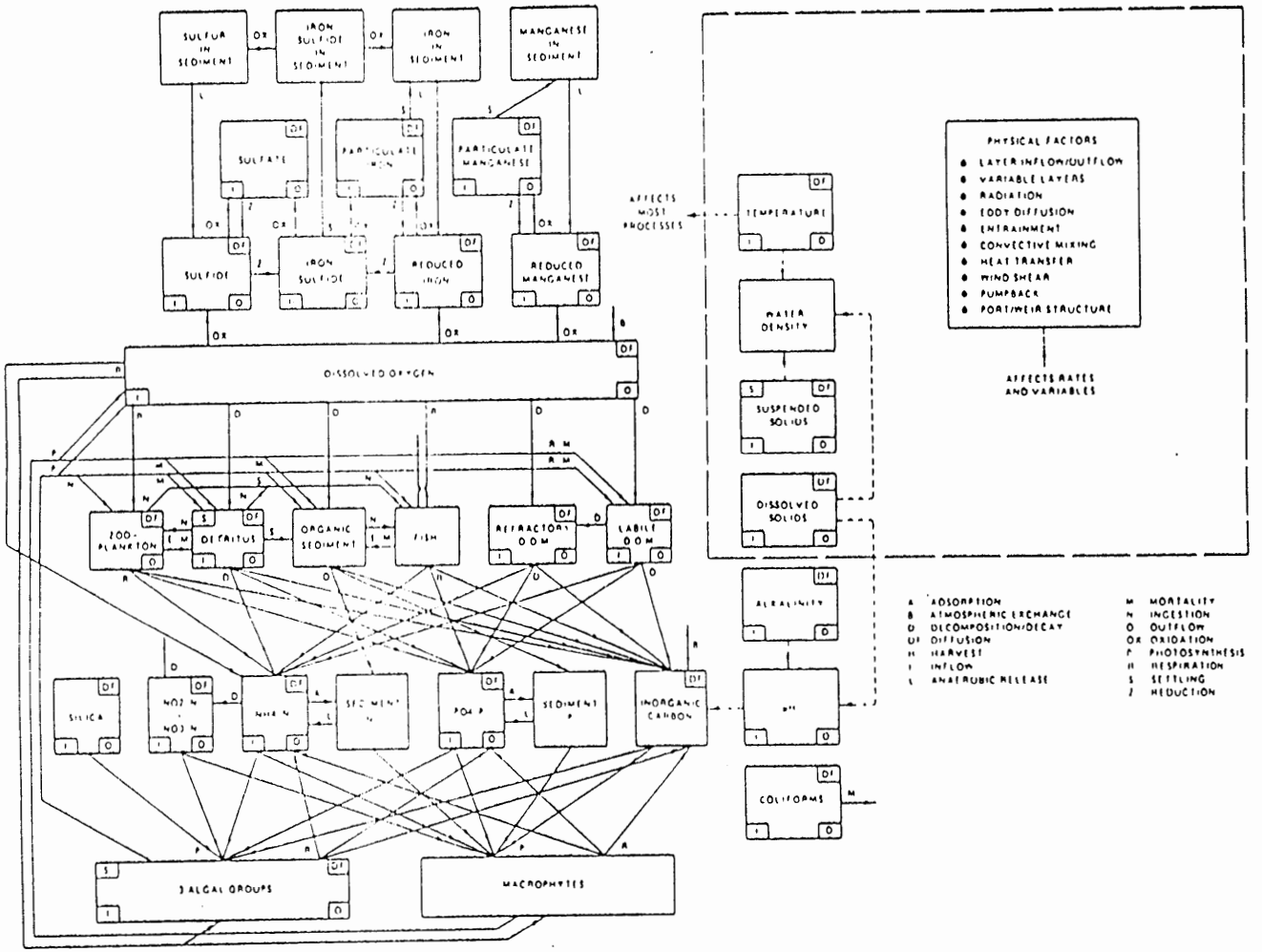

Figure 10. Organization of CE-QUAL-R1. CE-THERM-R1 is represented in the large dashed box on the right. Solid lines represent processes and the transfer of mass. Short dashed lines represent transfer information (Ford et al, 1980).

manual (Ford 1980) provides a detailed description of each of these processes.

MODELING PROCEDURES

Data Set Compilation

Extensive information including initial meteorological conditions, geometric and physical conditions, biological and chemical reaction rates, time sequences of hydrometeorological events and inflowing water concentrations was required to set-up the CE-QUAL-R1 model. An extensive amount of data were required and multidisciplinary effort was required to collect the data, correctly transpose the data into the required input file format, add site specific changes to the computer code and to correctly analyze the computer output results. The user's manual suggests that a specialized group of staff would require several months to create a representative model of a reservoir ecosystem.

Data from Kelly (1991) were used to create the model structure. A thermal model was developed for calculating thermal profiles for 1989 and 1990. However, with no information on inorganic suspended solids, the suspended solids were set to zero in the model and calibration parameters were adjusted to achieve model-data agreement.

The quality model required an array of biological and chemical reaction rates. Most of these rates have not been measured at Coldwater Lake and therefore numerous assumptions had to be made. Valerie Kelly and Dr. Richard Peterson

were consulted about typical magnitudes of the various reaction rates. All of the input parameters, their values and respective sources have been tabulated in Appendix A.

Calibration

Calibration of both CE-THERM-R1 and CE-QUAL-R1 was done by trial and error. The thermal model was calibrated using water temperature data collected in 1989. Once a satisfactory thermal profile was generated, the calibrated model was verified using water temperature data collected in 1990. The spreadsheet shown in Figure 11 was used to keep track of calibration parameter values and how they affected the thermal profile of the lake.

The thermal structure throughout the modeling period from the beginning of stratification in the spring to fall turnover was influenced by the mixing coefficients SHELCF, PEFRAC, CDIFW, and CDIFF. SHELCF, which is a wind sheltering coefficient and PEFRAC, which is a penetrative convection coefficient were used to match the timing and temperature of the onset of stratification, fall turnover and the depth of the epilimnion (Ford 1980). Once SHELCF and PEFRAC were set the eddy diffusion coefficients CDIFW and CDIFF were used to match the slope of the thermocline and temperatures in the hypolimnion.

The internal absorption of solar radiation was governed by EXCO, the extinction coefficient and SURFRAC, the fraction of solar radiation absorbed in the 0.6 m surface layer. Both these coefficients could be estimated from Secchi disk

	MODEL CALIBRATION														
	Calibration Parameters									Effects on Thermal Features of Lake on Julian Day 201					
Calibration Dates	Extinction Coeff. EXCO	Surface Solar Rad Fraction SURFRAC	Dust Attenuation Coefficient TURB	Wind Speed Function Coefficients AA	BB	Wind Sheltering Coefficient SHELCF	Penetrative Convection Fraction PEFRAC	Eddy Diffusion Coefficients CDIFW	CDIFF	Depth of Hypolimnion	Depth of Epilimnion	Gradient of Thermocline	Temperature of Hypolimnion	Temperature of Epilimnion	Timing o Fall Turnove
SAMPLE CALIBRATION															
11/8/92	0.30	0.29	0.06	2.50E-09	1.20E-09	0.90	0.30	0.00	0.00	50	6	54-50	4-6	20.5	10/12/89
		0.50								50	5	55-50	4-6	19.7	10/15/89
			0.30							50	7	53-50	4-6	17.3	10/24/89
	0.35									50	7	53-50	4-6	17.3	10/24/89
	0.40									50	7	53-50	4-6	17.3	10/24/89
	0.45									50	7	53-50	4-6	17.3	10/26/89
				3.50E-09						50	7	53-50	4-6	17.3	10/26/89
				4.18E-09						50	7	53-50	4-6	17.3	10/26/89
					1.51E-09					50	7	53-50	4-6	17.3	10/26/89
11/23/92						0.70				50	7	53-50	4-6	17.3	10/26/89
						0.80				50	7	53-50	4-6	17.3	10/26/89
						0.90				50	7	53-50	4-6	17.3	10/26/89
								1.00E-05		50	7	53-50	4-6	17.3	10/26/89
								1.00E-04		50	7	53-50	4-6	17.3	11/3/89
								5.00E-03		50	7	53-50	4-6	17.1	11/12/89
									1.00E-06	50	7	53-50	4-6	17.1	11/12/89
									1.00E-05	50	7	53-50	4-6	17.1	11/12/89

Figure 11. CE-THERM-R1 calibration spreadsheet

readings and should not have to be changed. Secchi disk depths taken by Kelly (1991) varied from 5 m to 8 m in 1989 and from 7 m to 9 m in 1990. If assumed that the Secchi disk disappeared from view at 10% of surface light intensity, the light extinction coefficient ranged from 0.29 m^{-1} to 0.46 m^{-1} for 1989 and from 0.26 m^{-1} to 0.33 m^{-1} in 1990. The extinction coefficients used in the model simulations were 0.45 m^{-1} for 1989 and 0.37 m^{-1} for 1990.

The water quality model was calibrated using dissolved oxygen concentrations collected in 1989. The data set from CE-THERM-R1 was transferred directly into the CE-QUAL-R1 after it was calibrated to match the thermal profile from collected field data. Many constituents in the quality model are interdependant, so calibration of one constituent changed the values of other constituents. Oxygen concentrations in the epilimnion were calibrated using the algal respiration rate, TPRESP, various rates involved in photosynthesis and the dissolved oxygen molecular diffusion coefficient, DMO2. Oxygen concentrations in the hypolimnion were mainly calibrated with the detritus decay rate, TDETDK and the dissolved organic matter (DOM) decomposition rates, TDOMDK and TRFRDK.

Algal concentrations were mainly calibrated using the primary productivity rate, TPMAX, respiration rate, TPRESP, settling rate, TSETL, and nitrogen and phosphorus half saturation coefficients. Algal concentrations were also dependant upon the light extinction coefficient, EXCO and the zooplankton grazing rate.

Nitrogen and phosphorus concentrations were mainly calibrated with algal nitrogen and phosphorus half saturation coefficients, the ammonia decay rate,

TNH3DK and DOM decay rates.

Zooplankton concentrations were mainly calibrated using the maximum ingestion rate, TZMAX, the assimilation efficiency, ZEFFIC, a feeding preference factor, PREF 1-4 and the zooplankton respiration rate, TZRESP. Their concentrations were also highly dependant upon the phytoplankton concentrations.

During the calibration of the water quality model spreadsheets similar to Figure 11 were used to keep track of how calibration parameters affected various water quality compartments.

RESULTS

LIGHT AND TEMPERATURE

Solar Radiation

The amount of energy Coldwater Lake received from solar radiation was a function of the angle of the sun, cloudiness of the sky, scattering and absorption of light by atmospheric dust and the relative earth-sun distance. These factors were predominantly controlled by latitude and season.

The energy input from solar radiation at Coldwater Lake changed as the angle of the sun changed throughout the season. The time of day also had a profound effect on the solar flux which reached the lake surface. The time of maximum solar radiation throughout the day was at the noon hour, when the sun reaches its maximum solar altitude (Ford 1980). The model output listed the maximum shortwave radiation (solar radiation) in units of $kcal/m^2/h$. The amount of shortwave radiation impinging on a lake surface strongly influenced the productivity of a lake ecosystem (Wetzel 1983). The model was run, setting the cloud cover to 0.0 throughout the modeling duration to determine the daily maximum shortwave radiation received on cloudless days that was available for primary productivity. (Figure 12) shows the maximum shortwave radiation at wavelengths of 700 nm and 350 nm as a function of the time of year.

Julian Day	350 nm S/W Rad (me/m²/s)	700 nm S/W Rad (me/m²/s)
19	256	512
49	391	781
67	506	1013
79	586	1172
88	647	1295
109	783	1566
117	826	1652
139	924	1848
143	937	1873
158	972	1943
168	981	1962
175	981	1962
182	976	1952
201	937	1873
205	924	1848
227	826	1652
235	783	1566
256	647	1295
265	586	1172
277	506	1013
295	391	781
325	256	512

me=microeinsteins

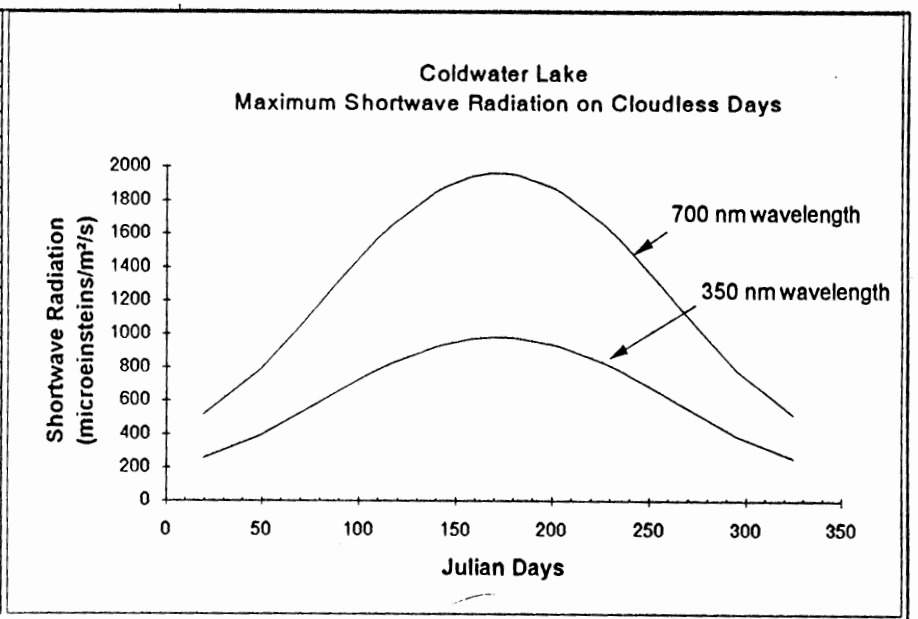

Figure 12. Coldwater Lake - maximum shortwave radiation on cloudless days at solar noon.

These results were presented in units of microeinsteins/m^2/s to correspond with units frequently used by limnologists in primary productivity calculations. The wavelengths spanned the photosynthetically available radiation (PAR) portion of the solar spectrum (Wetzel 1983).

In contrast to Figure 12, which shows the maximum shortwave radiation, Figure 13 shows the daily average solar radiation available to Coldwater Lake as a function of the time of year.

Photosynthetic efficiencies of light utilization can be determined for a lake ecosystem if the amount of photosynthetically stored energy (PSR) in a volume of water can be determined. An approximate conversion of assimilated carbon to energy equivalents is 1 mg carbon assimilated = 9.33 cal, assuming all photosynthesate is glucose (Wetzel 1983). The photosynthetic efficiency (ϵ) was calculated by dividing PSR in a volume in m^3 of water between two depths, z and z_2, by the PAR absorbed or dissipated in the water layer between $z_1$and z_2 (Wetzel 1983).

$$\epsilon = \frac{PSR}{PAR_{z_1} - PAR_{z_2}} \times 100[\%]$$

CE-QUAL-R1 gives an output value of carbon in the euphotic zone in g/m^3 as a measure of primary productivity. Therefore, the model output can be used to determine the photosynthetic efficiency of shortwave radiation utilization. For example; the 1989 model simulation estimated 0.01 g/m^3 of carbon in the euphotic zone on September 13, 1989. This corresponds to a photosynthetic efficiency of 0.09 % in the euphotic zone.

Julian Day	350 nm S/W Rad (me/m2/hr)	700 nm S/W Rad (me/m2/hr)
19	107	213
49	182	363
67	243	485
79	286	573
88	320	639
109	394	787
117	419	838
139	475	951
143	483	966
158	504	1008
168	510	1020
175	511	1022
182	508	1017
201	486	973
205	479	958
227	424	849
235	400	799
256	326	653
265	293	586
277	249	498
295	187	375
325	110	220

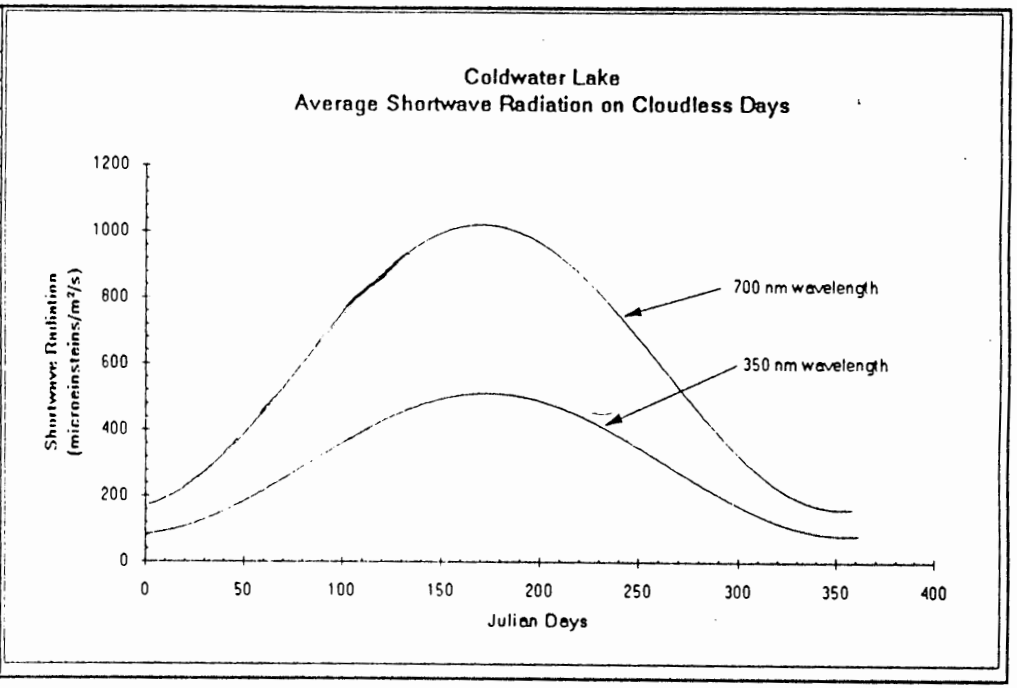

Figure 13. Coldwater Lake - daily average radiation on cloudless days.

This calculation for photosynthetic efficiency of shortwave radiation utilization was a gross approximation due to the lack of actual water quality data for input to the model.

Cloudiness of the sky also effects the amount of solar radiation available to a lake ecosystem. The atmospheric transmission of solar radiation is affected by scattering and absorption from cloud cover. The relationship between cloud cover and solar radiation available at the lake surface is shown in Figure 14. The scattering and absorption of light by atmospheric dust is adjusted in the model with the dust attenuation coefficient (TURB). A value of 0.4 was used to calibrate the model. This is an order of magnitude higher than the mean value of 0.06 which has been used in other studies (Ford et al 1980). The users manual recommends increasing TURB when there is too much heat in the lake throughout the entire simulation. This was the case, so TURB was increased to bring epilimnion temperatures in line with field measured values.

The relationship between TURB and the amount of solar radiaiton impinging upon the lake surface (Q_{ns}) on Julian day 182, assuming a cloud cover of 0.3 is shown in Figure 15. The relationship between cloud cover and Q_{ns}on Julian day 182 assuming TURB is equal to 0.4 is also shown in Figure 15. The slope of the Q_{ns} vs. cloud cover relationship increased with greater cloud cover in contrast to the linear relationship between TURB and Q_{ns}. This indicates that the model is more sensitive to variability in cloud cover measurements than in estimations of TURB.

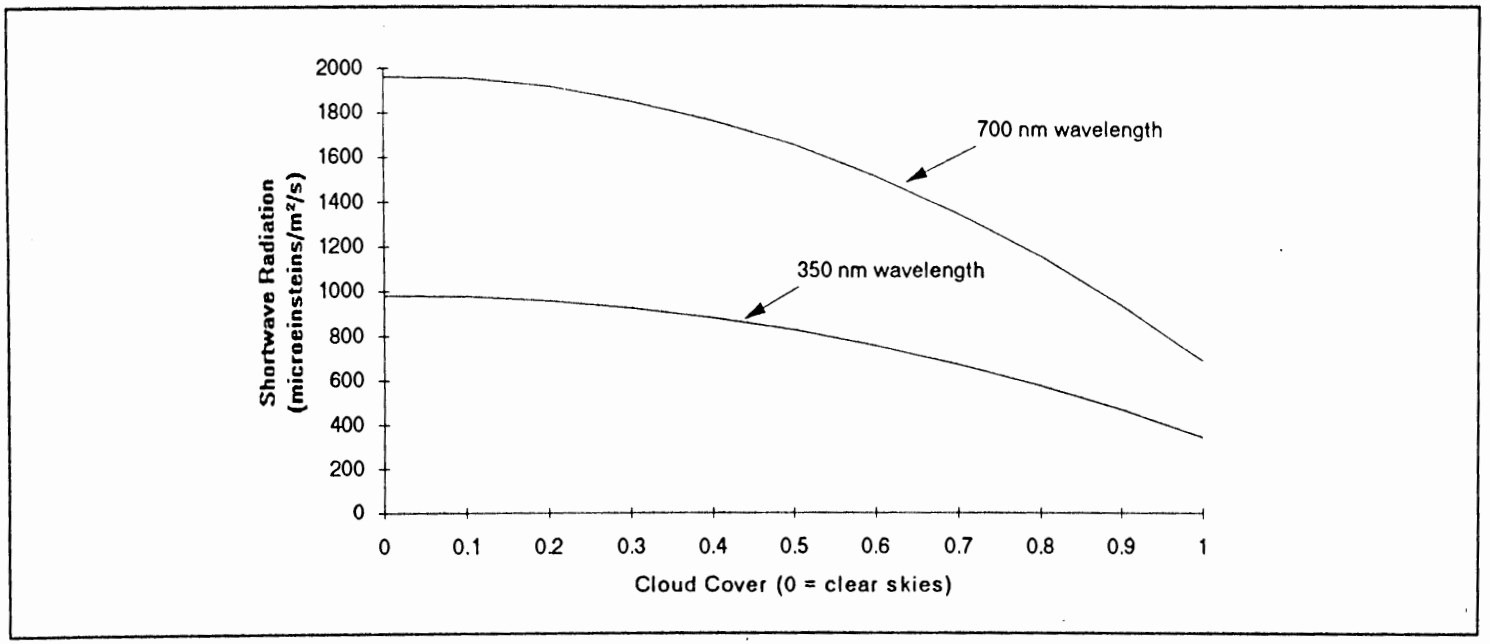

Figure 14. Cloud cover vs shortwave radiation at Coldwater Lake.

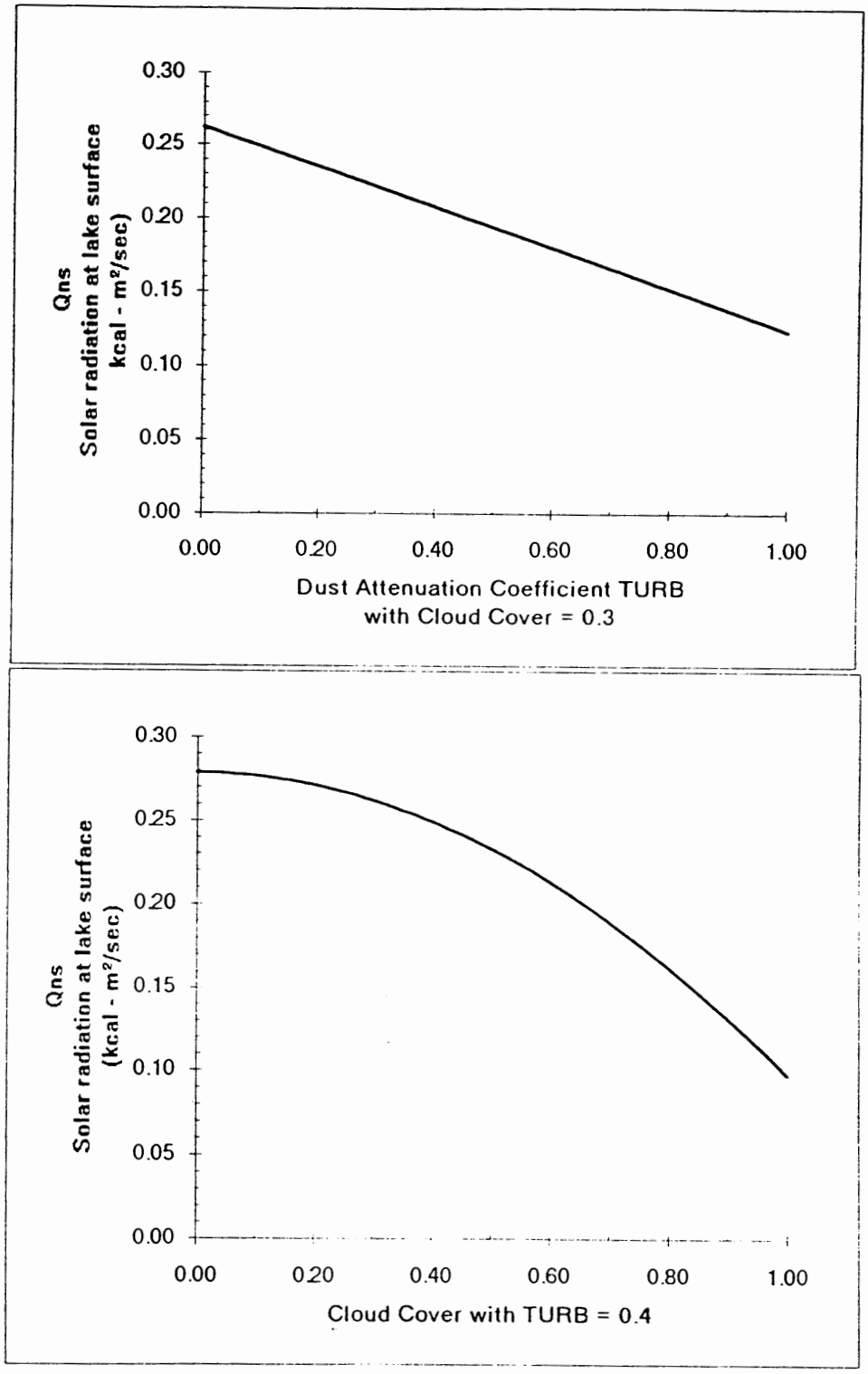

Figure 15. Model simulated relationship between solar radiation at the lake surface (Q_{ns}) vs. cloud cover and the dust attenuation coefficient, TURB on Julian day 182.

Poor availability of reliable cloud cover at Coldwater Lake is a source of error in the model simulations.

Thermal Stratification

Water temperature data for Coldwater Lake were collected nine times in 1989 and eight times in 1990. Data from 1989 were used to calibrate the thermal model (CE-THERM-R1) and data from 1990 were used to verify the modeled parameters developed in 1989.

A comparison of model results to field data as a function of depth are shown in Figure 16. The model effectively simulated the temperature of the epilimnion, temperature of the hypolimnion, depth of the epilimnion and the gradient of the thermocline. Field data were not available past October 4th, and fall turnover had not occurred by this time.

The stability of a lakes thermal structure, which determines how quickly fall turnover will occur, is controlled predominately by its size and morphometry. Coldwater Lake does not have a large surface area but is quite deep. Coldwater Lake has a volume of nearly $6.9 \times 10^7 m^3$, of which nearly $2.0 \times 10^7 m^3$ is in the warmer, epilimnion on October 4th.

The TKE generated by wind works at mixing the epilimnetic waters and hypolimnetic waters throughout the year. As air temperatures begin cooling the epilimnetic waters in the fall, the thermal barrier at the thermocline is broken down, and waters are allowed to mix to a greater depth.

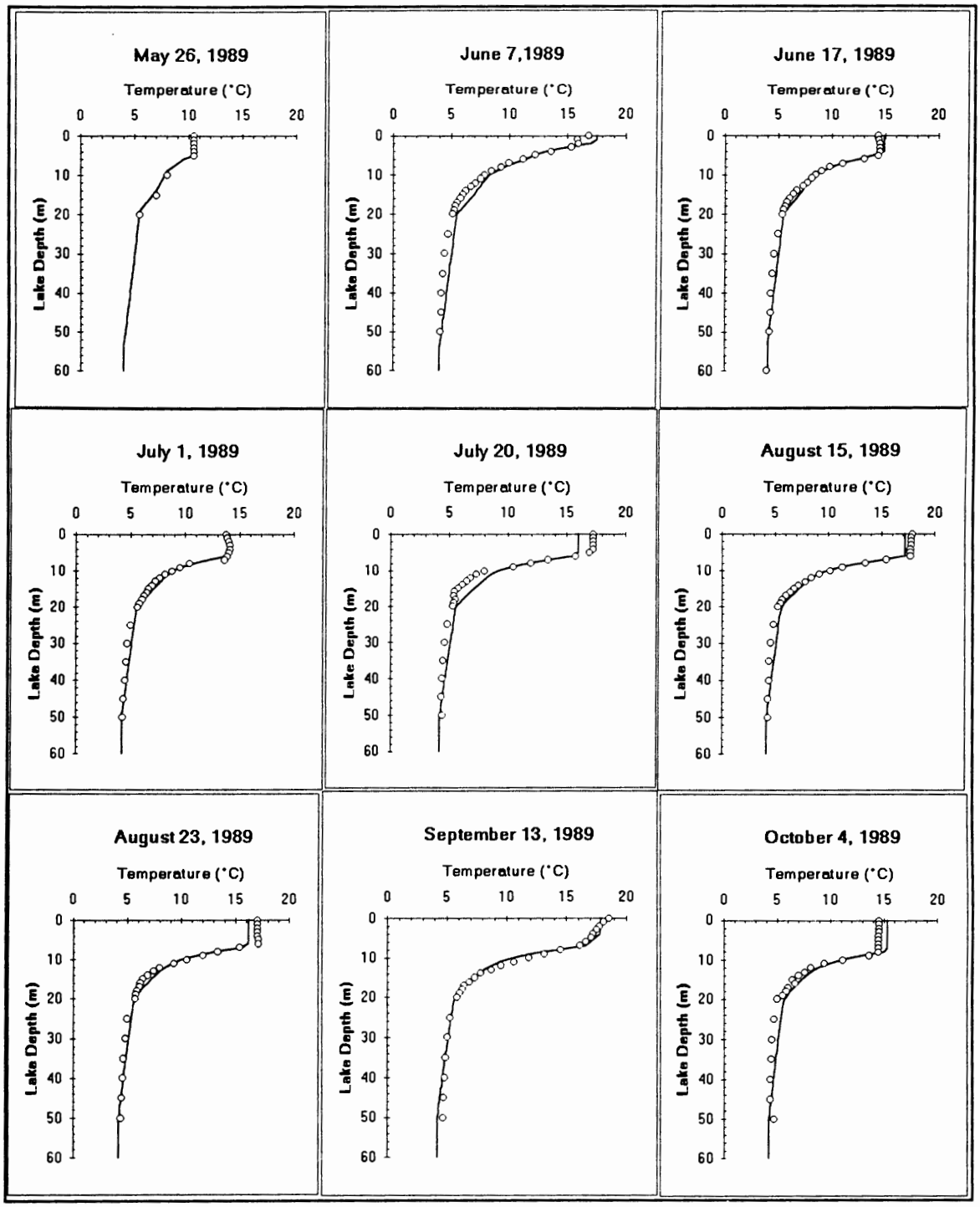

Figure 16. Temperatures as a function of depth simulation results using the calibrated thermal model CE-THERM-R1 for Coldwater Lake. Model simulation is shown as a continuous line and measured data as circles.

The model was run for two more simulation periods to determine when fall turnover occurred. Figure 17 shows that fall turnover was nearly complete by November 21, 1989.

Coldwater Lake had already become stratified by the first sampling period on May 26. The model and the field data both followed a rather typical stratification process for northern temperate lakes. The cycle of stratification followed expected trends of steady increase in the depth of the epilimnion and warming of hypolimnetic waters (Rice 1987). Deviations between model output and field measured data profiles included minor temperature differences in the epilimnion (Figure 16) from mid July throughout August. The model predicted slightly lower temperatures throughout this period.

Model Verification

Field data collected in 1990 were used to verify the model parameters used during the 1989 calibration. A comparison of model predictions to field data are shown in Figure 18.

Model prediction of the depth of the epilimnion, the gradient of the thermocline, and the temperature of the hypolimnion agreed well with field data. The temperature of the epilimnion and metalimnion, however, tended to be under estimated. This under estimation indicated there was not enough heat absorbed within the lake during the simulation period.

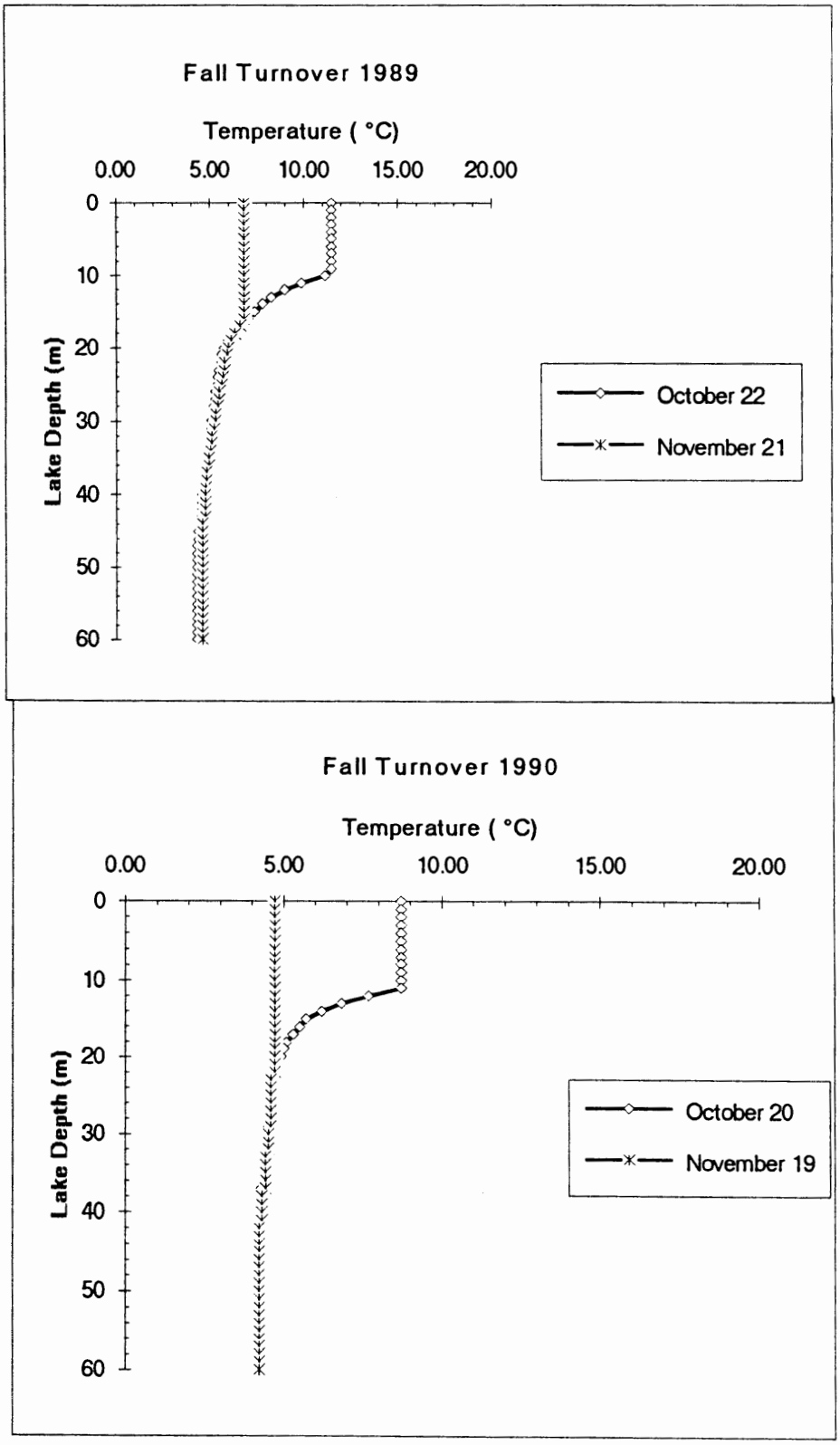

Figure17. Model simulated timing of fall turnover in Coldwater Lake for 1989 and 1990.

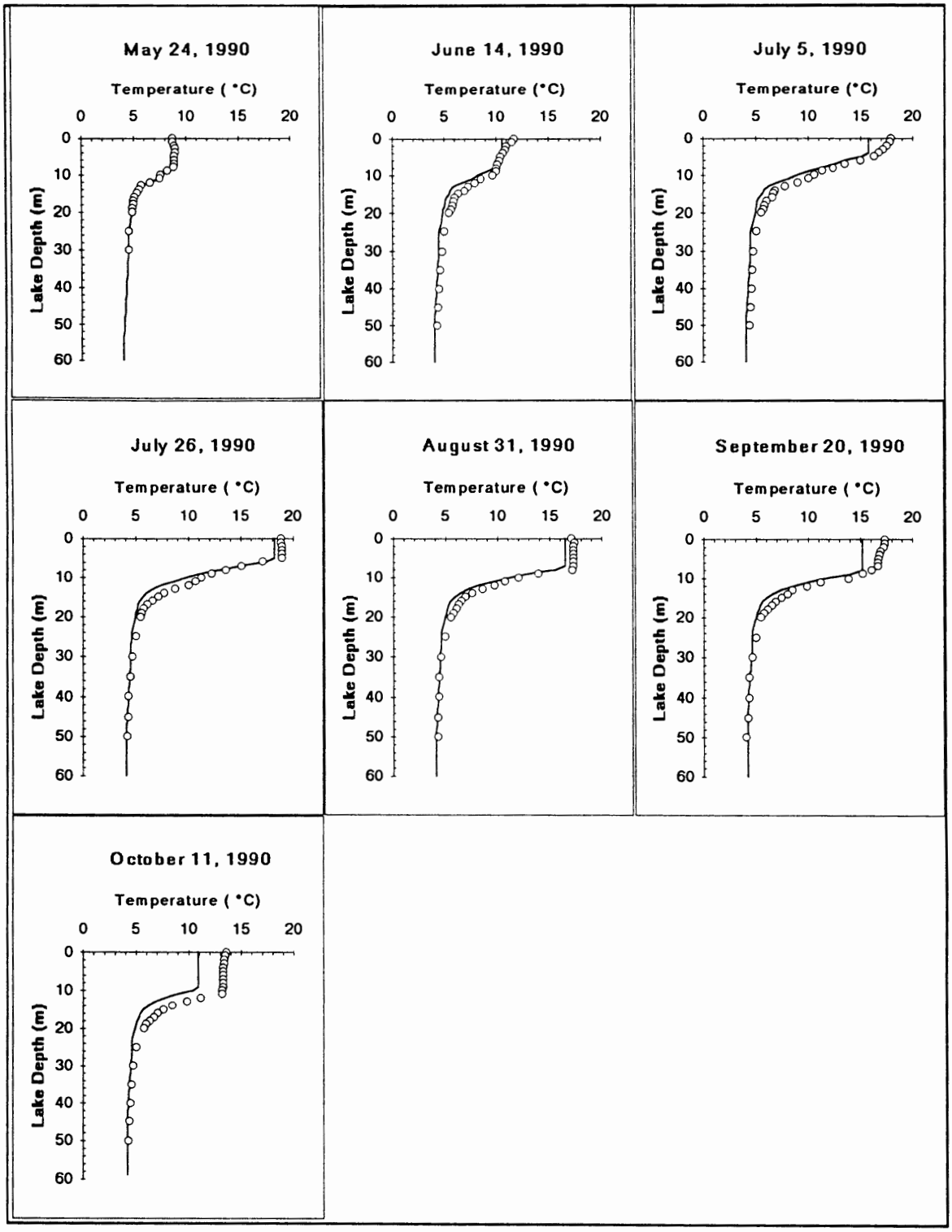

Figure 18. Temperature as a function of depth for 1990 verification using the calibrated thermal model CE-THERM-R1 for Coldwater Lake. Model simulation is shown as a continuous line and measured data as circles.

Temperature variations occur on an hourly as well as a seasonal time scale. Field data collected by Kelly (1991) were typically collected in early afternoon. Epilimnetic temperatures have been shown to vary 2°C - 3°C in temperate lakes with early afternoon temperatures the highest of the day (Fischer 1979). Since a daily computational interval was used, it was impossible to predict diurnal changes in temperature in Coldwater Lake.

Comparison of model prediction of the epilimnetic temperatures and slope of the thermocline with field values were consistently low throughout most of the simulation. The calibrated model parameters were fine tuned in an attempt to locate the reason for low temperature model prediction. The value for the dust attenuation coefficient was reduced to allow a greater amount of solar radiation to impinge upon the lake surface. This brought epilimnetic temperatures up but also increased the slope of the thermocline. The meteorological variables which affected the heat balance were re-calulated. Seven day moving averages of dry bulb temperature, wind speed and cloud cover were plotted in Figure 19 to determine similarities in meteorological conditions for 1989 and 1990.

Meteorological data were taken from three different locations during the 1989 and 1990 simulations. Different station locations were used because no one location had complete data throughout the simulation periods. Two of the stations were near Coldwater Lake and their locations are shown in Figure 2. Station CSLW was at a similar elevation as Coldwater Lake but was across the Toutle River Valley. Station

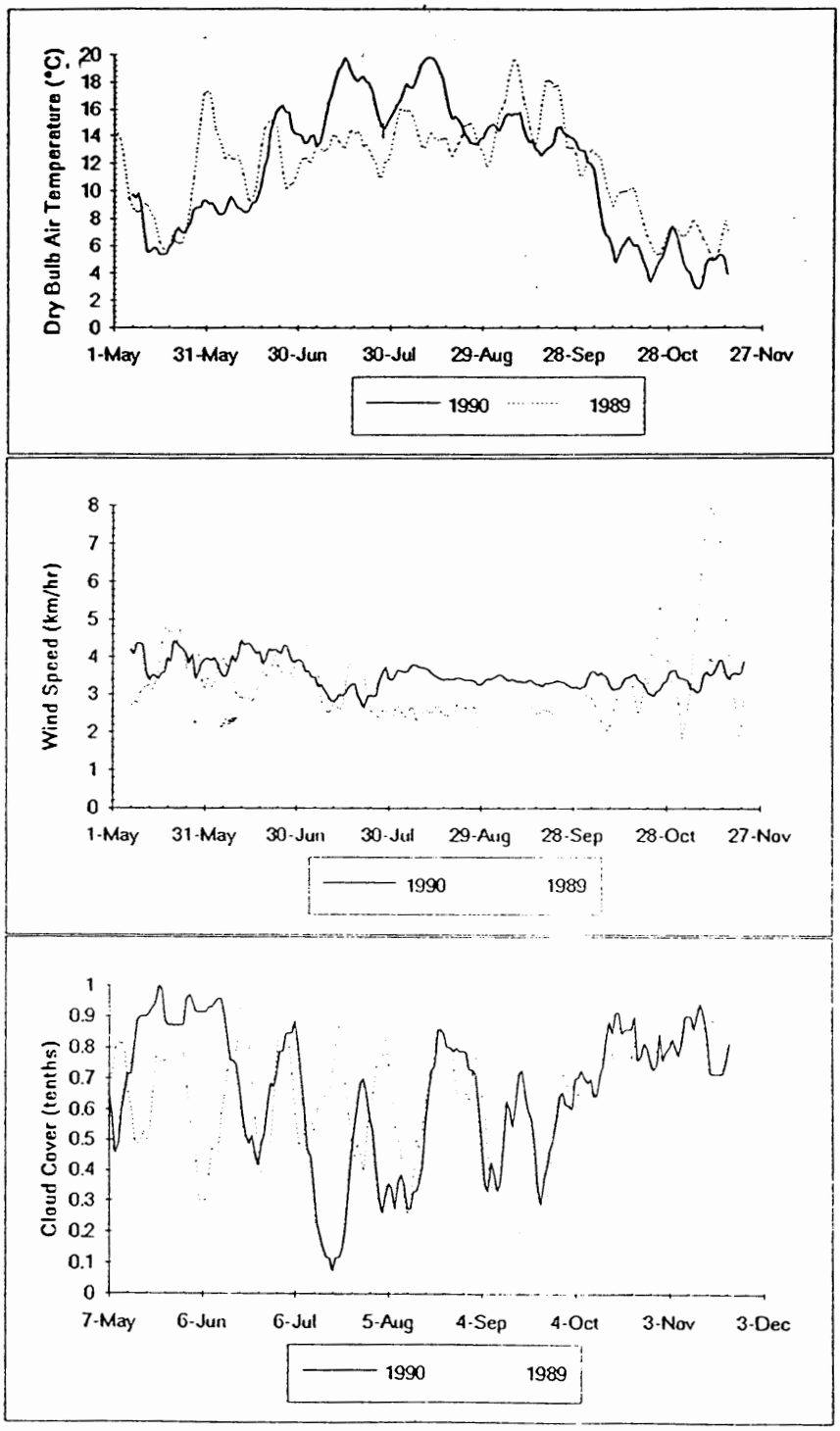

Figure 19. Seven day moving averages of meteorological conditions for 1989 and 1990. Dry bulb temperatures and wind speed were taken at station SLZW and CSLW. Cloud cover was taken at Portland International Airport.

SLZW was on a ridge north of the lake and is at an elevation approximately 250 m higher than Coldwater Lake. Therefore meteorological conditions did not exactly represent those at the lake and this may have been a source of error in the thermal predicitons.

The third meteorological station used was at the Portland International Airport, 50 kms south of the lake and at an elevation 750 m below Coldwater Lake. Cloud cover data were taken from this station. Cloud cover values were determined by human observation and were often difficult to obtain in remote areas such as Coldwater Lake.

Cloud cover throughout September 1990 was much greater than cloud cover during that same period in 1989. This was the same period in which the temperatures in the epilimnion and metalimnion were underpredicted. By using the dust attenuation coefficient as a calibrating parameter, the atmospheric transmission of solar radiation was reduced and this reduction was compounded by a greater amount of cloud cover. This compounded the absorption and scattering of shortwave solar radiation and appears to be the cause of the lack of heat in the epilimnion and metalimnion during September and the beginning of October 1990 (Figure 15).

Other significant meteorological occurences where field data were matched with model simulations are:

- Air temperature rose significantly in 1989 during the first week of June. This led to high epilimnetic temperatures during that period. Epilimnetic

temperatures dropped in the next thermal profile (Figure 16-June 17) which closely followed the drop in air temperature (Figure 19).

- Wind speeds from August through September 1990 were approximately 25% greater than wind speeds for that same period in 1989 (Figure 19). This led to a greater amount of TKE imparted upon the lake surface which caused a breakdown of the thermal stratification and a quicker fall turnover (Figure 17).

Morphometry

Simulations using a power function and a second degree polynomial function to represent the morphometry (the area as a function of lake depth) of Coldwater Lake were compared with the calibrated model which used a third degree polynomial to represent morphometry (Figure 20). All three simulations produced comparable results for the temperature of the epilimnion and hypolimnion, gradient of the thermocline and movement towards fall turnover. The second and third degree polynomial functions estimated the area of the lake at the water surface at 2.9×10^6 m^2 and 3.2×10^6 m^2, respectively. These both closely match the surface area of 3.4×10^6 m^2 calculated by the SURFER program from digitized field values and the area of 3.1×10^6 m^2 calculated by Kelly (1991). The power function underestimates the lake surface area by 1.0×10^6 m^2, but this seems to have little effect upon temperature calculations in the model. However, the power functions estimation of total lake volume of 6.6×10^7 m^3 was closely matched with the second and third degree polynomial volumes of 6.9×10^7 m^3 and 6.8×10^7 m^3. Therefore, the lake

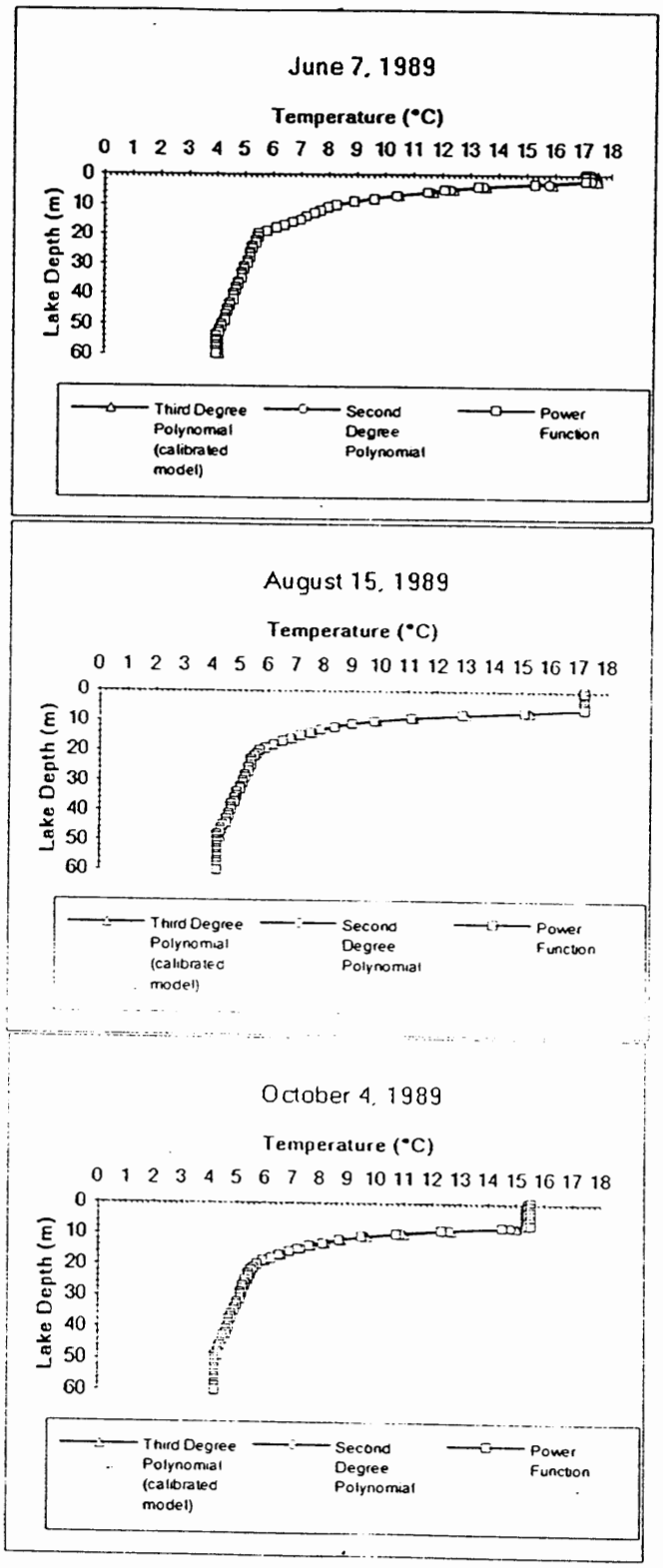

Figure 20. Temperature as a function of depth results for Coldwater Lake, 1989 using three different methods of determining layer surface area.

volume and volume at certain layers within the lake must have more influence on the temperature calculations than do the layer areas.

Rice (1987) found layer area to be of vital importance when modeling shallow (< 15 m) transparent Wood's Lake in the Adirondack mountains. The modeling of temperature in Coldwater Lake showed little effect to different methods of estimating layer area.

MIXING

Mixed Layer

The depth of the mixed layer (epilimnion) in Coldwater Lake during the 1989 and 1990 simulation periods varied from 3 m to 5 m in early summer and 10 m to 11 m at the end of the summer according to Kelly (1991). These depths were closely correlated in the modeling effort for both 1989 and 1990 with a closer correlation occurring in the 1989 calibration year (Figures 16 and 18). Mixing in the upper mixed layer was determined by the amount of turbulent kinetic energy (TKE) imparted upon the layer in the form of wind working on the surface of the layer and convective cooling within the layer. The degree of mixing in the upper mixed layer and throughout the water column was represented in the model output by an eddy diffusion coefficient. Daily values for the eddy diffusion coefficient in the upper mixed layer varied from 0.2 to 20 m^2/h. The value of these coefficients were directly related to wind speed (Figure 21).

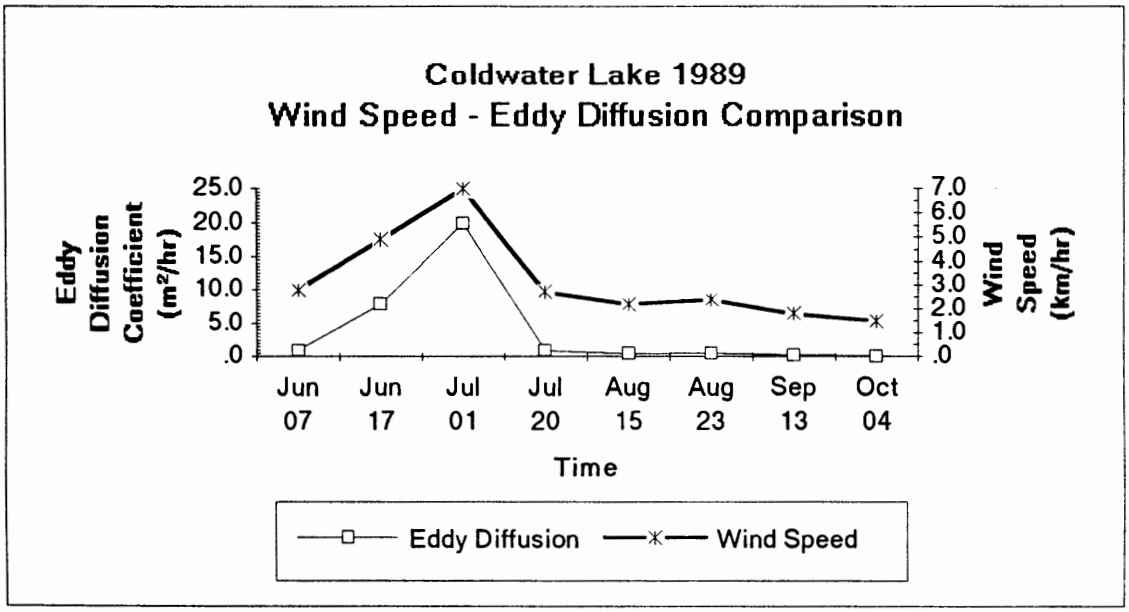

Figure 21. Eddy diffusion coefficients calculated by the model in the upper mixed layer vs. wind speed at Coldwater Lake, 1989.

Eddy diffusion coefficient values from the model represented conditions after a full day of mixing because of the daily model time step. The behavior of the diurnal mixed layer can typically be subdivided into 3 events throughout the day. There is the morning heating period when the upper water column is heated and stabilized. Next, there is the period during the early afternoon when the wind begins and the layer is deepened by a combination of surface induced turbulence, internal shear, penetrative convection and upwelling. Third, there is a period of pure penetrative cooling at night causing a net heat loss from the surface (Imberger 1985).

Wind stress across a lake introduces a shear along the base of the mixed layer. This shear force generates turbulence and enhances the ability of the wind to deepen the mixed layer (Imberger 1985). The model uses a Richardson number

function f(Ri) to evaluate the amount of turbulence at the base of the mixed layer. If Ri > 0.25, the thermocline remains a slippery surface with little mixing across it. If the shear at the thermocline increases, (Ri < 0.25) greater mixing occurs and the depth of the mixed layer increases (Wetzel 1983).

It was noted during field trips when the wind was blowing briskly that streaks occurred on the surface of the water which were parallel to the direction of the wind. These were indicators that Langmuir circulation was occurring. Langmuir demonstrated that turbulent transport under certain conditions was organized into vertical helical currents in the mixed layer (Wetzel 1983). The zones between the streaks are zones of upwelling. Langmuir circulation can occur in any lake of significant size when wind speeds reach 2-3 m/sec (Wetzel 1983). This circulation was a product of both wind speed and wave action and was one of the primary ways in which the mixed layer deepens.

Thermocline and Hypolimnion

Mixing in the thermocline and hypolimnion did not occur at the same scale as mixing in the upper mixed layer. The Coldwater Lake eddy diffusion coefficient values for the thermocline and hypolimnium were between one and five orders of magnitude less than values in the upper mixed zone (Figure 22). The water column from the base of the mixed layer to the bottom of the lake was effectively blocked from the mixing effects from surface wind shear during periods of stratification because of the stabilizing effects of density. gradients within the thermocline

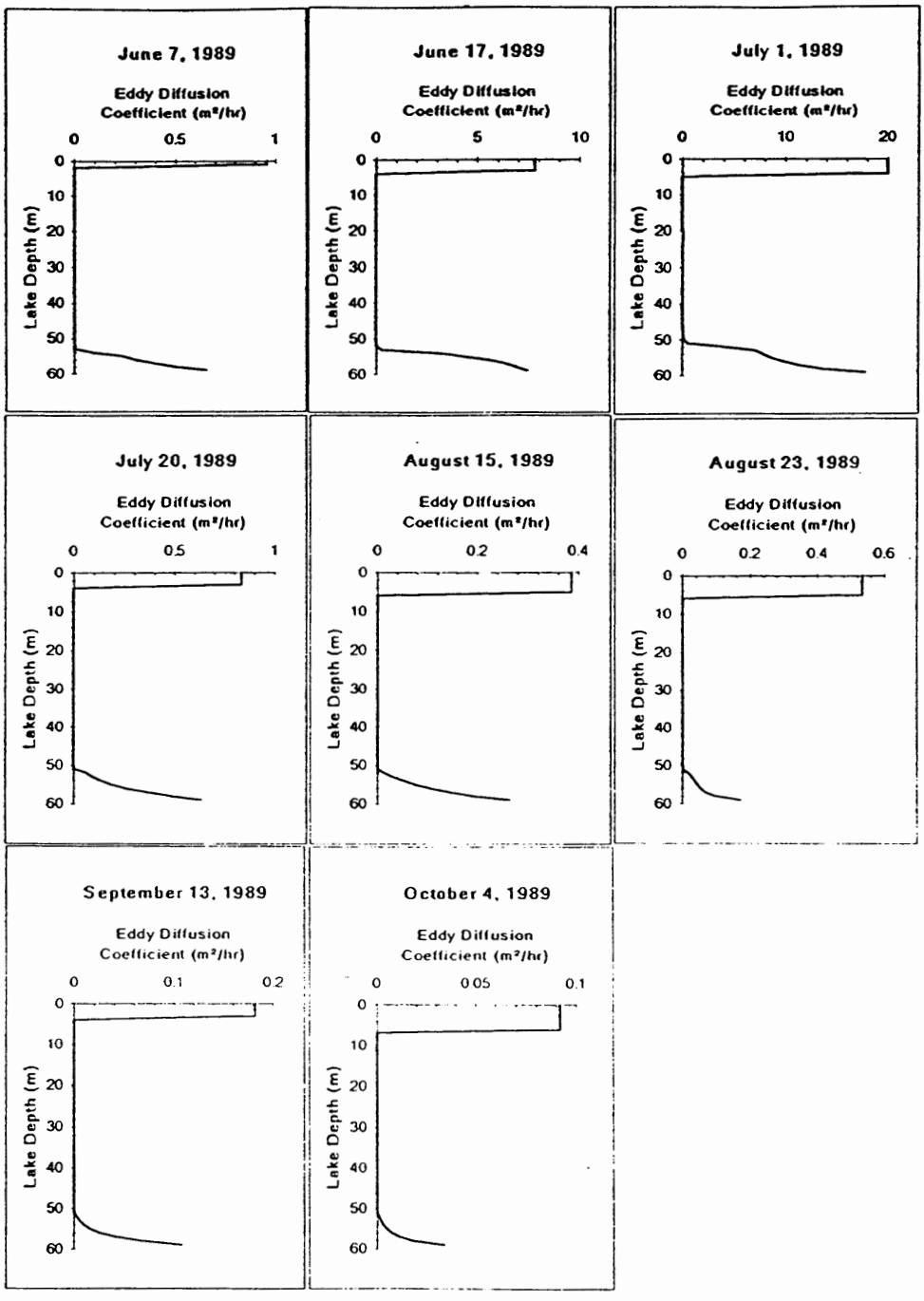

Figure 22. Model prediction of eddy diffusion coefficients in Coldwater Lake over the 1989 modeling period. (Note model predictions of eddy diffusion coefficients from 5 m to 50 m are shown in Table III.).

(Ford 1983). However, some mixing still occurred in these layers.

The vertical coefficient of eddy diffusivity was the dominant mixing mechanism in thehypolimnion. The mixing that took place was on a molecular scale with isolated periods of increased mixing which was derived from internal waves and from the potential energy of inflows (Imberger 1978). The eddy diffusion coefficient in CE-THERM-R1 was influenced by the calibration coefficients CIDFW and CDIFF. If the calculated vertical eddy diffusion coefficient, DC(I) (M^2/hr) was less than the molecular diffusion coefficient for temperature, it was set to the molecular diffusion coefficient, 5.148 x 10^{-4} m^2/hr. The maximum diffusion coefficient allowed is 20 m^2/hr which is similar to a value of 7 cm^2/s (19.44 m^2/hr) stated by Sweers (1970) for the upper mixed layer.

Eddy diffusion coefficient values from the model predictions and from field data are shown in Table III at depths of 10 m, 30 m and 50 m. The equation used to calculate field values for the vertical eddy coefficient in the hypolimnion assuming no inflows, no outflows, and no vertical transmission of light was:

$$Ez_{(i,n)} = \frac{\dfrac{T_i^{n+1} - T_i^n}{\Delta t}}{\dfrac{1}{\Delta z A_i}\left[A_{i+1/2}\dfrac{T_{i+1}^{n+1/2} - T_i^{n+1/2}}{\Delta z} - A_{i-1/2}\dfrac{T_i^{n+1/2} - T_{i-1}^{n+1/2}}{\Delta z}\right]} \qquad (16)$$

where:

T_i^{n+1} = temperature at layer i at time step n+1, °C
T_i^n = temperature at layer i at time step n, °C
T_{i+1}^n = temperature at layer i + 1 at time step n, °C
T_{i-1}^n = temperature at layer i at time step n, °C
A_i = area at layer i, m^2

$A_{i+1/2}$ = area at layer i + 1/2, m^2
$A_{i-1/2}$ = area at layer i - 1/2, m^2
Δz = layer thickness, m
Δt = time between field data, hr

Table III indicates that during much of the model simulation the mixing which took place in the hypolimnion and thermocline varied between molecular diffusion and the maximum allowed value of 20.0 m^2/hr. Minimum eddy diffusion coefficients were near the minimum value allowed by the model of 5 x 10^{-4} m^2/hr.

TABLE III

EDDY DIFFUSION COEFFICIENTS BELOW THE MIXED LAYER IN COLDWATER LAKE, 1989

Eddy Diffusion Coefficients (Ez) below the Mixed layer in Coldwater Lake (1989)			
Date	Lake Depth (m)	Field Ez (m^2/hr)	Model Ez (m^2/hr)
June 7	10	0.0377	0.0048
	30	0.1873	0.0139
	50	0.0513	2.6910
June 17	10	0.0304	0.1322
	30	0.0234	0.4438
	50	0.0518	20.0000
July 1	10	0.0487	1.1751
	30	0.0649	1.6653
	50	0.4122	6.6929
July 20	10	0.1176	0.0047
	30	0.0128	0.0024
	50	0.0086	20.0000
August 15	10	0.0273	0.0060
	30	0.1465	0.0070
	50	0.0060	1.2076
August 23	10	0.1385	0.0010
	30	0.0964	0.0011
	50	0.0408	0.0460
September 13	10	0.1871	0.0050
	30	0.3270	0.0050
	50	0.0013	1.0503

The calculated values from field data were near values predicted by the model

simulation. The field values compared more closely to literature values than did the model values. Wetzel (1983) reported eddy diffusion coefficient values of 2-6 cm^2/s x 10^{-2} (.007 - 0.02 m^2/hr) in Castle Lake in Northern California and Sweers (1970) reported a value of 0.15 cm^2/s (0.054 m^2/hr) as a typical value from dye experiments. An explanation for under prediction of the models eddy diffusion coefficients was the absence of the turbulence caused by plunging inflow since the model set up assumed there were no inflows. Internal waves caused by inflows which plunged to a lake depth of similar density are very influential in the transfer of heat and other properties through the metalimnion (Wetzel 1983).

McCormick and Scavia (1981) in studying mixing in Lake Washington found that by not limiting flux across the thermocline their modeling results matched temperatures in the hypolimnion more closely than if flux was limited at the thermocline. This suggests there are mixing mechanisms present in the hypolimnion other than surface induced mixing. In lakes with shallow thermoclines like Lake Washington and Coldwater Lake, mixing which results from bottom friction can play a significant part in the transport of heat (McCormick and Scavia 1981). The large eddy diffusion coefficients, predicted by the model simulation near the bottom of the hypolimnion in Coldwater Lake are similar to those found in Lake Washington.

Vertical diffusivities of heat in the hypolimnion range from molecular diffusion up to 0.36 m^2/hr (Fischer 1979). Though the hypolimnion is typically very stable, vigorous mixing could occur. This vigorous mixing could be the product of random external inputs, such as a plunging inflow intrusion into the stable hypolimnetic

waters or mixing due to seiche motion and internal waves.

The model simulation ignored lake inflows and outflows. Therefore, vigorous mixing near the lake bottom as shown in Figure 22 was caused by internal waves created by TKE imparted upon the lake surface by wind. TKE from wind is available for mixing the entire lake volume as shown by the equation:

$$DISW = TKE_w/\rho wV\Delta t \qquad (17)$$

where:

DISW = dissipation due to wind per unit mass, 1/kg
TKE_w = wind shear turbulent kinetic energy, kg - m^2/sec^2
ρw = density of water, kg/m^3
Δt = time step, hours

Internal wave energy mixed the lower hypolimnetic layers easier than upper hypolimnetic layers because water densities in the lower layers varied less between layer than in the upper layers. This led to the calculation of a small Richardson Number (typically $Ri < 0.25$) which corresponded to a region of rapid mixing. The relationship between the Richardson Number and the magnitude of the eddy diffusion coefficient is shown in equation 18:

$$DC(I) = \Delta t^2\left(\left[\frac{CDIFWxDISW}{1+Ri}\right] + \left[\frac{CDIFFx(DISF(I)+DISF(I+1))/2}{1+\left(\frac{1}{Fr}\right)^2}\right]\right) \qquad (18)$$

where:

DC(I) = vertical eddy diffusion coefficient, m^2/hr
Ri = Richardson Number
Fr = densimetric Froude number
CDIFW = eddy diffusion calibration coefficient for TKE_w

CDIFF = eddy diffusion calibration coefficient for inflows and outflows
DISF = dissipation due to inflows and outflows per unit mass, 1/kg

There is an inverse relationship between Ri and DC(I) which indicates greater mixing (a larger eddy diffusion coefficient, DC(I)) when there is a smaller Richardson Number, Ri.

DISSOLVED OXYGEN

Dissolved oxygen is one of the most important constituents within a lake and its measurement is often used when investigating aquatic environments. It provides important information about many of the biological and biochemical reactions which take place within a lake system.

CE-QUAL-R1 includes compartments for both aerobic and anaerobic constituents. Figure 23 shows the various compartmental fluxes interacting with oxygen.

The Coldwater Lake water quality model simulation was calibrated with 1989 dissolved oxygen (D.O.) data collected by Kelly (1991). Figure 24 shows a comparison between model predicted D.O.concentrations and field values. D.O. concentrations agreed well with field values near the beginning of the simulation (June 7). However, as the lake continued its summer stratification, the model did not correctly simulate the oxygen deficit in the epilimnion. D.O. field data were near 100 percent saturation in the epilimnion on June 7. A decline to 85% - 90% D.O. saturation occurred in the epilimnion over the remaining period of the simulation.

The model predicted that D.O. saturation levels in the epilimnion during the simulation period remained between the 95% and 100% saturation level. D.O. concentrations vary on an hourly as well as a seasonal time scale. Field data collected by Kelly (1991) were typically collected in late morning. Studies indicated that D.O. in the epilimnion in a stratified lake was at the lowest daily concentration during early morning darkness and increased until late afternoon (Wetzel 1983). The model simulation of D.O. in Coldwater Lake, which assumed a 24 hour time step, predicted the daily average D.O. concentration.

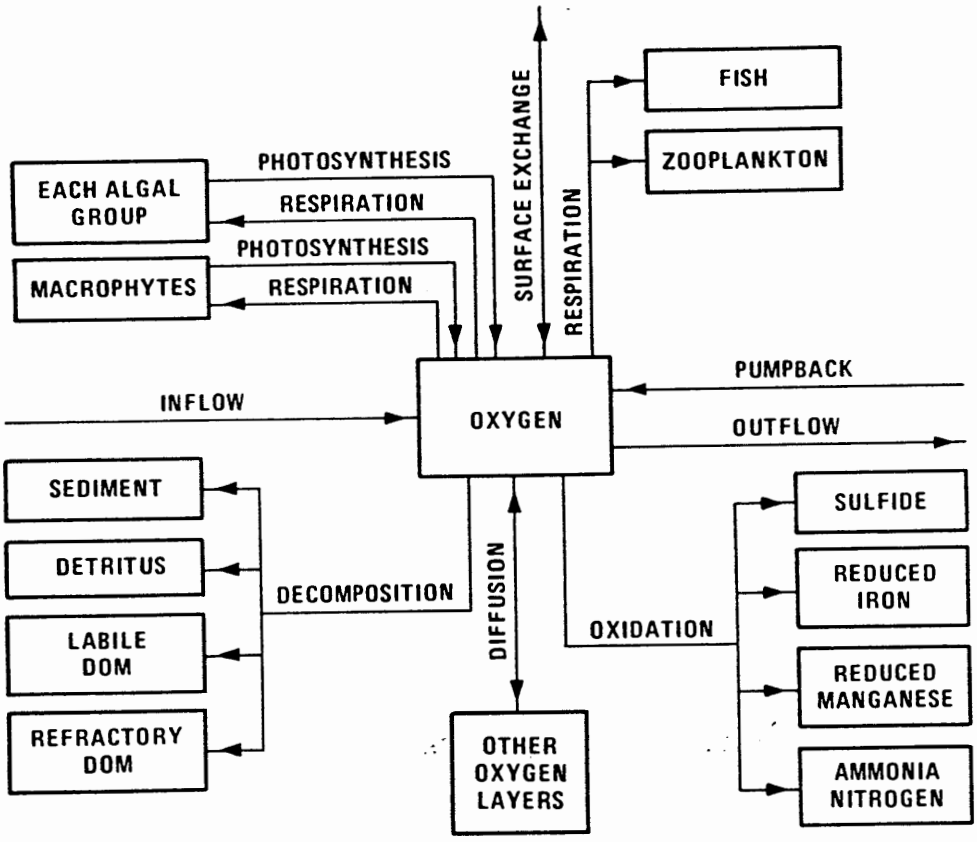

Figure 23. Fluxes among oxygen and other compartments (Ford 1980).

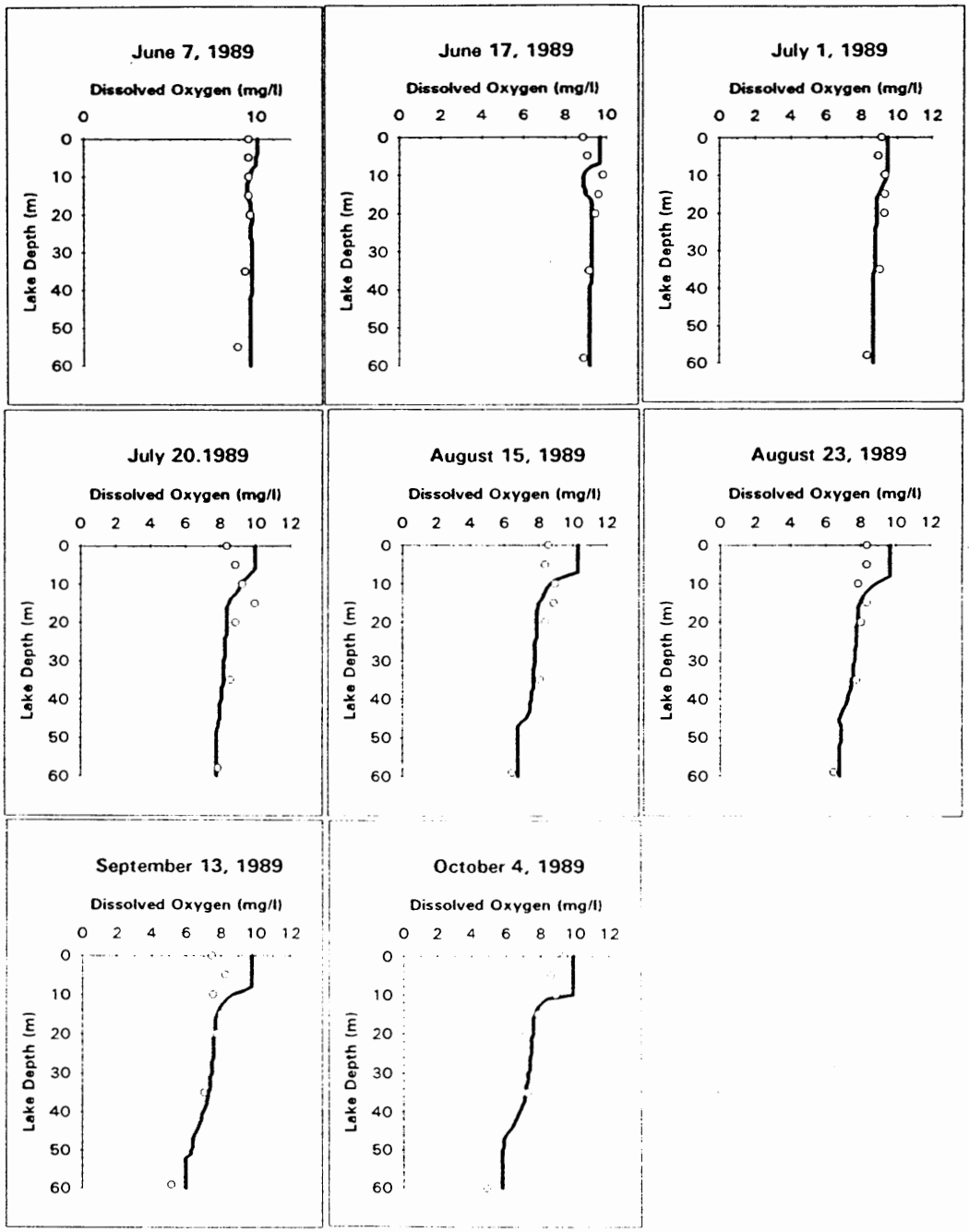

Figure 24. Vertical distribution of dissolved oxygen concentration for CE-QUAL-R1 model calibration of Coldwater Lake, 1989: simulation (solid line); measured data (circles).

Model simulated D.O. levels within the metalimnion showed a slight oxygen minimum on June 17. The metalimnetic minimum simulated by the model was representative of a system where oxidizable material produced in the epilimnion sank at a slower rate when it encountered the denser metalimnetic waters and where it decomposed at a higher rate than the cooler waters of the hypolimnion (Reid 1976). Model simulated residence time of oxidizable organic material in the metalimnion could be have been greater than the natural system on June 17 due to under prediction of the eddy diffusion coefficient (i.e., less mixing) in the metalimnion. This may have been caused by an innacurate wind speed measurement.

Field data indicated that D.O. was depleted in the hypolimnion during the summer stratification period. This was due to the consumption of oxygen by the decomposition of organic material. It is not typical for a lake with indicators of an oligotrophic status such as low nutrient concentration and high transparency to have such a high uptake of oxygen in the hypolimnion. However, Kelly (1991) stated that the trophic status of Coldwater Lake began as hyper-eutrophic due to high organic loading from the eruption of Mt. Saint Helens on May 18, 1980. There could still be high concentrations of dissolved organic matter (DOM) decaying which could create an oxygen deficit. The model simulation used initial conditions of 2 mg/l of refractory DOM throughout the water column. Refractory DOM was used to represent the majority of organic matter in the water column because allochthonous inputs from the eruption, such as woody debris, are more refractory in composition (Ford 1980). Decay of this initial concentration of refractory DOM produced results which agreed

well with field measured D.O. concentration in the hypolimnion.

Phytoplankton

Oxygen within natural waters is derived by photosynthetic activity according to the simplified formula

$$6CO_2 + 6H_2O \rightarrow C_6H_{12}O_6 + 6O_2$$

The vertical extent of photosynthesis was controlled by the depth of the euphotic zone. The average depth of the euphotic zone in Coldwater Lake was determined by Kelly (1991) to be 15.4 m, which is the depth at which light intensity is 1% of the surface intensity. The depth of the euphotic zone as measured by Kelly (1991) in 1989 ranged from 10 m to 15.8 m. The model was run with related light extinction coefficients of 0.45 m^{-1} and 0.30 m^{-1} to determine the effect on phytoplankton growth (Figure 25).

Model simulated phytoplankton densities more than tripled at the 10 m depth when the light extinction coefficient was lowered from 0.45m^{-1} to 0.30m^{-1}.

CE-QUAL-R1 sets the algal groups into three compartments. Various rates such as primary productivity, dark respiration, nitrogen uptake, and phosphorus uptake are calculated for each compartment. The dominant algal compartment was the diatom compartment which consisted mainly of a Cyclotella/Asterionella community. Verduin (1952) suggested a ratio of respiration to photosynthesis of 0.23 for a Cyclotella/Asterionella community in Lake Erie. A ratio of 0.21 was used in the model.

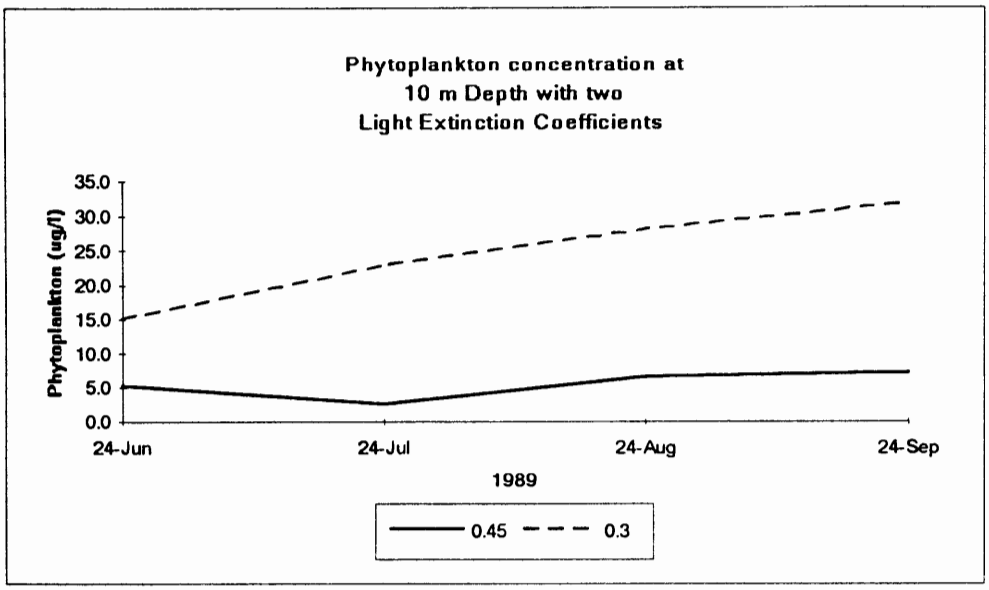

Figure 25. Model simulated phytoplankton concentrations in Coldwater Lake, 1989 at a 10 m depth with light extinction coefficients of 0.45 and 0.30.

Chlorophyll a, which is a primary pigment involved in the photosynthetic process, is often used as an indicator of phytoplankton distribution of biomass (Hutchison 1957). The phytoplankton density estimated by the model at the lake surface and depths of 10 m and 20 m was compared to chlorophyll a concentrations at those same depths (Figure 26). A ratio of 1 mg phytoplankton to 10 ug/l chlorophyll a was assumed for the initial conditions of the diatom phytoplankton compartment (Verduin 1952). The diatom population was the dominant phytoplankton population throughout the model simulation. Figure 26 showed the 1989 phytoplankton population at the lake surface ranging from 30 ug/l to 250 ug/l while chlorophyll a concentrations ranged from 0.45 ug/l to 1.59 ug/l. This gave an average ratio which

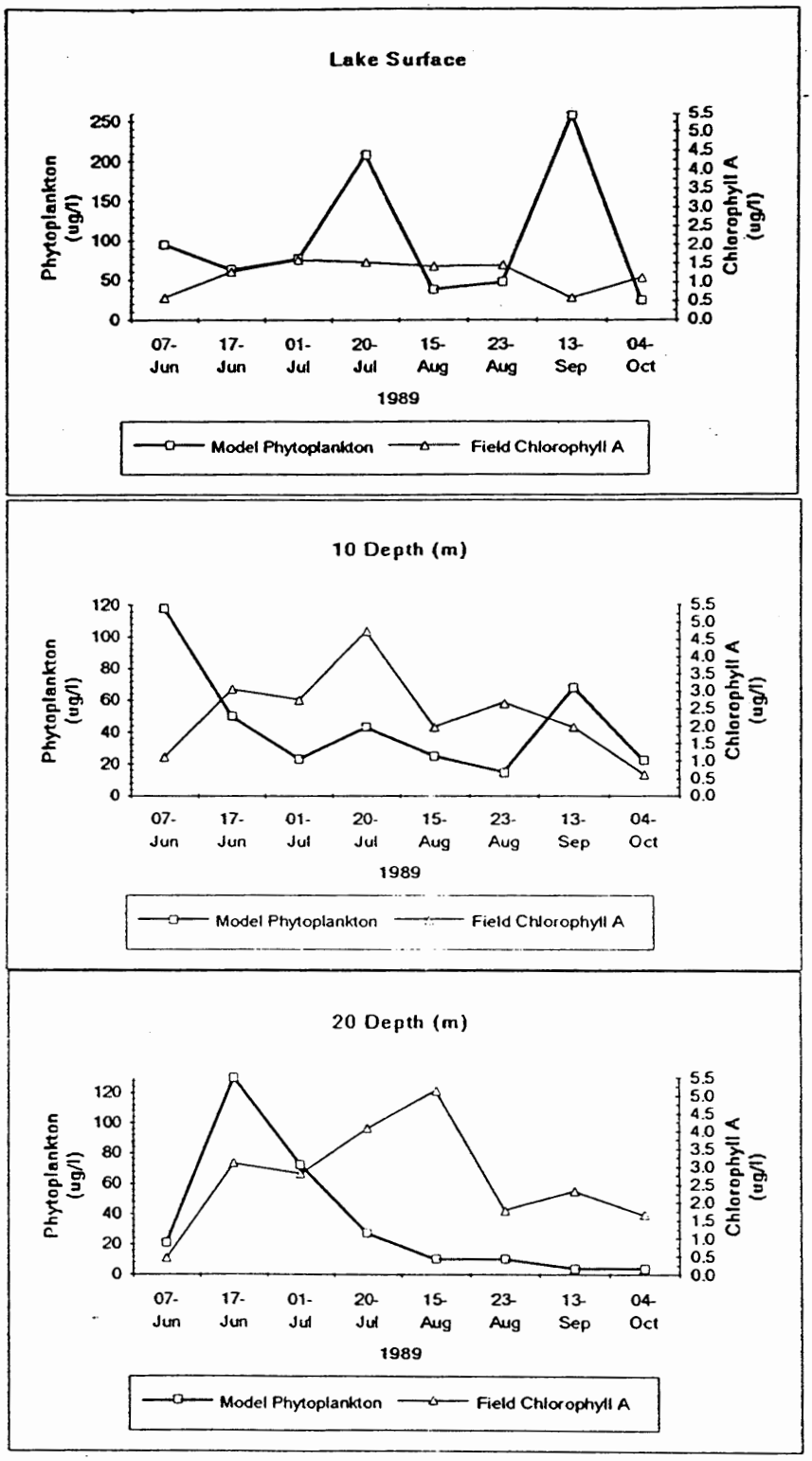

Figure 26. Distribution of model simulated phytoplankton concentrations vs. field measured chlorophyll a concentrations in Coldwater Lake.

was close to the initial condition ratio of 1 mg phytoplankton to 10 ug chlorophyll a. Phytoplankton concentrations at 10 m ranged from 18 ug/l to 120 ug/l while chlorophyll a concentrations ranged from 0.62 ug/l to 4.74 ug/l. This gave an average ratio of 1 mg/l phytoplankton to 25 ug/l chlorophyll a at a 10 m depth.

The initial condition phytoplankton - chlorophyll a ratio may not be valid for the 10 m or 20 m depths because a significant portion of algal cells within this region were non-viable and were found as particulate detritus in various stages of decomposition (Wetzel 1983).

Zooplankton

The 1989 model simulation had a mean zooplankton density in the epilimnion of the lake of approximately 100 ug/l. An estimate of weight per individual was not found but a comparison with mesotrophic lake biomass of zooplankton in Wetzel (1983) gave a range of 70 ug/l to 140 ug/l.

Anoxic Conditions

Dissolved oxygen concentrations did not drop low enough during the model simulation to trigger anaerobic processes which would cause anoxic conditions.

NUTRIENTS

Phosphorus

Two forms of phosphorus in fresh water are available for phytoplankton consumption: particulate phosphorus, which is contained within organisms, is found in the mineral form and is adsorbed onto dead organic particulates; orthophosphate phosphorus, which is found in the dissolved form, is the form which is most easily assimilated by phytoplankton (Kelly 1991).

Orthophosphate concentrations from the 1989 model simulation were compared to field data in Figure 27. The model simulated values for orthophosphate were near those measured in the field with concentrations below 7 ug/l, which is typical of oligo-mesotrophic lakes (Wetzel 1983).

The model simulation indicated that the dominant phytoplankton compartment (diatoms) were nitrogen limited throughout the simulation. Kelly (1993) believed that phytoplankton in Coldwater Lake were nitrogen limited because of the relatively high concentrations of total phosphorus as compared to the relatively low concentrations of nitrate. Assuming nitrogen limited growth this seemed reasonable as the field data showed nitrate levels decreasing throughout the summer.

Nitrogen

Nitrogen was typically present within a lake ecosystem in two forms: ammonia (NH_4), the easiest form of nitrogen for phytoplankton assimilation, and

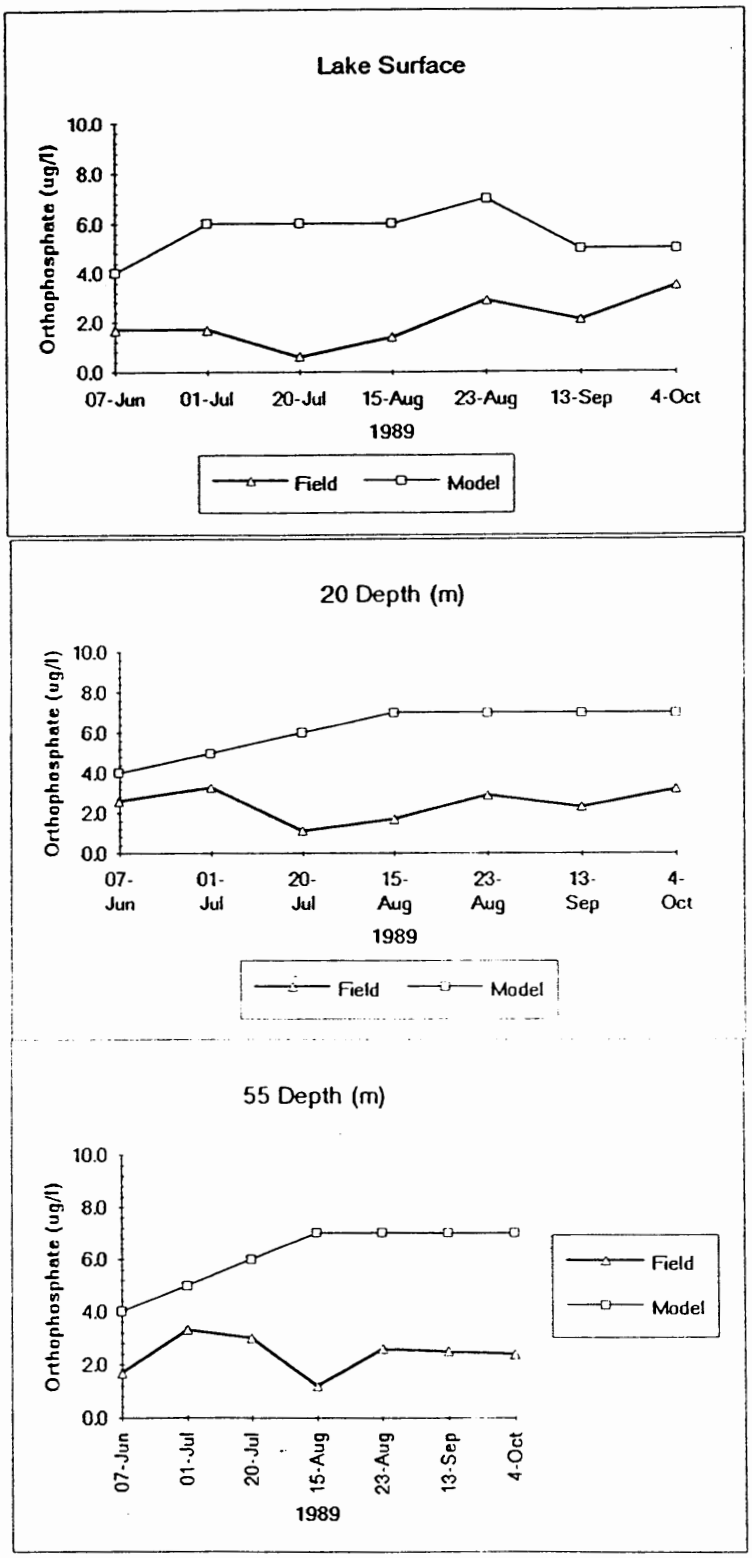

Figure 27. Model simulated orthophosphate concentrations vs. field values in Coldwater Lake, 1989.

nitrate (NO_3), which may be assimilated when limited ammonia is available for phytoplankton uptake (Wetzel 1983).

Model simulated concentrations of NO_3 and NH_4 were compared to field concentrations in Figure 28. NO_3 is stable throughout the water column at concentrations of 10 ug/l to 20 ug/l and NH_4 concentrations varied from 2 ug/l to 4ug/l. The model simulated concentrations agree well with the field data except for the depletion of NO_3 in the surface layers indicated in the field data. Kelly (1991) stated that the NO_3 depletion was probably a consequence of phytoplankton uptake. This uptake of NO_3 shown in the field data may also have been caused by bacterial consumption of NH4 and NO3 as proposed by Wissmar (1988).

The model simulation assumed no nitrogen fixation or lake inflows, so all nitrogen generated within the lake came from the decay of organic matter. Figure 29 shows the various compartmental fluxes which interact with NO_3 and NH_4. The model simulated increase in NO_3 concentration over the simulation period at 20m and 55m depths (Figure 28) comes from the decay of refractory DOM.

The model simulation assumed a major portion of the organic in Coldwater Lake was refractory and allochthonous in nature. A carbon to nitrogen ratio of 100:1 was assumed for the model simulation.

Model Verification

Field data collected in 1990 were used to verify model parameters used during the 1989 calibration. A comparison of model predicted D.O. concentration and field

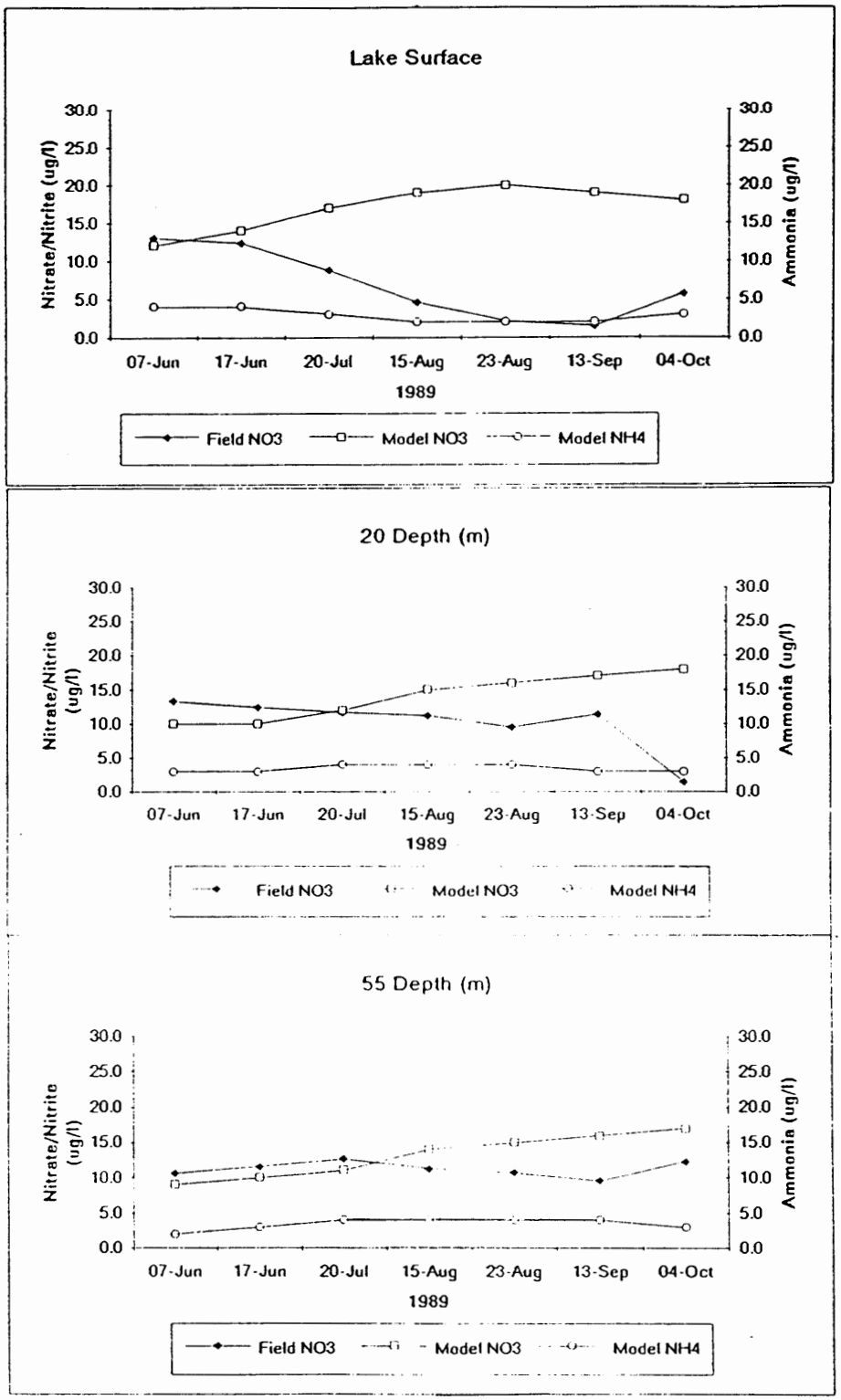

Figure 28. Model simulated concentrations of nitrate and ammonia vs. field values of nitrate in Coldwater Lake, 1989.

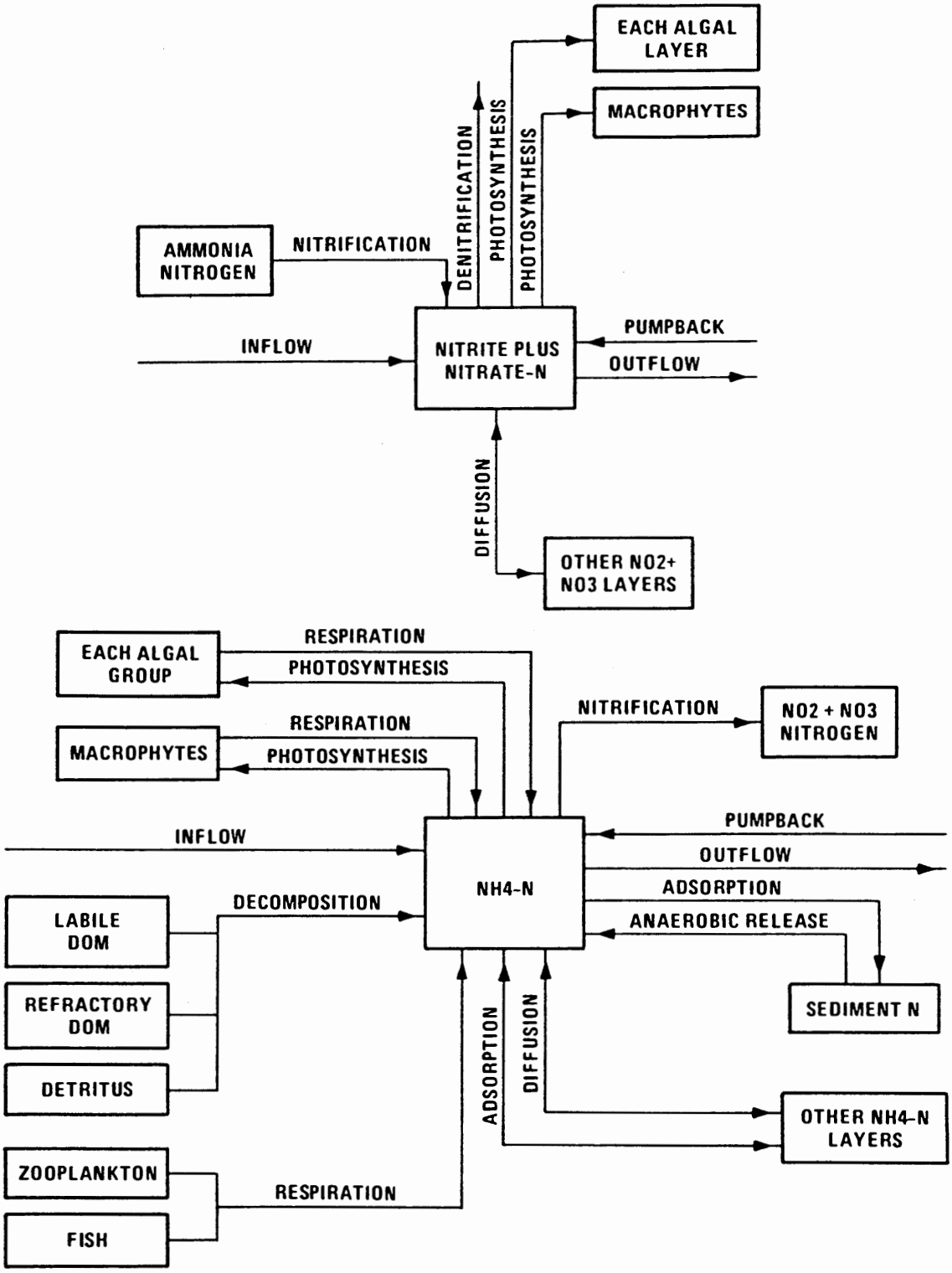

Figure 29. Fluxes between nitrate and ammonia and other compartments (Ford 1980)

concentration is shown in Figure 30. Model prediction showed an over prediction of D.O. concentration in the epilimnion during most of the simulation. Excessive oxidation in the metalimnion may have led to an under prediction of D.O. concentrations in the hypolimnion durin the 1990 model validation.

Phytoplankton densities for 1990 model verification ranged from a 105 ug/l mean concentration near the lake surface to a 60 ug/l mean concentration at a depth of 10 m (Figure 31). These results produced phytoplankton - chlorophyll a ratios of approximately 1 mg/l to 10 ug/l for the lake surface and 1 mg/l to 25 ug/l at the 10 foot depth. These concentrations are similar to those derived in the 1989 calibration.

Concentration of nitrogen and phosphorus during the 1990 model verification was similar to the 1989 calibration concentration (Figure 32 and 33). A slight increase in NO_3 and NH_4 concentration was noted in the hypolimnion which could be attributed to the D.O. deficit shown in Figure 30.

Zooplankton density during the 1990 model verification ranged from a low of 28 ug/l on September 20 to a high of 194 ug/l on July 20. Mean concentration throughout the simulation was approximately 100 ug/l, which is similar to the mean concentration in the 1989 model calibration .

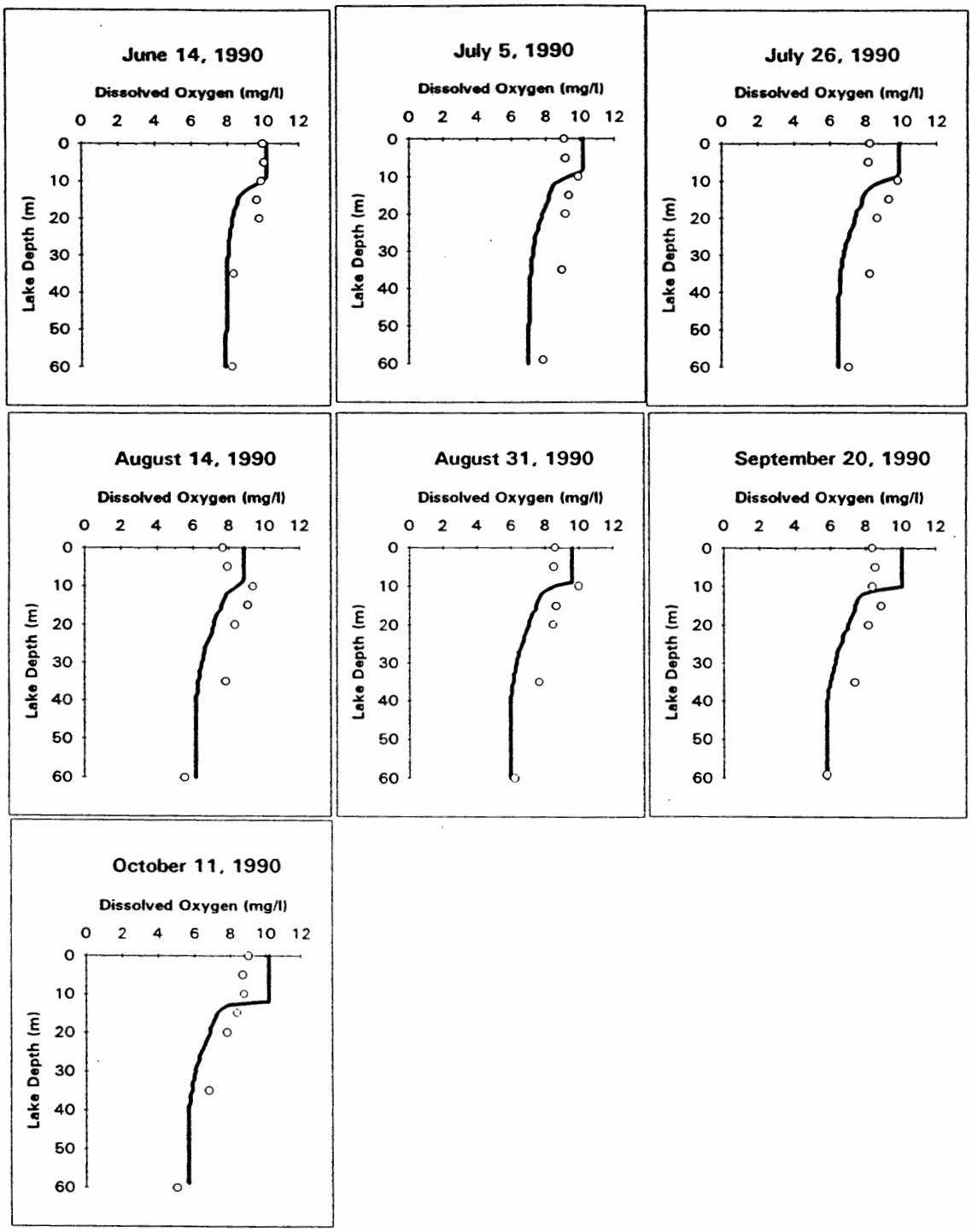

Figure 30. Vertical distribution of dissolved oxygen concentration for CE-QUAL-R1 model verification of Coldwater Lake, 1990: simulation (solid line); measured data (circles).

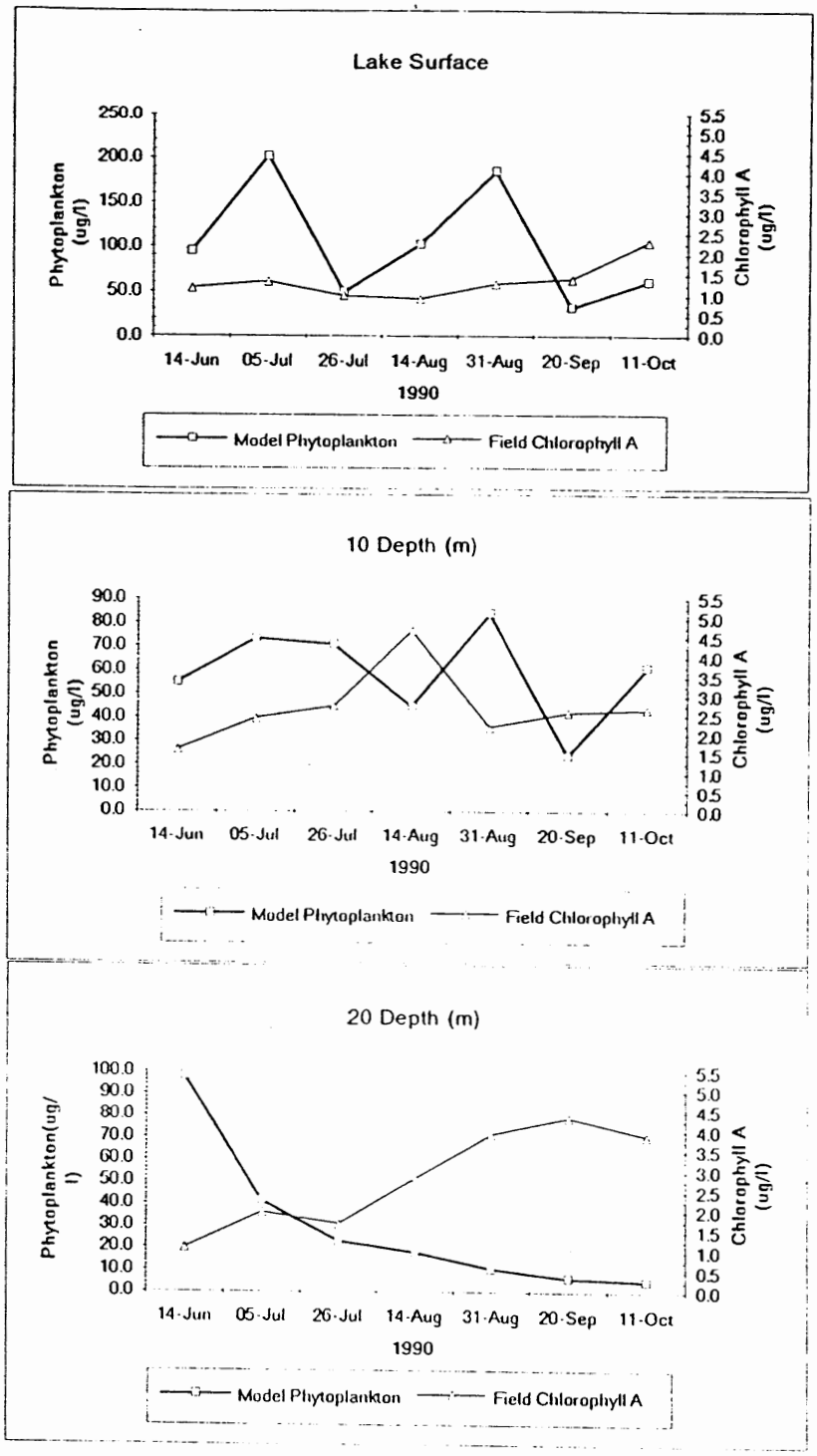

Figure 31. Model simulated phytoplankton concentration vs. field measured chlorophyll a concentration for model verification of Coldwater Lake, 1990.

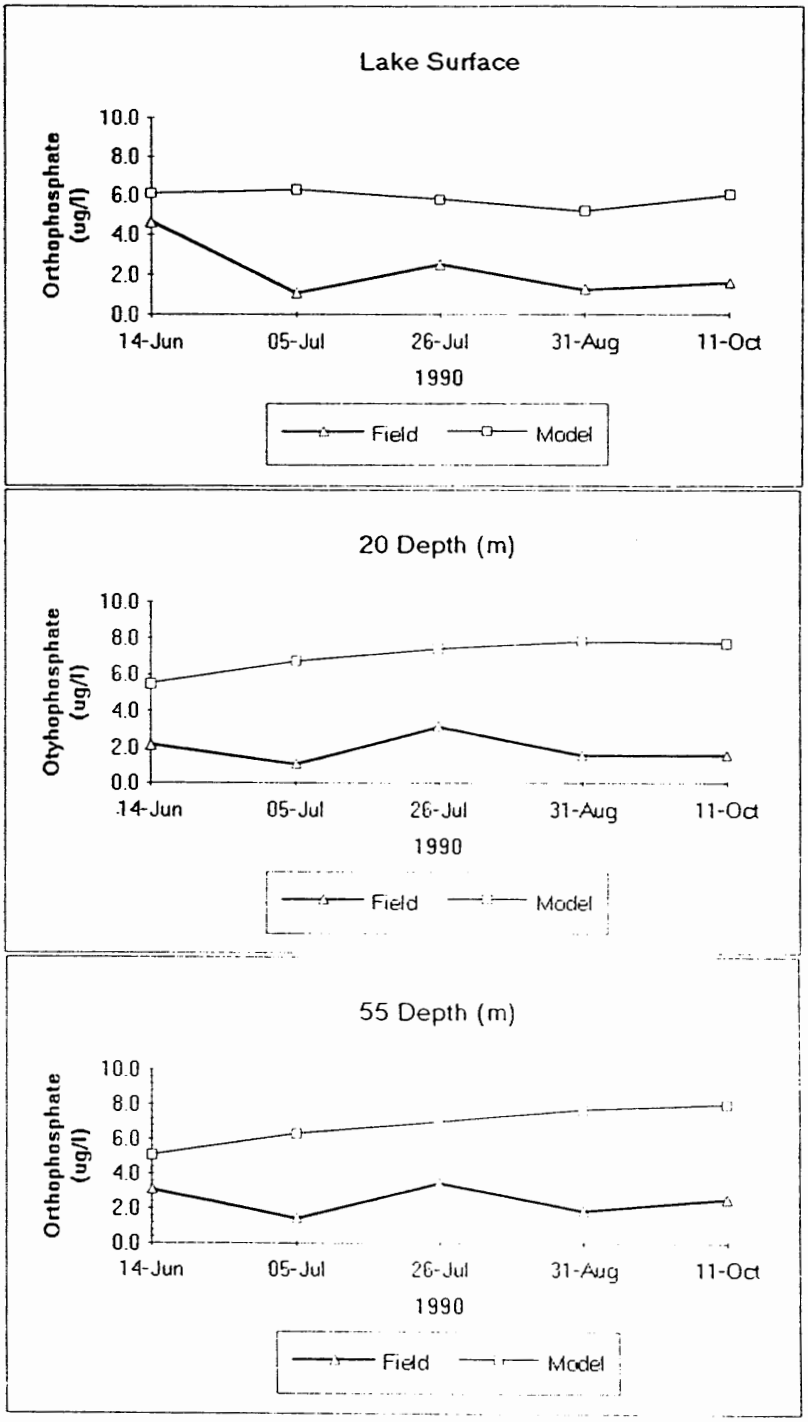

Figure 32. Model simulated orthophosphate concentration vs. field measured orthophosphate concentration for model verification of Coldwater Lake, 1990.

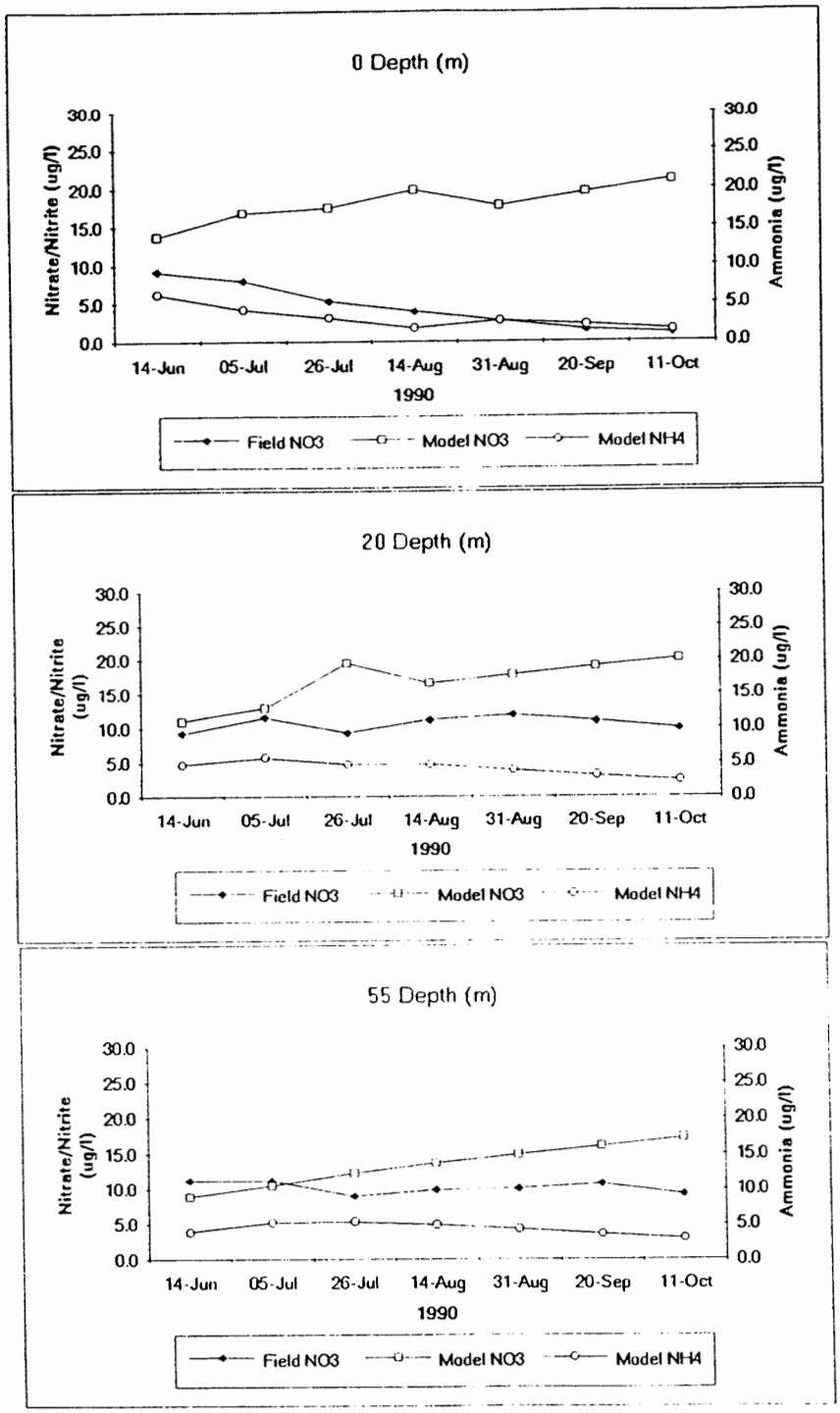

Figure 33. Model simulated concentrations of nitrate and ammonia vs. field measured concentration of nitrate for model verification of Coldwater Lake, 1990.

FISH PREDATION AND THERMAL CHARACTERISTICS

Thermal stratification of the water column occurs in most temperate lakes during the early spring and summer. A mixed zone (epilimnion) is formed at the top of the water column. The depth of this zone has a great effect on physical, biological and chemical characteristics of a lake.

Studies have been performed that indicate a relationship between abundance of planktivorous fish, large zooplankton, biomass of algae and water clarity. This relationship may effect the size distribution and biomass of plankton, which could influence the thermal structure of small lakes (< 20 km^2) by changing water clarity (Mazumder 1990).

Rainbow Trout have been stocked in Coldwater Lake since 1989 (Chrisifulli 1993). Rainbow Trout have been shown to eat few zooplanktons of a size less than 1.3 mm (Wetzel 1983). The dominant zooplankton in Coldwater Lake is the Daphnia pulicaria. Wetzel (1983) estimates the mean size of Daphnia at 1.3 mm. This would indicate that the Daphnia pulicaria could be a major food source for the Rainbow Trout.

The 1990 verification model was tested with a mean zooplankton concentration of 100 ug/l and an initial fish concentration of 200 kg/hectare. An ingestion rate which represented an optimum growth rate for fish was input into the simulation. Results indicated a mild raise in epilimnion temperatures of 0.1 - 0.2°C and a deepening of the Secchi disk depth of 1 m in September near the end of the

simulation. This change was not nearly as pronounced as results from Mazmuder (1990).

This relationship between zooplankton density and fish population could be further investigated since there is baseline data collected in 1989 before the planting of Rainbow Trout fingerlings.

MODEL SENSITIVITY

A sensitivity analysis was conducted for the 1989 modelling simulation to determine the sensitivity of two coefficients on model performance. The model coefficients TURB, which is an atmospheric dust attenuation coefficient and DISW, which is a calibration parameter used in the calculation of eddy diffusion coefficients were reviewed.

TURB, an atmospheric dust attenuation coefficient, represented the attenuation of solar radiation by dust due to scattering and absorption. A value of 0.40 (dimensionless) was used in the Coldwater Lake modeling simulations. Ford (1980) stated that a value of 0.06 had been used in previous CE-QUAL-R1 modelling studies. Figure 34 showed the relationship between dissolved oxygen (D.O.) concentrations and water temperature to values of 0.06, 0.20, and 0.40 for TURB. The value of TURB had little effect on D.O. concentrations but did cause a variance in temperature of up 2°C in the epilimnion. The larger values of TURB corresponded with the cooler epilimnion temperatures.

DISW was a calibration parameter used in the calculation of eddy diffusion coefficients which were due to turbulent kinetic energy imparted upon the lake surface by wind. Values of $5.0x10^{-1}$ and $5x10^{-3}$ (dimensionless) were used in the Coldwater Lake modelling simulations. Ford (1980) stated that values between $1.0x10^{-4}$ and $1.0x10^{-5}$ had been used in previous CE-QUAL-R1 modelling studies. Figure 35 shows the relationship between D.O. concentrations and model calculated eddy diffusion coefficients to values of $5.0x10^{-1}$, $5.0x10^{-3}$ and $5.0x10^{-5}$ for DISW.

A D.O. metalimnetic minimum occurred when DISW was set to $5.0x10^{-3}$ and $5.0x10^{-5}$ but did not occur when DISW was set to the higher value of $5.0x10^{-1}$. The elimination of the metalimnetic minimum using the higher value was due to greater mixing across the top of the thermocline. This allowed oxidizable material produced in the epilimnion to be transported more quickly through the metalimnion and to be distributed more evenly throughout the epilimnion. The bottom row of Figure 35 shows the relationship between water temperature and lake depth using the three DISW values. The $5.0x10^{-1}$ value provided the most mixing and therefore distributed more heat into the hypolimnion.

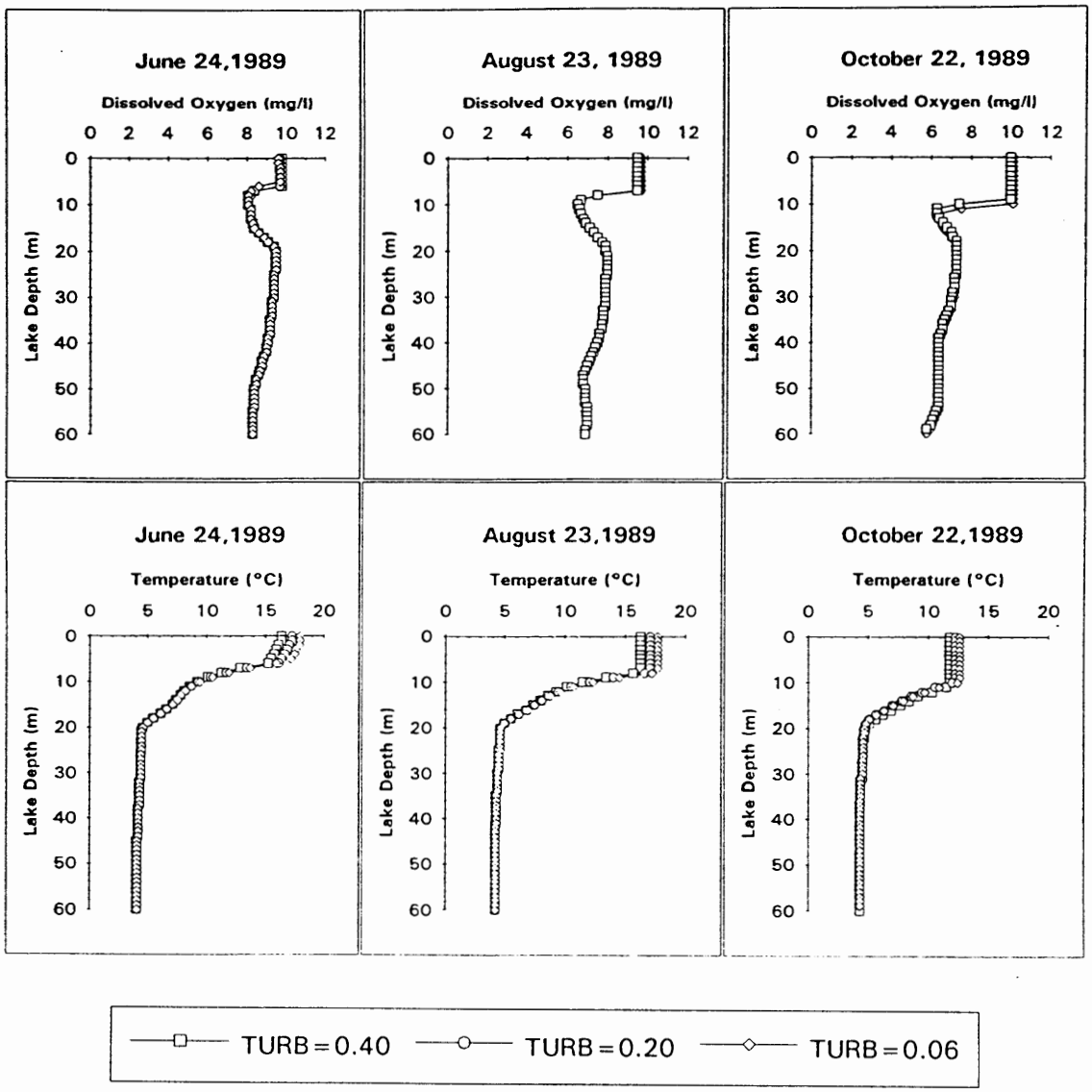

Figure 34. Sensitivity analysis of model simulated D.O. concentrations and water temperatures vs. an atmospheric dust attenuation coefficient, TURB.

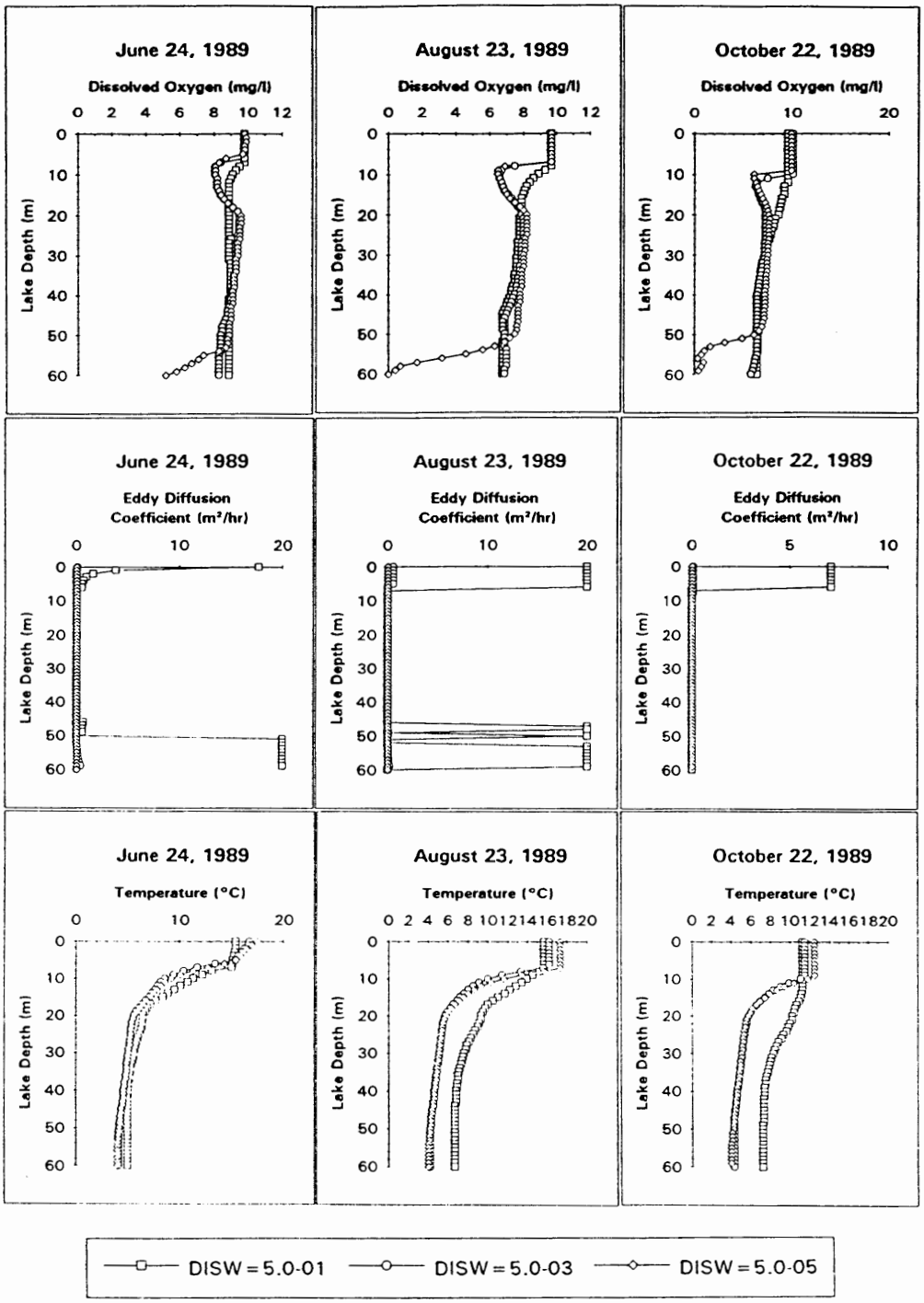

Figure 35. Sensitivity analysis of model simulated D.O. concentrations and water temperatures vs. a calibration parameter used in the calculation of eddy diffusion coefficients, DISW.

CONCLUSION

Thermal characteristics of Coldwater Lake were simulated using the U.S. Army Corps of Engineers one-dimensional thermal model CE-THERM-R1. Data from field research by Kelly (1991) were used to calibrate the model simulation in 1989 and to verify the model parameters in 1990.

The model accurately predicted the stratification process in 1989 by closely matching the depth and temperature of the epilimnion, the gradient of the thermocline and the temperature of the hypolimnion. During model verification in 1990 the model under predicted the temperature in the epilimnion and metalimnion by 1°C - 3°C in August and September. This may be attributed to denser mean cloud cover in 1990. Cloud cover data used in the model were collected from the Portland International Airport which is approximately 50 km south of Coldwater Lake. A dust attenuation coefficient was adjusted to attain good model agreement for 1989. Using the dust attenuation coefficient as a calibration tool was perhaps a method to account for lack of on-site cloud cover data. U.S. Forest Service personnel could be trained to take cloud cover readings at the new Mt. St. Helens Visitors Center scheduled for opening in May 1993.

Model simulations predicted eddy diffusion coefficients (Ez) throughout the water column. These were compared to Ez values in the hypolimnion calculated from temperature data collected by Kelly (1991). Model simulated Ez values in the

hypolimnion were one to two orders of magnitude greater than molecular diffusion and closely matched field calculated values . The model simulation assumed no lake inflow or outflow so the hypolimnion was more stable than the natural system. The model simulation predicted Ez values which were four to five orders of magnitude greater than molecular diffusion near the bottom of the lake. This may be attributed to minor variations in hypolimnetic temperatures which led to small density gradients between bottom layers. Small density gradients led to the calculation of a small Richardson number ($Ri < 0.25$) which corresponded to a region of rapid mixing.

CE-THERM -R1 was used to determine the photosynthetically available radiation (PAR) which was available for phytoplankton growth in Coldwater Lake. The daily average PAR in Coldwater Lake varied from 3.5×10^7 microeinsteins/m^2/day on Julian day 100 (April 10), approximately the time when summer stratification begins, to 4.3×10^7 microeinsteins/m^2/day on Julian day 172 (June 21), the day with the greatest hours of sunlight.

The water quality characteristics of Coldwater Lake were simulated using the U.S. Army Corps of Engineers one dimensional water quality model CE-QUAL-R1. Oxygen, algae and nutrient data from field research by Kelly (1991) were used to calibrate the model.

Dissolved oxygen (D.O.) concentration were used to calibrate the model. D.O. concentration in the hypolimnion agreed well with the field data throughout the simulation. D.O. concentration in the epilimnion was over predicted for much of the simulation. This was thought to be a function of the time of day D.O. concentration

was taken. The model output average daily D.O. concentration during the 24 hour model time step. Field measurement of D.O. was typically taken in late morning before D.O. reached maximum daily concentration.

Model simulation of mean phytoplankton concentration, at the lake surface, agreed well with field data, assuming a ratio of 1 mg/l phytoplankton to 10 ug/l chlorophyll a. Phytoplankton concentration at 10m and 20m depths was under predicted assuming the phytoplankton-chlorophyll a ratio of 1 mg/l to 10 ug/l. However, this ratio may not be valid for these depths because a significant portion of the algal cells within this region were non-viable and were found as particulate detritus in various stages of decomposition. The model did not precisely predict timing of phytoplankton blooms.

Concentration of nitrogen and phosphorus in the model simulation agreed well with field measured concentration for much of the simulation. The model predicted that the dominant phytoplankton compartment (diatoms) were nitrogen limited. The Coldwater Lake model simulation assumed no lake inflow or nitrogen fixation, so any increase in nitrogen concentration within the lake came from decay of organic matter. The model prediction of a slight increase in NO_3 concentration in the hypolimnion was mainly due to decay of refractory dissolved organic matter (DOM). A carbon to nitrogen ratio of 100:1 was assumed for model simulation because much of the DOM within the water column is from humic matter deposited during the May 18, 1980 eruption of Mt Saint Helens.

The model simulated zooplankton concentration in the epilimnion, of 100 ug/l,

was similar to biomass found in other mesotrohpic lakes.

The introduction of fish into Coldwater Lake during the 1990 model verification was found to have minimal effects on water clarity and temperature in the epilimnion and metalimnion. An initial concentration of 200 kg/hectare of Rainbow Trout with a high growth rate, reduced the temperature in the epilimnion 0.2°C and reduced the depth of the epilimnion by 1 m on September 20, 1990. The relationship between zooplankton density and fish population could be further investigated since there is baseline data collected in 1989 before the planting of Rainbow Trout fingerlings.

The 1990 model verification under estimated the amount of D.O. in the hypolimnion. This may be attributed to the large D.O. depletion in the metalimnion. Nutrient, phytoplankton and zooplankton concentrations calculated in the 1990 model verification agree well with 1990 field data.

Sensitivity analyses were performed for the variables TURB and DISW to determine how they effected model performance. TURB, an atmospheric dust attenuation coefficient had little affect on D.O. concentrations but did effect water temperatures in the epilmnion. The 0.40 value used in the Coldwater Lake modelling simulation predicted water temperatures in the epilimnion which were approximately 2°C cooler than those predicted when using a value of 0.06, which had been used in previous CE-QUAL-R1 modelling studies. DISW, a calibration parameter used in the calculation of eddy diffusion coefficients affected D.O. concentrations in the metalimnion. The 5.0×10^{-3} value used in the Coldwater Lake modelling simulation

predicted a D.O. metalimnetic minimum which was not indicated in the field data collected by Kelly (1991). A value of $5.0x10^{-1}$ predicted no metalimnetic minimum because of greater mixing across the top of the thermocline. Values between $1.0x10^{-4}$ and $1.0x10^{-5}$ had been used in previous CE-QUAL-R1 modelling studies.

In review, data which would be quite useful in further modeling studies of the lake are:

- Cloud cover estimates from spring turnover to fall turnover.
- Primary production rate, dark respiration rate and sinking rate of the dominant phytoplankton.
- An estimation of dissolved organic matter contributed to Coldwater Lake by the eruptive process of Mt. St. Helens in 1980.
- Fish density per hectare of lake surface.
- Nutrient loading balance from inflows to verify importance in relation to initial conditions.

The CE-QUAL-R1 water quality model for Coldwater Lake can be used to predict interactions of physical factors, chemical factors, and biological assemblages in both aerobic and anaerobic environments. The model could be of use to those who wish to predict the effect that building campsites around the lake would have on the nutrient balance within the lake. It could also be useful in predicting Coldwater Lake's transition to a different trophic status.

Coldwater Lake provides a unique opportunity to examine the freshwater ecology of a newly formed lake. The use of the CE-QUAL-R1 water quality model could be a useful tool for this examination.

REFERENCES

Anderson, R.Y., E.B. Nuhfer, and W.E. Dean. 1985. Sedimentation in a blast-zone lake at Mount St. Helens, Washington -- Implications for varve formation. Geology 13:348-352.

Chrisafulli, Charlie. March 12, 1993. Personal conversation.

Fairchild, L.H., 1985. Ph.D. dissertation: *Lahars at Mount St. Helens, Washington.* Doctor of Philosophy, University of Washington, Washinton.

Fischer, Hugo B., E. John List, Robert C.Y. Koh, J. Imberger, Norman H. Brooks. 1979. Mixing in Inland and Coastal Waters. Academic Press, Inc., San Diego, California.

Ford, Dennis E., Kent W. Thornton, Allan S. Lessem, and Joseph L. Norton. June 1980. Environmental Laboratory, U. S. Army Engineer Waterways Experiment Station, Vicksburg, MS. CE-QUAL-R1: A water quality management model for reservoirs.

Hutchinson, G.E. 1957. A Treatise on Limnology, I. Geography, Physics and Chemistry, John Wiley and Sons, New York.

Imberger, J. 1985. "The diurnal mixed layer," *Limnol Oceanogr.*, 30(4), 1985, pp 737-770, copyrighted 1985, by the American Society of Limnology and Oceanography, Inc.

Imberger, J., John Patterson, Bob Hebbert, and Ian Loh. May 1978. "Dynamics of Reservoir of Medium Size," *Journal of the Hydraulics Division*, pp 725-743.

Janda, R.J., et al. 1981. "Lahar movement, effects, and deposits", *US Geological Survey Professional Paper 1250.* Peter Lipman and Donal Mullineaux, Ed. pp. 461-478.

Janda, R.J., D.F. Meyer, and D. Childers. Showa 59. 1985. Sedimentation and geomorphic changes during and following the 1980-83 eruptions of Mount St. Helens, Washington. *Shin sa bo.*37(2): 10-19.

Kelly, Valerie Jean. 1991. Thesis: *Limnology Of Two New Lakes, Mount St. Helens, Washington*. Master of Science in Biology, Portland State University, Oregon.

Kelly, Valerie Jean. March 18, 1993. Personal conversation.

Larson, D.W. and M.W. Glass. 1987. Spirit Lake, Mount St. Helens, Washington: Limnological and Bacteriological Investigations. U.S. Army Corps of Engineers.

McCormick, Michael J., and Donald Scavia. April 1981. "Calculation of Vertical Profiles of Lake-Averaged Temperature and Diffusivity in Lakes Ontario and Washington," *Water Resources Research*, Vol 17, No. 2, pp 305-310.

Mazumder, A., W.D. Taylor, D.J. McQueen, and D.R.S. Lean. June 1990. *Science* Vol. 24. Effects of fish and plankton on lake temperature and mixing depth.

NOAA 1990. Monthly local climatological data summary 1990.

Reid, G.K., and R. D. Wood. 1976. Ecology of Inland Water and Estuaries. New York, D. Van Nostrand Co. 485 pp.

Rice, Dale Allan. 1987. Abstract of thesis: *Thermal Stratification Modeling of a Transparent Adirondack Lake*. Master of Science in Environmental Engineering, Syracuse University, New York.

Rice, Dale Allan, et al. 1989. "Modeling Thermal Stratification in Transparent Adirondack Lake," *Journal of Water Resources Planning and Management*, Vol. 115, No. 4, July, 1989. Copyrighted by ASCE, ISSN 0733-9496/89/0004-0440. Paper No. 23673.

Stefan, H.G., and Ford, D.E. (1975). "Temperature dynamics in dimictic lakes." *J. Hydr. Div.*, ASCE, 101(1), 97-114.

Sweers, H.E. 1970. "Vertical Diffusivity Coefficient in a Thermocline," Dept. of Energy, Mines and Resources, Marine Sciences Branch, Ottawa, *Limnology and Oceanography*, Vol 15, No. 2, March 1970, pp 273-280.

Uhrich, M.A., 1990. Precipitation data for the Mount St. Helens area, Washington 1981-1986. U.S.G.S. Open File Report 90-117, 1990.

Van Nostrand. 1983. Van Nostrand Scientific Encyclopedia. Van Nostrand Reinhold Co. 3067pp.

Verduin, J. 1952. "Photosynthesis and Growth Rates of Live Diatom Communities in Western Lake Erie," *Ecology*, Vol 33, pp 163-169.

Wetzel, R.G. 1983. Limnology. Saunders College Publishing. 767 pp.

Wissmar, R.C., J.A. Baross, M.D. Lilley and C.N. Dahm 1988. "Nitrogen Cycling in Altered and Newly Created Lakes Near the Mount St. Helens Volcano." *Journal of Freshwater Ecology*, Vol. 4, No. 4, December 1988, pp 551-568.

APPENDIX A

INPUT VALUES FOR 1989 COLDWATER LAKE

CE-QUAL-R1

COMPUTER SIMULATION

APPENDIX A

INPUT VALUES FOR 1989 COLDWATER LAKE CE-QUAL-R1 COMPUTER SIMULATION

INPUT PARAMETER	UNITS	COMPUTER NAME	INPUT VALUE	SOURCE
First Julian day for update data	day	IFIRST	121	NA
Last Julian day for update data	day	ILAST	325	NA
Computation interval	hour	NHOI	24	QUAL Manual
Output Interval	hour	IPRT	720	QUAL Manual
First simulation day	day	ISTART	146	Kelly (1991)
Simulation year	NA	IYEAR	1989	NA
Number of algal compartments	each	NALG	3	QUAL Manual
Reservoir operation	NA	MODE	NORMAL	QUAL Manual
Reservoir operation	NA	STRUCT	WEIR	QUAL Manual
Reservoir operation	NA	CHOICE	SPECIFY	QUAL Manual
Calibration temperature profiles	NA	CALBRAT	YES	QUAL Manual
Number of inflow tributaries	each	NTRIBS	0	Detention Time
Initial number of layers	each	NUME	61	NA
Latitude	decimal degrees	XLAT	45.3	Topographic Map
Longitude	decimal degrees	XLON	122.25	Topographic Map
Dust Attenuation Coefficient	NA	TURB	0.40	Calibration
Wind Speed Coefficient	m/mb-sec	AA	4.18×10^{-9}	Calibration
Wind Speed Coefficient	m/mb-sec	BB	1.50×10^{-9}	Calibration
Full pool elevation	MSL	ELEMSL	701	Topographic Map
Reservoir length	m	RLEN	5400	Topographic Map

APPENDIX A

INPUT VALUES FOR 1989 COLDWATER LAKE CE-QUAL-R1 COMPUTER SIMULATION

INPUT PARAMETER	UNITS	COMPUTER NAME	INPUT VALUE	SOURCE
Minimum layer thickness	m	SDZMIN	0.5	QUAL Manual
Maximum layer thickness	m	SDZMAX	2.0	QUAL Manual
Initial layer thickness	m	SDZ(1)	1.0	QUAL Manual
Area vs. depth curve coefficient	NA	ACOEF(1)	96420.8	Curve Fitting
Area vs. depth curve coefficient	NA	ACOEF(2)	59379.4	Curve Fitting
Area vs. depth curve coefficient	NA	ACOEF(3)	-1963.33	Curve Fitting
Area vs. depth curve coefficient	NA	ACOEF(4)	30.028	Curve Fitting
Reservoir width coefficient	NA	WCOEF(1)	12	Bathymetric map
Reservoir width coefficient	NA	WCOEF(2)	0.55	QUAL manual
Sheltering coefficient	0.0 to 1.0 in tenths	SHELCF	0.9	Topo map
Penetrative convection fraction	NA	PEFRAC	0.5	Calibration
Eddy diffusion calibration parameter	NA	CDIFW	5×10^{-1}	Calibration
Eddy diffusion calibration parameter	NA	CDIFF	1×10^{-5}	Calibration
Critical density for inflows	kg/m^3	CDENS	0.1	QUAL manual
Extinction coefficient	1/m	EXCO	1989 - 0.45 1990 - 0.37	Calibration
Solar radiation in 0.6m surface layer	NA	SURFAC	0.39	Calibration
Self shading coefficient	1/m * mg/l	EXTINS	0.3	QUAL manual
Molecular diffusion for D.O.	m^2/s	DM02	1.42×10^{-9}	QUAL manual
Molecular diffusion for CO_2	m^2/s	DMC02	2.04×10^{-10}	QUAL manual

APPENDIX A

INPUT VALUES FOR 1989 COLDWATER LAKE CE-QUAL-R1 COMPUTER SIMULATION

INPUT PARAMETER	UNITS	COMPUTER NAME	INPUT VALUE	SOURCE
Stoichiometric equivalent between organic matter and orthophospate	NA	BIOP	.0025	Calibration
Stoichiometric equivalent between organic matter and carbon	NA	BIOC	.050	Calibration
Stoichiometric equivalent between organic matter and nitrogen	NA	BION	.005	Calibration
Self-shading coefficient due to particulate matter	1/m * mg/*l*	EXTINP	0.1	QUAL manual
Fraction of algal biomass lost by nonpredatory mortality to the detritus compartment	NA	ALDIGO	0.8	QUAL manual
Stoichiometric equivalent for silica for the third algal compartment	2-15% of algal dry weight	ALGAS	0.1	QUAL manual
Maximum gross photosynthetic or production rate (diatoms)	1/day	TPMAX1	1.20	Calibration
Phytoplankton settling rate (diatoms)	m/day	TSETL1	0.24	QUAL manual
Phosphorus half-saturation coefficient (HSC) (diatoms)	mg/*l*	PS2P041	0.002	Calibration
HSC for nitrogen (diatoms)	mg/*l*	PS2N1	0.025	Calibration
HSC for carbon dioxide (diatoms)	mg/*l*	PS2C021	0.1	Calibration
Saturating light intensity at the maximum photosynthetic rate (diatoms)	Kcal x m^{-2} x hr^{-1}	PISAT1	72	QUAL manual
Maximum excretion rate or photorespiration rate, rate ofextracellular release of organic compounds (diatoms)	1/day	TPEXCR1	0.044	QUAL manual
Maximum algal nonpredatory mortality rate (diatoms)	1/day	TPMORT1	0.030	QUAL manual
Maximum dark respiration rate of algae (diatoms)	1/day	TPRESP1	0.250	Calibration
HSC for silica	mg/*l*	PS2SI	0.05	QUAL manual
Lower temperature bound at which phytoplankton metabolism continues (diatoms)	°C	ALGxT1	4	QUAL manual
Lowest temperature at which processes are occurring near the maximum rate (diatoms)	°C	ALGxT2	26	QUAL manual
Upper temperature at which processes are occurring at the maximum rate (diatoms)	°C	ALGxT3	32	QUAL manual

APPENDIX A

INPUT VALUES FOR 1989 COLDWATER LAKE CE-QUAL-R1 COMPUTER SIMULATION

INPUT PARAMETER	UNITS	COMPUTER NAME	INPUT VALUE	SOURCE
Upper lethal temperature - biological temperature curves are generally asymmetrical, with the maximum rates occurring nearer the upper lethal temperatures than the lower temperatures (diatoms)	^{o}C	ALGxT4	37	QUAL manual
Value of the temperature rate multiplier corresponding to the lower temperature, ALGxT1	^{o}C	ALGxK1	0.1	QUAL manual
Value of the temperature rate multiplier corresponding to the upper temperature, ALGxT4	^{o}C	ALGxK4	0.1	QUAL manual
Maximum gross producion rate for macrophytes	1/day	TPLMAX	0.0	QUAL manual
Maximum dark respiration rate for macrophytes	1/day	TMRESP	0.2	QUAL manual
Maximum excretion or photorespiration rate for macrophytes	1/day	TMEXCR	0.1	QUAL manual
Maximum nonpredatory mortality rate for macrophytes	1/day	TMMORT	0.05	QUAL manual
Fraction of macrophytes, dying during the time step, that increment the labile DOM compartment	%	PLDIGO(1)	0.4	QUAL manual
Fraction of dead macrophytes that increment the detritus compartment	%	PLDIGO(2)	0.3	QUAL manual
Fraction of dead macrophytes that increment the sediment compartment	%	PLDIGO(3)	0.3	QUAL manual
Maximum drop in temperature that macrophytes can withstand within a 7-day period	^{o}C	TMPMAC	1.5	QUAL manual
Self-shading coefficient for macrophytes	1/m x mg/l	EXTINM	0.2	QUAL manual
HSC of macrophytes for inorganic carbon limitation	mg/l	PLIMC	.05	QUAL manual
HSC of macrophytes for nitrogen limitation	mg/l	PLIMN	0.01	QUAL manual
HSC of macrophytes for phosphorus limitation	mg/l	PLIMP	0.005	QUAL manual
Species-specific or mixed community coefficient representing the average density of plants	grams-plant dry weight/m^3	PLDENS	10	QUAL manual
Saturating light intensity at the maximum production rate	Kcal/m^2/hr	PLITE	30	QUAL manual
Fraction of nutrients that is obtained from the water column	%	PLFRAC	0.5	QUAL manual

APPENDIX A

INPUT VALUES FOR 1989 COLDWATER LAKE CE-QUAL-R1 COMPUTER SIMULATION

INPUT PARAMETER	UNITS	COMPUTER NAME	INPUT VALUE	SOURCE
Depth below which no macrophytes will grow	m	PLNTDEP	0.5	QUAL manual
Critical low temperatures below which macrophyte processes stop	^{o}C	PLTT1	2.0	QUAL manual
Low optimum temperature for photosynthesis by macrophytes	^{o}C	PLTT2	25.0	QUAL manual
High optimum temperature for photosynthesis by macrophytes	^{o}C	PLTT3	29.0	QUAL manual
Critical high temperature above which no macrophyte photosyntheses occurs	^{o}C	PLTT4	38.0	QUAL manual
Temperature rate multiplier at temperature PLTT1	dimensionless	PLTK1	0.1	QUAL manual
Temperature rate multiplier at temperature PLTT4	dimensionless	PLTT4	0.1	QUAL manual
Maximum ingestion rate for zooplankton	1/day	TZMAX	1.0	Calibration
Maximum nonpredatory mortality rate for zooplankton	1/day	TZMORT	0.01	Calibration
Zooplankton assimilation efficiency - it is the proportion of food assimilated to food consumed	dimensionless(A/G)	ZEFFIC	0.60	Calibration
Feeding preference factor of zooplankton for the first algal compartment	dimensionless	PREF1	0.3	Calibration
Feeding preference factor of zooplankton for the second algal compartment	dimensionless	PREF2	0.0	Calibration
Feeding preference factor of zooplankton for the third algal compartment	dimensionless	PREF3	0.4	Calibration
Feeding preference factor of zooplankton for the detritus algal compartment	dimensionless	PREF4	0.3	Calibration
Maximum zooplankton respiration rate	1/day	TZRESP	0.1	Calibration
Threshold food concentration at which zooplankton feeding begins	g/m^3	ZOOMIN	.01	Calibration
Zooplankton HSC for grazing algae and detritus	mg/l	ZS2P	0.16	QUAL manual
Critical temperature below which zooplankton processes stop	^{o}C	ZOOT1	4.0	QUAL manual
Low optimum temperature for zooplankton processes	^{o}C	ZOOT2	20.0	QUAL manual
High optimum temperature for zooplankton processes	^{o}C	ZOOT3	26.0	QUAL manual

APPENDIX A

INPUT VALUES FOR 1989 COLDWATER LAKE CE-QUAL-R1 COMPUTER SIMULATION

INPUT PARAMETER	UNITS	COMPUTER NAME	INPUT VALUE	SOURCE
Critical high temperature or lethal temperature for zooplankton	°C	ZOOT4	36.0	QUAL manual
Temperature rate multiplier at temperature ZOOT1	dimensionless	ZOOK1	0.1	QUAL manual
Temperature rate multiplier at temperature ZOOT4	dimensionless	ZOOK4	0.1	QUAL manual
Detrital settling velocity	m/day	TDSETL	0.5	QUAL manual
Represents the lower temperature bound at which detritus decomposition continues	°C	DETT1	0.0	QUAL manual
Temperature at which decomposition occurs near the maximum rate	°C	DETT2	28.0	QUAL manual
Maximum ingestion rate of fish	1/day	TFMAX	.01	QUAL manual
HSCs that represent the amount of food present that results in fish ingestion at half the maximum growth rate	mg/l	FS2FSH	.01	QUAL manual
Preference factor of fish for benthos and sediment	dimensionless	FPSED	0.6	QUAL manual
Preference factor of fish for algae(1)	dimensionless	FPALG(1)	0.3	QUAL manual
Preference factor of fish for algae(2)	dimensionless	FPALG(2)	0.0	QUAL manual
Preference factor of fish for algae(3)	dimensionless	FPALG(3)	0.4	QUAL manual
Preference factor of fish for zooplankton	dimensionless	FPZOO	0.3	QUAL manual
Preference factor of fish for detritus	dimensionless	FPDET	0.1	QUAL manual
Critical temperature below which fish processes stop	°C	FSH1T1	1.0	QUAL manual
Low optimum temperature for fish processes	°C	FSH1T2	24.4	QUAL manual
High optimum temperature for fish processes	°C	FSH1T3	28.4	QUAL manual
Critical high temperature or lethal temperature for fish	°C	FSH1T4	35.2	QUAL manual
Temperature rate multiplier at temperature FSH1T1	dimensionless	FSH1K1	0.1	QUAL manual

APPENDIX A

INPUT VALUES FOR 1989 COLDWATER LAKE CE-QUAL-R1 COMPUTER SIMULATION

INPUT PARAMETER	UNITS	COMPUTER NAME	INPUT VALUE	SOURCE
Temperature rate multiplier at temperature FSH1T4	dimensionless	FSH1K4	0.1	QUAL manual
Assimilation efficiency for fish	dimensionless	FEFFIC	0.8	QUAL manual
Nonpredatory mortality rate for fish	1/day	TFMORT	0.01	QUAL manual
Fish respiration rate	1/day	TFRESP	0.01	QUAL manual
Decomposition rate of labile DOM	1/day	TDOMDK	0.10	Calibration
Decomposition rate of refractory DOM	1/day	TRFRDK	0.05	Calibration
Process by which labile DOM becomes refractory DOM	1/day	TDOMRF	0.10	Calibration
Ammonia decay rate	1/day	TNH3DK	0.10	Calibration
Detritus decay rate	1/day	TDETDK	0.10	Calibration
Coliform decay rate	1/day	TCOLDK	1.4	QUAL manual
Sediment decomposition rate	1/day	TSEDDK	0.016	QUAL manual
Denifitrification rate	1/day	TNO3DK	0.01	QUAL manual
Lower temperature bound at which dissolved organic matter decays	^{o}C	DOMT1	0.0	QUAL manual
Lowest temperature at which decomposition is occurring near the maximum rate	^{o}C	DOMT2	25.0	QUAL manual
Rate multiplier corresponding to DOMT1	dimensionless	DOMK1	0.12	QUAL manual
Lower temperature bound at which ammonium nitrification continues	^{o}C	NH3T1	0.0	QUAL manual
Lowest temperature at which nitrification is occurring near the maximum rates	^{o}C	NH3T2	25.0	QUAL manual
Rate multiplier corresponding to NH3T1	dimensionless	NH3K1	0.1	QUAL manual
Lower temperature bound at which denitrification continues	^{o}C	NO3T1	0.0	QUAL manual
Lowest temperature at which denitrification occurs at its maximum rates	^{o}C	NO3T2	25^{o}C	QUAL manual

APPENDIX A

INPUT VALUES FOR 1989 COLDWATER LAKE CE-QUAL-R1 COMPUTER SIMULATION

INPUT PARAMETER	UNITS	COMPUTER NAME	INPUT VALUE	SOURCE
Rate multiplier corresponding to NO3T1	dimensionless	NO3K1	0.1	QUAL manual
Suspended solids settling velocity	m/day	TSSETL	0.5	QUAL manual
Adsorption coefficient of phosphorus for use in the Langmuir isotherm	$m^3\ g^{-1}$	ADSRBP	30.0	QUAL manual
Adsorption coefficient of nitrogen for use in the Langmuir isotherm	$m^3\ g^{-1}$	ADSRBN	40.0	QUAL manual
Maximum amount of phosphate adsorbed per gram of solids	g P m^{-3}/g solid m^{-3}	ADMAXP	0.003	QUAL manual
Maximum amount of ammonia adsorbed per gram of solids	g N m^{-3}/g solid m^{-3}	ADMAXN	0.005	QUAL manual
Formulation to modify the coliform die-off rate as a function of temperature	Q_{10}	Q10COL	1.04	QUAL manual
Number of grams of oxygen required to oxidize 1 g of NH_4(as N) to NO_3	g	O2NH3	4.57	QUAL manual
Stoichiomettric requirement for oxygen during the deomposition of detritus and organic sediment (assuming a constant organic composition)	dimensionless	O2DET	1.4	QUAL manual
Oxygen requirement for biological respiration (conversion of carbohydrate to CO_2 and H_2O)	dimensionless	O2RESP	1.1	QUAL manual
Stoichiometric equivalent for oxygen production during photsynthesis taking into account the formation of proteins	dimensionless	O2FAC	1.4	QUAL manual
Stoichimetric requirement for oxygen in the deomposition of DOM is assumed to be the same as for detritus	dimensionless	O2DOM	1.4	QUAL manual
Indicates the oxygen requirement for comverting reduced manganese to manganese oxyhydroxide	dimensionless	O2MN2	0.15	QUAL manual
Describes the oxygen requirement for oxidizing reduce iron	dimensionless	O2FE2	0.14	QUAL manual
Demonstrates the oxygen requirement for the oxidation of sufide to sulfate	dimensionless	O2S2	2.0	QUAL manual

APPENDIX B

INITIAL VALUES FOR 1989 COLDWATER LAKE

CE-QUAL-R1

COMPUTER SIMULATION

APPENDIX B

INITIAL VALUES FOR 1989 COLDWATER LAKE CE-QUAL-R1 COMPUTER SIMULATION

INITIAL VALUE	UNITS	COMPUTER NAME	INPUT VALUE	SOURCE
Number of layers for which initial conditions are specified	NA	NPOINT	11	NA
Fish are expressed on a kilogram per hectare basis for the entire reservoir.	kg/hectare	FISH	0.0	Calibration
Elevations are specified from the bottom up to the surface. Highest elevation cannot be greater than the midpoint of the surface layer	m	ELEV	NA	NA
Initial condition for the first algae compartment	mg/l dry weight	DALGA1	0.080	Kelly (1991)
Initial condition for the second algae compartment	mg/l dry weight	DALGA2	0.004	Kelly (1991)
Initial condition for the third algae compartment	mg/l dry weight	DALGA3	0.200	Kelly (1991)
Initial condition for total alkalinity	mg/l as $CaCO_3$	DALKA	65.0	Kelly (1991)
Initial condition for ammonia	mg/l as N	DCNH3	0.0001	Calibration
Initial condition for nitrate	mg/l as N	DCNO3	0.012	Kelly (1991)
Initial condition for refractory DOM	mg/l dry weight	DCRFR	2.0	Calibration
Initial concentration of coliform bacteria	colonies/100 ml	DCOLIF	0.0	Calibration
Initial condition for organic detritus	mg/l dry weight	DDETUS	0.1	Calibration
Initial condition for labile DOM	mg/l	DDOM	0.2	Calibration
Initial condition for dissolved oxygen	mg/l	DOXY	10.20 (surface)	Kelly (1991)
Initial condition for available phosphorus (orthophosphate)	mg/l as P	DPO4	0.002	Kelly (1991)
Initial condition for organic sediment	g/m^2	DSEDMT	.0001	Calibration
Initial condition for temperature	^oC	DTEMP	10.5(surface)	Kelly (1991)
Initial condition for total dissolved solids	mg/l	DTDS	0.1	Kelly (1991)
Initial condition for the zooplankton compartment	mg/l dry weight	DZOO	0.050	Kelly (1991)

APPENDIX B

INITIAL VALUES FOR 1989 COLDWATER LAKE CE-QUAL-R1 COMPUTER SIMULATION

INITIAL VALUE	UNITS	COMPUTER NAME	INPUT VALUE	SOURCE
Initial condition for pH	unitless	DPH	7.7	Calibration
Initial condition for suspended solids	mg/*l*	DSSOL	0.0	Calibration
Initial condition for Mn(IV)	g/m^3	DCMN4	0.01	Calibration
Initial condition for Mn^{+2}	g/m^3	DCMN2	0.0	Calibration
Initial condition for Fe(III)	g/m^3	DFE3	0.0	Calibration
Initial condition for Fe^{+2}	g/m^3	DFE2	0.0	Calibration
Initial condition for FeS in the water column	g/m^3	DFESB	0.0	Calibration
Initial condition for SO_4^{-2}	g/m^3	DSO4	0.60	Calibration
Initial condition for S^{-2}	g/m^3	DS2	0.0	Calibration
Initial condition for Mn in sediments	g/m^3	DCMN	600.0	Calibration
Initial condition for Fe in sediments	g/m^3	DFE	120.0	Calibration
Initial condition for FeS in sediments	g/m^3	DFESA	0.0	Calibration
Initial condition for S in sediments	g/m^3	DS	20.0	Calibration
Initial condition for inorganic P in sediments	g/m^3	DXPO4	1.0	Calibration
Initial condition for inorganic N in sediments	g/m^3	DCN	10.0	Calibration
Initial condition for silica in the water column	g/m^3	DSI	16.0	Calibration
Initial condition for macrophytes	g/m^2	PLCOL (1-9)	0.0	Calibration